water

MDPI

Review

Solar Desalination by Humidification–Dehumidification: A Review

Nejib Ghazouani [1,2,*], Alaa A. El-Bary [3], Gasser E. Hassan [4], Nidhal Becheikh [1], Abdulhakim Bawadekji [5] and Mahmoud M. Elewa [3,*]

1 College of Engineering, Northern Border University (NBU), Arar 73222, Saudi Arabia
2 Civil Engineering Laboratory, National Engineers School of Tunis (ENIT), University of Tunis El Manar, Tunis 1002, Tunisia
3 Arab Academy for Science, Technology and Maritime Transport, College of Engineering and Technology, P.O. Box 1029, Alexandria 21934, Egypt
4 City for Scientific Research and Technological Applications, New Borg El Arab City, Alexandria 21934, Egypt
5 College of Science, Northern Border University (NBU), Arar 73222, Saudi Arabia
* Correspondence: nejib.ghazouani@nbu.edu.sa (N.G.); mahmoud.elewa@aast.edu (M.M.E.)

Abstract: The scarcity of drinkable water supplies is becoming a serious and troubling challenge to long-term development. This issue emphasises the urgency of implementing rapid water desalination options. However, desalination is a capital-intensive process that requires a significant amount of energy, and since it is now mostly powered by fossil fuels across the globe, it has the potential to leave a significant carbon footprint. In this light, transitioning to green energy sources for desalination is a necessity in today's society. Humidification–dehumidification (HD) is one of the most effective desalination procedures to consider for distant places with modest fresh water demands for household and agricultural demands. This is mostly because it requires minimal operational and maintenance concerns. The current article examines the many kinds of HD desalination systems driven by solar energy sources and their key components. The current study established that the seawater HD system is viable for producing fresh water, especially for greenhouses and dispersed demand. HD is an effective technique for eluting fresh water from concentrated brines, boosting production, and minimising harmful environmental impact, benefitting ecosystems and human services. The packed bed humidifier is the most commonly used kind of humidifier in the HD water desalination system. Additionally, as compared to an indirect dehumidifier, the direct dehumidifier improves the performance of the HD desalination system. According to the findings of this research, hybrid energy systems have the greatest gain output ratio (GOR). Solar water heating significantly increases system productivity as compared to solar air heating. When combined with a heat pump, the HD delivers optimal system productivity and GOR at the lowest cost per litre. The conclusion is that, even though humidification–dehumidification is a promising method for decentralised small-scale fresh water production applications, it needs additional improvement to optimise system performance in terms of economy and gain output ratio.

Keywords: greenhouse desalination; humidification–dehumidification of air; renewable energy

check for updates

Citation: Ghazouani, N.; El-Bary, A.A.; Hassan, G.E.; Becheikh, N.; Bawadekji, A.; Elewa, M.M. Solar Desalination by Humidification–Dehumidification: A Review. *Water* **2022**, *14*, 3424. https://doi.org/10.3390/w14213424

Academic Editors: Chunyan Wang, Lu Lin, Chao Zhang and Shen Qu

Received: 15 September 2022
Accepted: 19 October 2022
Published: 27 October 2022

Publisher's Note: MDPI stays neutral with regard to jurisdictional claims in published maps and institutional affiliations.

Copyright: © 2022 by the authors. Licensee MDPI, Basel, Switzerland. This article is an open access article distributed under the terms and conditions of the Creative Commons Attribution (CC BY) license (https://creativecommons.org/licenses/by/4.0/).

1. Introduction

Water is essential to the beginning and continued existence of humanity. Because it covers almost three-quarters of the earth's surface, water is one of the most abundant resources on the planet. The oceans contain approximately 97% of the water on Earth, which is salt water. The remaining 3% of the water on Earth is fresh water, which can be found at the poles (in the form of ice), in ground water, lakes, and rivers. Fresh water supplies the majority of the water that is needed by humans and animals. Glaciers, areas with permanent snow cover, ice, and permafrost are home to over 70% of the world's tiny 3% fresh water supply, respectively. Thirty per cent of the world's fresh water is found

underground, most of which is located in very deep aquifers and difficult to access. Rivers, lakes, and underground water reserves have traditionally served as man's primary sources of water for domestic, agricultural, and industrial uses. Around 70% of the world's fresh water is used for agricultural purposes, whereas only 20% is used for industrial purposes and only 10% for residential uses [1].

According to the UN-Water Annual Report 2021, published in June 2022, 2 billion people in underdeveloped nations lack access to clean drinking water. Additionally, 3.6 billion people (46% of the world population) lack access to appropriate sanitation [2]. According to some recent forecasts, about half of the world's population will experience genuine water supply problems [3]. Around 3 billion of the world's population lack access to adequate quality and/or quantity of fresh water, and 107 countries are not on track to have sustainability-managed water resources by 2030 [2]. Currently, one-fifth of the world's population lives in places with insufficient fresh water supply. In many developing nations, 80% of the population lives in rural areas with much poorer access to fresh water than in metropolitan areas [4]. By 2025, it is anticipated that up to two-thirds of the world's population will live in nations with water scarcity [5].

However, increased industrialisation and the global population boom have significantly increased the need for fresh water for home use and crops to generate sufficient food. Additionally, there is the issue of river and lake contamination caused by industrial pollutants and vast volumes of sewage released. Water demand doubles every 20 years on average, making the water problem all the more alarming [1,2]. The seas are the only essentially limitless supply of water. Their primary disadvantage is their excessive salinity. As a result, it would be desirable to address the water scarcity issue by desalination this water. Salinity in water is limited to 500 parts per million (ppm) and up to 1000 ppm in rare instances, but most of the accessible water on Earth has a salinity of up to 10,000 ppm and salt water typically has a salinity of 35,000–45,000 ppm in the form of total dissolved salts [1,6].

Excessive water salinity results in a loss of flavour, gastrointestinal discomfort, and laxative effects. A desalination system's objective is to clean or purify brackish or salt water and deliver drinkable and irrigation water with TDS of less than 500 ppm or from 500–1500 ppm for irrigation [7]. This is performed via a variety of desalination procedures that will be investigated; as a result, desalination operations use a large amount of energy to separate salts from salt water. Renewable energy systems produce energy from renewable sources such as geothermal energy, solar energy, low-grade energy sources, photovoltaic thermal (PV/T) panels, and power plant waste heat. Their primary feature is that they are environmentally friendly. The production of fresh water using desalination technology powered by renewable energy systems is considered a possible solution to the problem of water scarcity in distant places that lack access to potable water and traditional energy sources such as heat and electricity. Numerous renewable energy desalination pilot plants have been erected worldwide, with the majority operating effectively for several years. Almost the majority of them are custom-designed for particular locales and generate fresh water by solar or geothermal energy [8]. Although renewable energy-powered desalination systems cannot compete with traditional desalination systems in terms of the cost of water produced, they are appropriate in specific places and are projected to shortly become more broadly practicable. El-Ghonemy [9] analysed water desalination systems driven by renewable energy sources, highlighting current advances in the area of renewable energy-based desalination, with a concentration on technology and economics. Some broad recommendations for the selection of desalination and renewable energy systems, as well as the factors for examination, were provided. Figure 1 depicts the technical state of renewable energy desalination methods [10].

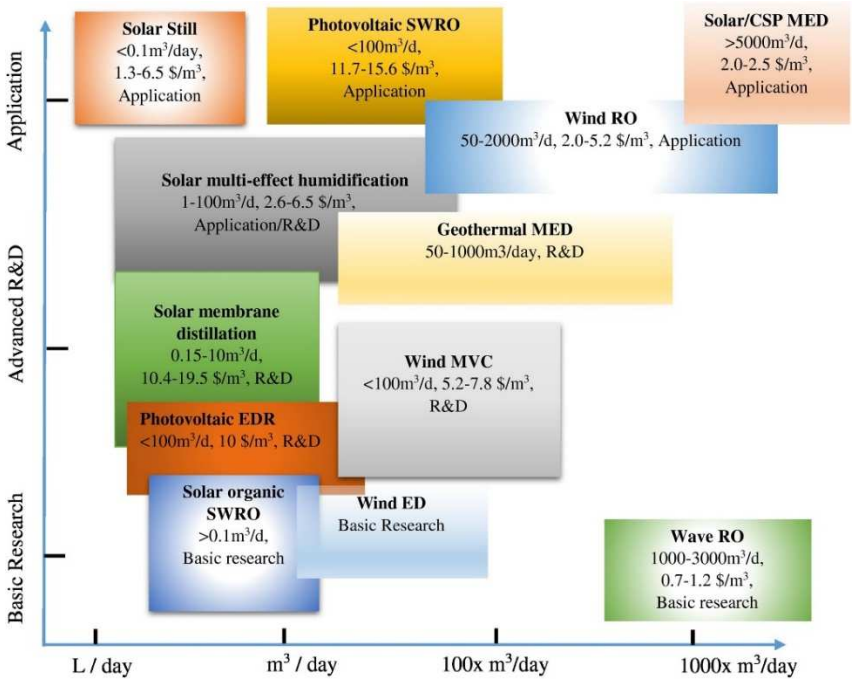


Figure 1. The technological state of desalination technology for renewable energy. Reproduced with permission from. Reproduced with permission from Farah Ejaz Ahmed, Raed Hashaikeh, Nidal Hilal, Desalination Journal, published by Elsevier, 2019 [10].

Desalination methods available today are mostly classified into two categories: thermal and membrane approaches. The former is prohibitively expensive, has corrosion issues, and requires large, difficult-to-maintain installations (e.g., multi-stage flash (MSF)), while the latter suffers from membrane fouling and demands water pre-treatment before being delivered into the desalination modules, as well as post-treatment. Other less prevalent desalination systems are less established, and each has its own set of advantages and disadvantages.

Desalination is characterised by fast technological advancements. Each year, several new desalination facilities are tested and implemented globally. Desalination methods have matured technologically and economically, enabling them to play a larger part in the future water supply. These installations may be built using a variety of different technological approaches and provide a great deal of versatility in terms of size and energy use (a function of energy resources and the situation). MSF is the most often thermal-based utilised method. This approach is used in about 50% of all installations worldwide. On the other hand, when production scales down, the efficiency of conventional distillers falls due to the difficulty of implementing a given number of effects in small installations. For these smaller installations (in rural areas, for example), conventional distillers are unsuitable: the installation costs, energy usage, and hence water costs, are too expensive.

Several well-established desalination techniques exist, including reverse osmosis (RO), MSF, and multi-effect distillation (MED); however, these technologies are often inappropriate for developing countries because of their high infrastructure requirements, reliance on fossil fuels as a source of energy, and cost-effectiveness on very large scales.

Greenhouses (GHs) are a critical component of the food supply chain as they increase crop yield [11]. The productivity of GHs is commonly known to be 7–10 times that of an open field. Furthermore, it only uses 10% of the water required for open field agriculture [12]. They protect the plants while conserving resources such as electricity and water [13]. GHs are utilised to chill or heat the air within the GH depending on their geographical location and season [14]. The grown crop's production is heavily reliant on the GH environment, namely, the GH temperature and relative humidity (RH) [15]. Plant photosynthesis has a diverse spectral profile; however, in vitro, most photosynthe-

sis chemicals exhibit narrow spectral absorbance maxima in the blue (400–500 nm) and red (600–700 nm) wavelength bands, which account for less than 30% of the incoming solar spectrum [16]. The remaining 70% of solar energy is in the near-infrared (NIR) band (700–2500 nm), where photons do not drive photosynthesis but do raise the ambient temperature within a GH. Temperature is recognised to have a crucial role in regulating plant development [17]. However, the transfer of NIR radiation into greenhouses often leads to excessive solar heating and increased water demand for evaporative cooling, particularly in hot and dry locations. Heat stress occurs when plants are exposed to high temperatures for an extended length of time, resulting in decreased output [18]. Similarly, high RH promotes the growth of pathogens such as fungi, whereas low RH causes plants to lose too much water to the GH air, resulting in wilting [19]. As a result, it is critical to maintaining an optimal temperature and relative humidity within the GH for growing high-quality produce. Additionally, year-round crop production is required to make the GH commercially viable in dry locations. However, in desert areas, high temperatures and a scarcity of water restrict crop production to a few months, making agriculture economically unviable and difficult. Due to the paucity of fresh water, farmers are sometimes obliged to utilise salty ground water for agriculture to satisfy irrigation needs [20]. Additionally, the cooling burden rises dramatically during the summer, resulting in temperatures that exceed the optimal range, which is harmful to plant growth. As a result, numerous methods have been developed to control the GH microclimate and meet irrigation needs in dry places [21,22]. However, the microclimate of the greenhouse is reliant on dynamic, non-linear, and uncertain parameters such as solar irradiation, outside temperature, air speed, and inside conditions [23].

In dry areas, natural ventilation alone is inadequate to manage the temperature within the GH during the summer season, when solar gains and outside temperatures are high [24]. While coupling natural ventilation with shade screens may help reduce cooling loads, restricting solar irradiance entering the GH canopy affects plant growth since sunlight is necessary for photosynthesis [25]. Evaporative or fan and pad cooling is another way of lowering the temperature of the air passing through the GH and converting it to latent heat. However, evaporative cooling is temperature and relative humidity dependent; in dry climates, when temperature and relative humidity rise, the air's wet-bulb temperature increases as well, resulting in inefficient cooling within the GH [26]. As a result of these considerations, active mechanical heating, ventilation, and air conditioning (HVAC) systems scheduling and decision-making may be improved by anticipating factors many hours in advance. In addition, the link between the GH's cooling load and water demand in an environment with high temperatures and a scarcity of fresh water is evaluated. Crops yield and output are greatly reliant on the microclimate created by the HVAC system in the GH. Maintaining optimal conditions in the greenhouse necessitates monitoring and managing temperature and relative humidity, as well as identifying potential scenarios/techniques to decrease energy and water usage. In the summer, when sun irradiance and temperature reach 1000 W/m^2 and 45 °C, respectively, it is difficult to maintain optimum growth conditions while minimising energy and water use. In order to operate a GH efficiently, it is required to calculate the cooling and water requirements under various climatic conditions/seasons [27]. HVAC systems are the most effective technique for controlling the GH microclimate, but they use a significant amount of energy. The majority of energy is generated by fossil fuels, which contribute to damaging greenhouse gas (GHG) emissions. As a result, GHs powered by renewable energy and equipped with active mechanical cooling systems provide a viable option for sustainable agriculture in comparison to traditional food production systems fuelled by fossil fuels.

The sun, the sea, and the environment are used to generate fresh water and cool air in a seawater greenhouse. Within a controlled setting, the procedure recreates the natural hydrological cycle. The building's front wall is a salt water evaporator. It is made of a honeycomb lattice and confronts the wind. Air movement is controlled by fans. Seawater drips down the lattice, cooling and humidifying the air that passes through into the planting area. The sun is diffused by a specifically designed roof. The roof absorbs infrared heat

while allowing visible light to pass through to encourage photosynthesis. This results in ideal growing conditions, which are cold and humid with high light intensity. Seawater heated in the roof goes through a second evaporator, producing hot, saturated air that flows through a condenser. Incoming salt water cools the condenser. Because of the temperature differential, fresh water condenses out of the air stream. Air temperature, relative humidity, solar radiation, and airflow rate all influence the amount of fresh water. With adequate meteorological data, these circumstances may be modelled, allowing the design and procedure to be optimised for any acceptable site [28–30].

In a salt water greenhouse, substantially more water evaporates than condenses back into fresh water. Because of the high rates of ventilation used to keep the crops cool and supplied with CO_2, this humid air is 'lost.' The greater humidity of the exhaust air aids in the development of more hardy crops downwind of the greenhouse. This phenomenon may allow biofuel crops to be grown in the region around the seawater greenhouse.

A seawater GH is a GH structure that permits the cultivation of crops and the generation of fresh water in approximately one-third of the planet's dry areas. This is in reaction to the worldwide water shortage, peak water, and soil salinisation. The system is powered by solar energy. It employs a construction similar to the pad-and-fan GH, but with added evaporators and condensers. The salt water is pumped into the GH to generate the best circumstances for the development of temperate crops: a chilly and damp atmosphere. [31] Using the idea of solar desalination, which eliminates salt and contaminants, fresh water is generated in a concentrated form. The residual humidified air is then removed from the GH and utilised to enhance outside plant growth conditions.

The current article classifies and discusses recent technical advancements in the area of solar HD based on the technique used in the research endeavour. This strategy is adopted to better understand the field's research gaps and to arrange the results. Throughout the document, the article identifies and analyses the gaps, as well as the existing and future state of each area. The present review included flat plate collectors, evacuated tube collectors, bubble columns, concentrating collectors, photovoltaic modules, solar ponds, and hybrid systems. Following that, current improvements in HD desalination systems and subsystems for by-product treatment are analysed and addressed. The concluding part makes recommendations for further study.

2. Solar Desalination Technologies

As previously stated, the majority of desalination procedures use a significant quantity of energy. The bulk of desalination facilities now operating on a global scale is powered by fossil fuels. However, the majority of places that face increased fresh water demand also obtain significant quantities of solar energy. Thus, solar energy might be an excellent source for this purpose since it is plentiful and emits few pollutants. Solar desalination methods are divided into direct and indirect categories across the literature. In this context, if solar radiation is absorbed directly by the desalination plant's input feed water, the plant is regarded to be of the direct kind. Solar energy is collected by solar thermal collectors and then transmitted to the salty water in indirect plants, or it is converted to electricity and then utilised to power the plant. In both scenarios, solar energy might be utilised to power the plant using a heat engine. Adapted from [32], Figure 2 displays this categorisation of solar desalination modules. However, this reference classifies HD as a straight drive. This is because, in an HD system, saline water may absorb sun energy directly or via solar thermal collectors. It might be either direct or indirect in this sense.

Numerous aspects must be considered while selecting technology for a desalination project. It is highly dependent on the demand side, available resources, economic considerations, maintenance concerns, and the projected lifespan of the project, among other factors. For example, the simultaneous need for fresh water and energy may necessitate the use of poly-generation plant technology. Additionally, surplus heat generated by solar thermal collectors in the desalination plant might be used to meet heating needs. The magnitude of the demand sector may have a significant impact on the design process since certain

technologies are incapable of meeting large demand levels. The operation and maintenance sectors are also important to examine since certain technologies are capable of working for an extended period without requiring significant upkeep. Another factor to consider is the amount of available land and the potential market. Additionally, environmental concerns should not be overlooked since they may be addressed in economic calculations. The benefits and disadvantages of various methods of solar desalination are listed in Table 1 in terms of environmental, economic, energy consumption, construction, material availability, efficiency, and distilled water quality, among other aspects. This table may provide relevant information on the comparison of several desalination systems.

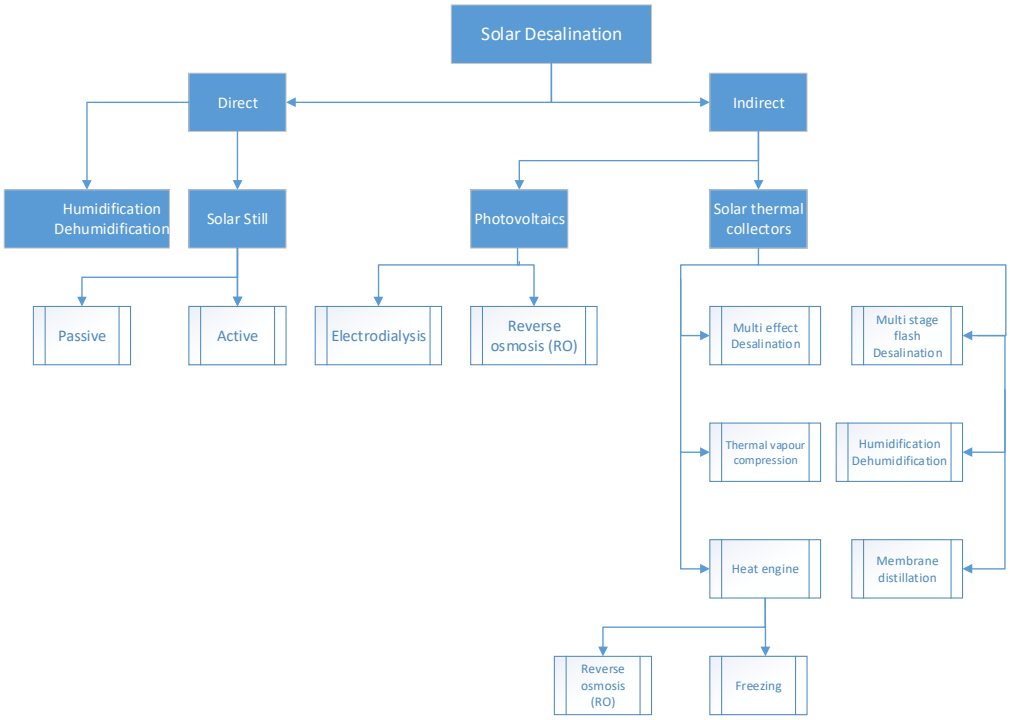


Figure 2. Classification of desalination processes based on solar energy.

Table 1. Merits and demerits of various solar desalination technologies.

Desalination Type	Merits	Demerits
Solar still (SS) [33]	• Environmentally friendly • Low operation and maintenance costs • High-quality produced water • Available building materials • Suitable for homes and communities living on islands • Removal of fluoride, arsenic, bacteria, and other contaminants from the water	• Occupies a large area • Is inefficient • Is not suitable for high-capacity water production
HD [34,35]	• High flexibility • Suitable for decentralised operation • Simpler brine pre-treatment • Operates with any form of energy • Low installation and operating costs	• High capital investment costs • High total expenses of generated water • Availability of requirements
Solar chimney [36,37]	• Long operating lifespan • Simple and robust construction • Low maintenance cost • Environmental friendliness • Production of by-products such as salt • Use of waste barren land • Low generated water prices • Generate electricity and fresh water at the same time	• Large area of occupation • Extremely expensive capital investment expenses

Table 1. *Cont.*

Desalination Type	Merits	Demerits
Multi-stage flash desalination (MSF) [38]	• Produces high-quality distilled water • Reliable device operation • Ideal for large-scale distillation operations • Water of any grade may be processed • Minimal or no pre-treatment of the feed water is necessary	• Excessive energy use • Excessive operating temperature results in device corrosion • Heavy structure • Excessive capital cost
Multi-effect distillation (MED) [38]	Compared to multi-stage flash desalination, this process uses less thermal energy, produces better distilled water, and emits less CO_2 since it doesn't need a high operating temperature or feed water pre-treatment.	• Expensive and hefty construction. • Vacuum pump power consumption
Vapour compression desalination (VC) [38]	There are several advantages to using this technology, including: • Low energy consumption • High operational efficiency • Size depends on compressor size • High quality produced water • Appropriate for low-capacity operation • No additional cooling medium • Less pre-treatment of feed water • Low environmental impact	• High capital investment • Corrosion of the compressor • Water production costs
Natural vacuum desalination [39]	• Wastewater, seawater, and sewage may all be treated. Low-temperature heat sources are adequate; water production costs are reduced; tall structures may be integrated; organic substance in the product is not destroyed because of the heat.	• Removal of non-condensable gases created during water evaporation is necessary • High building heights beyond 10 m are required
Solar-powered RO [10,40–44]	Several advantages include smooth operation, low energy consumption, flexibility in capacity expansion, and the ability to be built as a compact or portable device. However, the membranes can become fouled by biological organisms, so pre-treatment of the feed water is required. Using a battery is not recommended because of the high capital cost and the need for battery replacement.	• It is not suggested to use a battery because of the high capital cost and the need for battery maintenance. • Membranes have a limited lifespan • High-pressure pump is necessary • Requires pre-treatment of feed water
Solar thermal powered RO [40,45–47]	Minimal batteries are needed; a low-temperature source is adequate; solar collectors could cover a broad temperature range; no efficiency losses; low operation and maintenance costs; and non-skilled labour would suffice for large-capacity operation. Solar collectors, on the other hand, use less energy for post-treatment.	• No potential demerits
Electrodialysis (ED) [45,48,49]	Inverter-free DC operation means lower losses, longer membrane lifetimes, higher water recovery, and less fouling and scaling on the membrane. Less pre-treatment of the feed water is needed. Devices are easier to start and stop. Low efficiency since energy is required.	• Every 20 min, the polarity must be reversed • The generated water is expensive and consumes a lot of energy
Membrane distillation (MD) [50–56]	• Reduced leakage compared to RO • Pre-treatment of feed water is not necessary • Pipelines are thinner • Reduced operation in low temperatures • High salt feed water may be treated	• Membrane wetting • High membrane prices • Due to low driving force, a large membrane surface is needed
Freezing [57,58]	• It takes just 420 kJ of energy to remove salt and create 1 kg of fresh water, which is six times less than what MSF needed • Due to the low working temperature, they are tolerant to corrosion issues and may function for a long period with minimum maintenance	• After the desalination process, ice handling is one of the most difficult tasks

To create a drinkable water product, three processes are required: pre-treatment, treatment, and post-treatment. Different desalination systems need varying degrees of pre- or post-treatment. In comparison to thermal desalination, membrane-based desalination techniques may be more susceptible to the presence of unwanted organic or inorganic chemicals or pathogens in the product water. Specifically, higher temperature desalination facilities with water temperatures more than 70 °C are considered to be rather safe in terms of the safety and quality of the generated water. This is because at high temperatures, any

extant microbes are killed and dangerous inorganic compounds such as Boron products are eliminated by the distillation process, resulting in water with an acceptable purity. On the contrary, RO is unable to successfully remove Boron from seawater and other salty water sources. Additionally, ED cannot ensure pathogen elimination. In these circumstances, extensive post-treatment and water quality testing are necessary, increasing the plant's capital cost. However, further measures should be employed in thermal plants operating at temperatures below 50 °C, since this temperature is insufficient for reliable pathogen elimination. Additionally, it should be emphasised that water quality problems may be highly dependent on the quality and circumstances of the water supply.

In comparison to other desalination systems, HD has a smaller capacity. However, it also takes very little care throughout the plant's life. While the generated water is more expensive than that produced by other technologies such as reverse osmosis, other aspects make solar HD a viable option for distant places with low-to-moderate demand levels. It is not dependent on electricity or other energy sources, and solar energy can generate the necessary thermal energy. Solar HD plants might be an excellent alternative for tiny locations that lack enough access to potable water networks. Additionally, as solar collector technology advances, the total cost of the generated water decreases, making it a viable choice for small-scale applications.

Global Water Intelligence (GWI DesalData) desalination and reuse markets [59] classified desalination technologies according to Table 2.

Table 2. Industrial solar desalination technologies classifications.

Established	Emerging
• Reverse osmosis (RO) • Nanofiltration (NF) • Multi-effect distillation (MED) • Multi-stage flash distillation (MSF) • Electrodialysis/electrodialysis reversal (ED/EDR) • Electrodeionisation (EDI) • Falling film evaporators • Direct contact evaporation • Forced circulation crystallises	• Capacitive deionisation (CDI) • Humidification–dehumidification (HD) • Membrane distillation (MD) • Forward osmosis (FO) • Chemical solute extraction

Figure 3 illustrates a technology's path to commercialisation depicting the early enthusiasm around a new idea, followed by disappointment when practical challenges arise, and then the last push for commercialisation and widespread adoption.

Management of brine is now a major driver of adoption. Except for semi-batch RO, almost all the methods undergoing the gradual march to widespread usage are largely utilised for brine concentration.

Materials such as graphene and carbon nanotubes are among the slowest-maturing technologies due to the time required to develop dependable and cost-effective production processes.

'Operational R&D' designs, such as semi-batch or counter-flow RO systems, are expected to gain traction considerably more swiftly.

Despite the capabilities of thermal desalination methods to use waste heat, research undertaken by MIT into primary energy usage demonstrates that even when waste heat is utilised, thermal procedures are less energy efficient than membrane processes. These primary energy values represent the value of the energy in the source, including generating losses and are based on the energy produced by a combined cycle gas turbine.

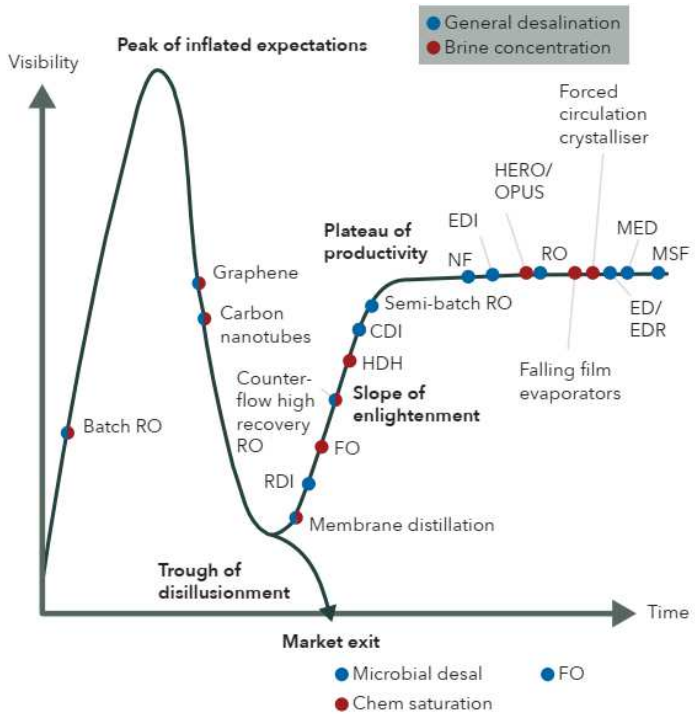


Figure 3. The commercialisation of innovative desalination and brine concentration technologies [59].

3. Humidification–Dehumidification of Air

The HD desalination method is based on converting salt water to water vapour in the humidifier and then condensing it over the condensing coils in the dehumidifier at a surface temperature lower than the dew point of the air. To boost HD's fresh water production, the evaporation process is accelerated by heating either the water or the air, or both, to enhance the air's capacity to transport more water vapour as the temperature rises. In theory, 1 kg of dry air may transport 0.5 kg of vapour with an energy cost of 2814 kJ when the temperature is increased from 30 to 80 °C. [60]. A defined quantity of water vapour is removed throughout the humidification process by flowing air that is maintained in contact with salt water. When humid air comes into touch with a cold surface, water vapour condensation occurs, providing the necessary fresh water. The condensation method uses the latent heat of condensation to pre-heat the salt water going through the condensing coils [35,60–63]. The seawater cycle may be either open or closed in the HD desalination technology. The evaporation of 1 kg of water leads to a 60 °C fall in the temperature of 10 kg of salt water in the open cycle. The amount of fresh water recovered varies between 5% and 20% of the volume of salt water cycled. This indicates that a little amount of fresh water is produced at a high rate of heat loss. In a closed-cycle system, increased fresh water output is maintained at a low energy cost [60,62]. Figure 4 illustrates a basic form of the HD water desalination method. The HD system is simply a pair of vertical/horizontal ducts joined at the top to circulate the air [64]. The HD desalination system may be operated in natural or forced draught mode, depending on the air circulation. The dehumidifier is comprised of a single duct that includes the condenser that generates the unsaturated air. An atomiser is used to flash salt water within the humidifier, resulting in small droplets. This maximises the surface area of contact between the flashed salt water and the surrounding air [65]. A packing material used in the other duct to effectively humidify the air is referred to as a humidifier delivering saturated air. To maximise system efficiency, the air and/or water are heated utilising a variety of energy sources, including thermal, solar, geothermal, and hybrid energy. HD systems are categorised according to their energy source, their air and water circulation cycles, and their water and/or air heating sources [66]. No high temperatures are required for the revolutionary HD of air technology [67]. Solar energy can

provide all of the thermal energy necessary in these systems [68]. Solar HD desalination systems are well-known for their efficiency in delivering clean water to isolated areas [68]. HD systems are straightforward in design and operation, but their poor thermal energy efficiency is a major disadvantage. Typically, the poor thermal efficiency of HD systems is attributable to the limited thermodynamic availability of low-grade heat. Moreover, HD systems often use natural draught to circulate air inside the system, which is linked with lower heat and mass transfer coefficients than forced draught air flow. Typically, film condensation over metallic tubes is used to condense airborne water vapour and recover the latent of condensation. Due to the poor rate of heat transmission, often a large metallic surface area is needed, which raises the cost of the system. Solar HD technologies have considerable potential for decentralised small-scale water production applications, but more system efficiency improvements are required to minimise the capital cost [69].

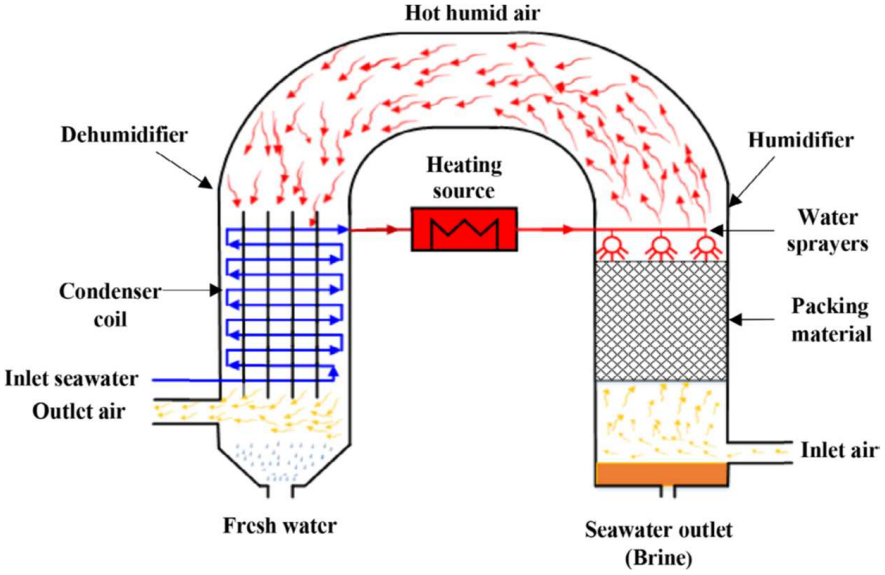


Figure 4. Desalination of HD in a straightforward manner. Reproduced with permission from A. S. A. Mohamed, M. Salem Ahmed, Hussein M. Maghrabie, Abanob G. Shahdy, International Journal of Energy Research, published by John Waley and Sons, 2020 [70].

3.1. Parameters Impacting the HD System's Performance

The HD's performance is quantified using a variety of indicators, including GOR, specific water production, recovery ratio (RR), mass flow rate ratio (MR), energy reuse factor (F), and specific entropy generation (S_{gen}).

3.1.1. Gain Output Ratio (GOR)

The gain output ratio (GOR) is one of the primary performance measures used to evaluate HD's performance. It may be computed as the ratio of the latent heat of vaporisation of generated fresh water to the total energy input to HD [71]:

$$\mathrm{GOR} = \frac{m_{fw \cdot \lambda}}{Q_{in}} \quad (1)$$

where m_{fw} is the mass flow rate of fresh water; λ is the latent heat of vaporisation, and Q_{in} is the total energy input.

A high GOR value indicates that a low heat input per unit quantity of fresh water is wanted. As a result, employing fossil fuels as a source of heat and reaching a higher GOR value results in cheaper fuel costs, whereas, when solar energy is used as a heat source, sustaining a greater GOR needs a smaller solar collector, lowering initial expenses [60].

3.1.2. Specific Water Production

The daily amount of fresh water obtained per square metre of collector area is referred to as the specific water production. This indicator is mostly used to determine the efficiency of the HD when it is powered by solar energy. Additionally, a capital cost evaluation of HD is necessary if the cost of solar collectors varies between 40% and 45% for air heating systems [34,60] and between 20% and 35% for water heating systems [34,60,72].

3.1.3. Recovery Ratio (RR)

The recovery ratio (RR), defined as the quantity of fresh water recovered per kilogram of input salt water, is greatly increased as a consequence of the improved salt rejection. The recovery ratio (RR) for seawater desalination with a salinity of 35 g/L was about 25% in the 1980s but increased to over 35% in the 1990s. Recently, the recovery ratio (RR) has reached about 45% and may reach 60% when combined with a second stage system [73]. It is computed using the formula [74]:

$$\mathrm{RR} = \frac{m_{fw}}{m_{sw}} \tag{2}$$

where m_{sw} is the mass flow rate of feed seawater.

3.1.4. Mass Flow Rate Ratio (MR)

The mass flow rate ratio (MR), which is defined as the ratio of the intake seawater mass flow rate to the dry air mass flow rate supplied to the system, has a significant influence on the performance of HD [75]. It is approximated by [76]:

$$\mathrm{MR} = \frac{m_{sw}}{m_{air}} \tag{3}$$

where m_{air} is the flow rate of dry air.

3.1.5. Energy Reuse Factor (F)

In the water desalination system powered thermally by HDH, there have been several efforts made to recover heat in order to reduce the amount of money spent on energy. The energy reuse factor, denoted by the letter '*F*' is the ratio of the energy that is obtained from the heated working fluid to the energy that it provides [77]. It is an essential indication of the HD system's ability to reclaim lost heat. There is a range of possibilities for the economic value of the energy reuse factor in the HD system, from 6 to 12 [34]. The energy reuse factor, denoted by the letter '*F*' may be calculated as follows [77]:

$$F = \frac{V_{dh,in} - V_{dh,out}}{V_{dh,in} - V_{h,out}} \tag{4}$$

where V is the vapour loading in moles of water vapour per moles of carrier gas.

3.1.6. Specific Entropy Generation

The total specific entropy generation ($S_{gen,total}$) of the humidification–dehumidification desalination cycle is equal to the sum of the entropies created by each component of the HD system divided by the produced water flow rate. $S_{gen,total}$ may be computed using the least work of separation and classical thermodynamic concepts as follows [78]:

$$S_{gen,total} = \frac{\dot{S}_{gen,total}}{m_{fw}} \tag{5}$$

where $S_{gen,total}$ is the total specific entropy generation for each system component.

3.2. Humidifier and Dehumidifier

As a result, HD technology is a viable desalination approach for small-scale potable water needs [34,79]. In comparison to the thermal and membrane desalination processes described previously, HD systems are relatively insensitive to high feed salinity and can operate efficiently at low operating pressures (1 bar) and temperatures, making them suitable for decentralised production of potable water from high salinity seawater [80]. The HD process is analogous to the rain cycle, in which salt water evaporates into the air or other carrier gases such as Ar, He, or CO_2 [81,82] when heated by solar radiation; air transports water vapour at higher altitudes and condenses at very low pressures and temperatures. Similarly, water vapour is removed from a humidifier by air interaction with the hot feed, followed by condensation of water vapour in a condenser or dehumidifier, where humid air interacts with a cold surface to generate distillate/fresh water [83].

The HD desalination method utilises packing materials in the humidifier to increase the amount of time that air has contact with the water [66,84,85]. This increases heat and mass transfer efficiency (which is the foundation of the HD desalination process) and humidification efficiency. In other words, the humidifier's packing material has a significant effect on HD efficiency. Numerous research has been undertaken to determine the efficacy of various humidifier packing materials in improving HD processes [86–88]. Yuan et al. [89] employed honeycomb paper in an HD solar desalination unit's humidifier tower. A mathematical model was constructed to investigate the system's behaviour, and the findings indicated that closed air and water circulation contributed to the system's superior performance when compared to open circulation. Yamali et al. [90] investigated the impacts of different operating conditions on solar-powered HD desalination machines by incorporating four plastic honeycomb structures into the humidifier unit and developing a mathematical model. Increased feed and coolant flow rates were shown to boost system productivity. The air flow rate, on the other hand, had a negligible influence on the system's performance. Amer et al. [91] conducted a similar investigation, comparing HD performance with three different kinds of humidifier packings (wooden slats, gunny bag cloth, and polyvinyl chloride). The influence of operational parameters on system performance revealed that forced air circulation increased system productivity considerably only at lower feed temperatures; however, the effect was minor at higher feed temperatures.

Hermosillo et al. [92] evaluated the possibility of condensation enthalpy recovery throughout the dehumidifier unit using a cellulose paper humidifier. It was discovered that by reducing the input flow rate, a maximum latent heat recovery of roughly 100% could be attained while maintaining better yields. Muthusamy et al. [93] analysed the energy and exergy consumption of an HD system loaded with sawdust and gunny bag humidifier packing materials. The performance of the system was improved by installing inserts in the air heater and dehumidifier units. The findings indicated that the gunny bag humidifier improved energy and exergy efficiency by 44% and 38%, respectively when compared to the sawdust humidifier. Al. Hallaj et al. [94] incorporated wooden slats into a wooden-framed humidifier tower. Experiments with the closed-air cycle solar HD process showed that yield was heavily reliant on feed flow rate and that air velocity had an influence only at lower intake water temperatures. Nematollahi et al. [95] conducted an in-depth investigation of the exergy consumption of an HD system integrated with a pall rings humidifier. It was discovered that when the diameter of the humidifier unit rose, its length and incoming air temperature declined, and the exergy efficiency improved. Nafey et al. [96] investigated the performance of a solar HD unit equipped with a canvas humidifier in an experimental setting. The distillation rate was found to be predominantly dependent on system characteristics (e.g., feed and air input temperatures/flow rates), with wind speed and ambient temperature having a minimal influence. Ben Bacha et al. [97] demonstrated a solar multiple condensation evaporation cycle (SMCEC) desalination method using a thorn tree humidifier. In comparison to other aspects, it was discovered that fresh water productivity was significantly dependent on the water entry temperature of the humidifier and dehumidifier units.

A spray tower is the second form of humidifier. It is a cylindrical structure in which water is disseminated downward by spray nozzles while air flows upward. The pressure drop is minimal on the air side, but the humidifier can hold a large amount of water and air. The humidifier's effectiveness is limited due to the short contact time between the air and the water stream [65]. As a result, the length of a humidifier may enhance its efficiency [98,99]. The upward hot-water injection [100] increased humidifier efficiency and fresh water production. As a result, increasing the humidifier's length may boost its efficiency. Numerous heat and mass transport characteristics must be determined in order to determine the humidifier's efficiency. Kreith and Boehm [101] discussed several empirical correlations and design methods. Other researchers [102–104] discovered that when the flow of sprayed water rises, the absolute outlet humidity increases as well. As a result, multi-stage humidification is necessary to optimise the generation of fresh water.

A bubble column represents the third type of tower that is characterised by the injection of a light gas or fluid into its base at the same time that it produces bubbles. The movement of fluid is extremely intricate in this column, even though its structure is quite straightforward. There have been some experimental investigations carried out on the flow of fluid through bubble columns. Computational fluid dynamics techniques are used for the majority of the work involved in conducting numerical evaluations. Schmack et al. [105] offered a new bubble column-HD module that could be scaled down to a small size and connected with a straightforward flat plate condenser for use in distant areas. The proposed desalination method using a condenser measuring 1 m^2 could produce roughly 19 L of water distillate on a daily basis and was effective at temperatures lower than the point at which water boils. In another attempt, Rajaseenivasan et al. [106] analysed a bubble column-HD unit integrated with solar collectors in three different configurations. These configurations included a conventional solar air heater, a solar air heater containing turbulators, and a dual-purpose solar collector containing turbulators. The conventional solar air heater was found to be the most efficient of the three. In the three situations that were discussed, the highest daily productivity reached was determined to be 16.32, 20.61, and 23.92 L, respectively. In the case of solar air heaters featuring turbulators, the maximum possible overall efficiency reached up to 78%. Abd-ur-Rehman et al. [107] designed and improved an innovative bubble column humidifier that could be combined with an HD module. They studied the relationship that existed between the fluctuations in air pressure and air superficial velocity and the height of the water column. Additionally, they looked into the impact that the temperature of the water had on the vapour density. According to the findings, there was a correlation between the rise in water temperature and the increase in the air's surface velocity, which led to a higher vapour density. In addition, the least amount of pressure decrease was seen at air superficial velocities that were lower, as was the case for the height of the water column. In a different attempt, Srithar et al. [108] evaluated the functionality of an HD module that had been improved by the addition of a solar collector and a bubble column humidifier. It was discovered that the performance may be improved by preheating the air supply, increasing the air mass flow, reducing the water depth, and including turbulators within the absorber plate. The design of concave-shaped turbulators produced the highest daily productivity, which amounted to 20.61 L per day. El-Agouz and Abugderah [109] demonstrated the performance of a bubble column employing air bubbles travelling through heated seawater for the HD. They discovered that the air vapour content difference was 222 g/kg of dry air at both water and air temperatures of 75 °C. Additionally, Khalil et al. [110] discovered that increasing both the water temperature and the airflow rate increases the plant's production and efficiency, whereas increasing the water height in the humidifier had a negligible impact.

Wetted-wall towers as the fourth form of humidifier were employed by [104,111]. In a wetted-wall tower, a thin film of water is created as it flows downhill within a vertical pipe, either co-currently or counter-currently. Additionally, Zamen et al. [112] used vertical polypropylene fleeces to slow the downward flow of water. On the other hand, Orfi et al. [104] used a cotton wick to cover the tower walls to aid in the evaporation process.

There are several different varieties of heat exchangers that may be used in HD settings as dehumidifiers. For instance, Müller-Holst et al. [111] made use of heat exchangers that consisted of flat plates. Others used finned-tube heat exchangers [72,109,113]. One research [114] employed a horizontal falling film-type condenser that consisted of a long tube with longitudinal fins. In contrast, another studies [115,116] used a stack of plates with copper tubes placed on them to create the same effect. In some additional investigations [117], direct contact heat exchangers were also employed as a condenser. These heat exchangers were used in conjunction with a shell-and-tube heat exchanger to give better condensation and improved heat recovery for the cycle. The humidifier exits humid air and enters the dehumidifier to be cooled. Different forms of heat exchangers are employed, including plate–fin tubes, bubble columns, and desiccants. While the humid air cools, the salty water somewhat warms up before reaching the heater. As the temperature of the air lowers, its specific humidity decreases as well. This ejects moisture carried by the humid air.

The vast majority of the publications that were evaluated [34] make reference to plate–fin tube heat exchangers (FTHE) (Figure 5), which are the form of heat exchanger that is the most cost-effective for HVAC dehumidification. This kind is often used for HD procedures as well as other kinds. While salty water travels down the tubes, air flows around them and along the plate fins in the direction of gravity. Either salty water may be pumped through all of the tubes at once using a port manifold, or alternatively, the tubes can be arranged in a multi-pass design. Equal mass-flow rates may be achieved in all tubes of an HVAC system or a process sector HVAC system by the use of a z-configuration and the modification of the flow cross-section. In a heat exchanger with many passes, the return bends directly the salty water to go through several tubes. The outcome is either a crossflow setup with a single pass or several passes.

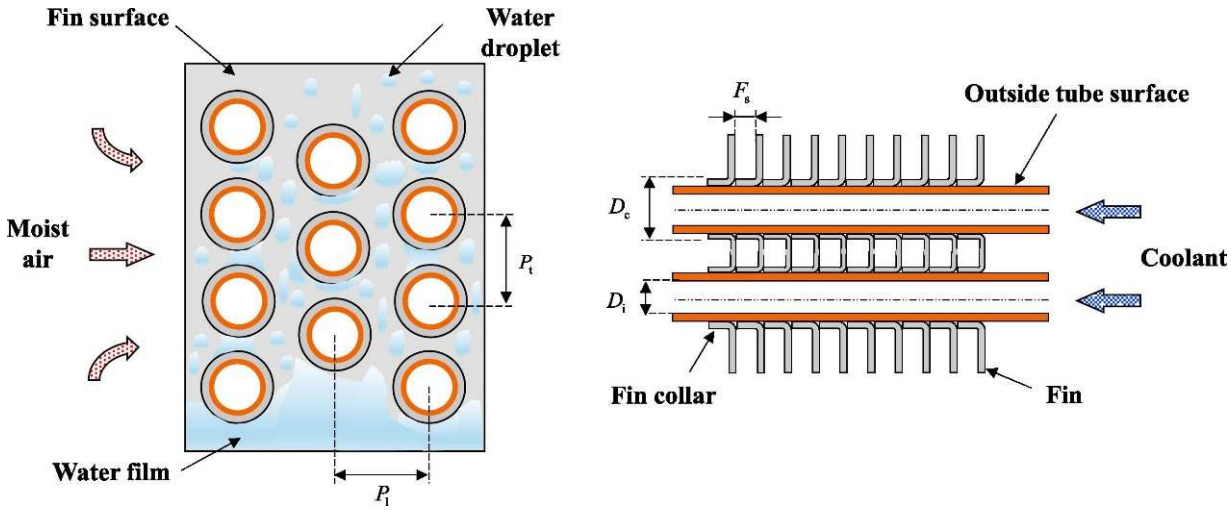


Figure 5. Schematic representation of the cross-section of a fin-and-tube heat exchanger. It also includes certain geometric features. Reproduced with permission from Guohui Zhang, BaolongWang, Xianting, Li, Wenxing Shiab, Yang Cao, Applied Thermal Engineering Journal, published by Elsevier, 2019 [118].

Plain louvre fins [119–124], plain fins [125–127], slit fins [121,125,128], and wavy fins [120,128–130] have all had their effect on thermal performance studied in order to investigate the cooling and dehumidifying capabilities of FTHEs. The influence of the number of tube rows on thermal performance has been studied [120,125,126,128], whereas the effect of the fin spacing on thermal performance has been addressed [121,122,125,131]. Additionally, FTHEs with a tiny diameter have been investigated in [119,128,132]. The papers referenced in [122,128,133] discuss the transverse tube spacing as well as the longitudinal tube space, also known as row space.

Plate–fins increase the amount of surface area that is exposed to the air, which results in improved air-side heat transfer. They might have a smooth surface, or they can be perforated or corrugated to create turbulence. Commonly used standardised geometries for air-cooling and dehumidifying heat exchangers include the following, according to [134]: outside tube diameters of 8.0, 10.0, 12.5, 16.0, 20.0, and 25.0 mm; longitudinal and transverse tube spacing ranging from 15 to 75 mm; fin spacing ranging from 1.4 to 6.4 mm; and according to [135] fin thickness ranging from 0.005 to 0.008 inches (0.127 to 0.203 mm). In modern refrigeration applications, outer tube diameters that are no more than 10 mm are often used. It is advised that seawater velocities be between 1.5 and 2.4 m/s [134] in order to minimise severe fouling and erosion.

When choosing a material for a heat exchanger, it is important to consider factors such as cost, mass, resistance to corrosion, thermal conductivity, and the ability to be machined. Plate–fin tube heat exchangers are often used in HVAC systems [134]. These heat exchangers are generally made of copper tubes with aluminium fins, which enables great thermal conductivity at a reasonable cost. The round tubes are extended so that they may press-fit into the plates that surround them.

This common Cu-Al combination, on the other hand, will create an electrochemical cell in an environment where corrosion is present, which will cause corrosion to occur. CuNi alloys, which have stronger corrosion resistance, are often used for the tubes of plate–fin tube heat exchangers used in maritime applications. Chafik [72] suggests using CuNi 90/10 for the tubes, Al or Cu for the fins, and stainless steel 304 L for the frames, casing, and collecting basin in HD dehumidifiers that are powered by salt water. After just six months of use, Houcine et al. [136] found that the materials of these dehumidifiers started to corrode. By adding a little percentage of iron, or Fe, to the tube alloy, improved corrosion resistance may be accomplished. Happ [137] suggests using CuNiFe 90/10 tubes with copper fins on the basis of more than 20 years of expertise gained at a salt water corrosion testing centre located in Helgoland, which is located in the North Sea in Germany. It is helpful to have a coating layer on the air side of the dehumidifier, as this will slow down or even prevent the corrosion of the fins and lengthen the life of the device. The design of the system must exclude any possibility of salty water droplets being transferred from the humidifier to the dehumidifier. The analyses of modified fundamental HDH desalination systems are included in Table 3.

In summary, the above presentation of published literature demonstrates a strong interest in increasing the efficiency and fresh water production of HD desalination, as well as the progress made via the use of packing-bed materials inside the humidifier. As a result, it has been determined that regardless of the system or fluid preheated, the following humidifiers have the highest utilisation: cellulose (34%), plastic packed bed (14%), fibre (12%), polyethylene balls and rings (10%), wood-based (10%), bubble column (8%), metal-based (4%), thorn trees (4%), ceramic packed bed (2%), and aspen pads (2%). Similar to dehumidifiers, finned tube heat exchangers (FTHE) (56%), shell and tube heat exchangers (STHE) (38%), plate heat exchangers (4%), and bubble column heat exchangers (2%) are used [148].

3.3. HD System Classification Based on Cycle Configurations

HD systems function below the boiling point, providing an operational advantage over other technologies, since they may be powered by thermal energy supplied at a temperature of 30 °C. Additionally, unlike MSF and MED, this system may be linked with a thermosiphon system because of its ability to function at low flow rates and low temperatures, obviating the need for pumps to assure the circulation of hot fluid. It is easy to use and maintain, requiring no specialist technical expertise or automation. Its mobility is proportional to the system's size, taking into account that the available prototypes is suited for small-scale applications [149,150].

Regarding its environmental effect, it is worth noting that HD is a new technology that has emerged as a means of mitigating the environmental harm caused by traditional

technologies. HD consumes less thermal energy than MSF and MED [149], owing to the system's current capacity, which concentrates on small-scale systems [151]. Additionally, it generates less brine [149] and is a simple technology that can be constructed, maintained, and operated using local resources in urban and remote places [152].

Table 3. Experimental HD and humidifier/dehumidifier types.

Year	Humidifier Type	Dehumidifier Type	Major Conclusions	Ref.
2000	Packed bed	Finned-tube heat exchanger	• When solar irradiation was 700 W/m^2 during continuous systematic operation for 8 h, the system's fresh water productivity was 6.2 kg/m^2/d.	[138]
2002	Packed bed	Finned-tube type condenser	• The effects of some operational factors, such as flow rates, temperatures of feed water, air, and cooling water, were carefully researched in order to maximise system performance.	[139]
2015	Bubble column	Shell and tube heat exchanger	• The maximum fresh water production rate was 21 L/d.	[110]
2008	Packed bed	Finned-tube heat exchanger	• The fresh water output was 2.5 L/h.	[90]
2014	Packed bed	Shell and long tubes of copper with fins	• The greatest water productivity was 41.6 L/h, which was considerably affected by the temperature of cycled hot seawater.	[140]
2013	Packed bed	Coil tube condenser	• Four different hybrid HD system designs were analysed, all of which mixed flash evaporation with or without an air heater. • The inlet cooling temperature and cooling water mass flow rates influenced the peak productivity of 11.4 kg/m^2/d.	[141]
2014	Packed bed	Shell and Tube heat exchanger	• The largest amount of fresh water produced was 41.8 L/d. • The water mass flow rate had a greater impact on humidifier efficiency than the air mass flow rate.	[142]
2016	Bubble column	Shell and Tube heat exchanger	• The production of fresh water was 6275 kg/m^2/day. The authors analysed the relationship between the initial water level in the humidifier and the air flow rate.	[143]
2014	Packed bed	Finned-tube heat exchanger	• Both the air-heated and water-heated HD cycles demonstrated comparable GOR. • The air-heated cycle requires a larger humidifier and a smaller dehumidifier due to its greater air pumping capacity. • The water-heated cycle required a more powerful water pump, a smaller humidifier, and a larger dehumidifier.	[74]
2015	Packed bed	Coiled condenser	• This system's water output varied between 17.7 to 52 kg/h. • Two designs of parabolic trough solar air collector integration with HD systems were examined.	[144]
2016	Packed bed	Surface heat exchanger	• The water production rate of this system was 70.8 kg/h. • Analysis of entropy and energy balance was conducted.	[145]
2018	Packed bed	Packed bed	• The cost of producing 1 kg of water could rise from USD 6.20 to USD 13.41 if the dry air flow rate were increased from 0.1 kg/s to 0.5 kg/s.	[146]
2017	Direct contact packed bed	Indirect contact surfaces heat exchanger	The scientists compared an energy and water cogeneration system to both ORC and HD systems, with the water production rate at 19.53 kg/h.	[147]

There are three primary categories of HD systems. One categorisation is based on the source of energy, which may be solar, heating, geothermal, or hybrid. This classification emphasises a positive feature of the HD concept: the prospect of obtaining water with less energy, most notably industrial waste heat or renewable energy sources such as solar or biomass. The second categorisation is determined by the configuration of the cycle (Figure 6). A closed-water open-air (CWOA) cycle is one in which ambient air is drawn into the humidifier, heated, and humidified, and then transported to the dehumidifier, where it is partly dehumidified and drained in an open circuit to create a closed circuit. Air circulates in a closed circuit between the humidifier and the dehumidifier. This procedure is repeated until the brine reaches the required level of recovery. Mechanical or natural convection fans may circulate the air in these systems, and a pump is often used to circulate the feed water. It is vital to understand the technical advantages of each of these circuits and to choose the design that optimises efficiency while minimising water production expenses. The third kind of HD system is classified according to the type of heating used

(water or air). The temperature of the fluid being heated has a considerable effect on the system's performance [153].

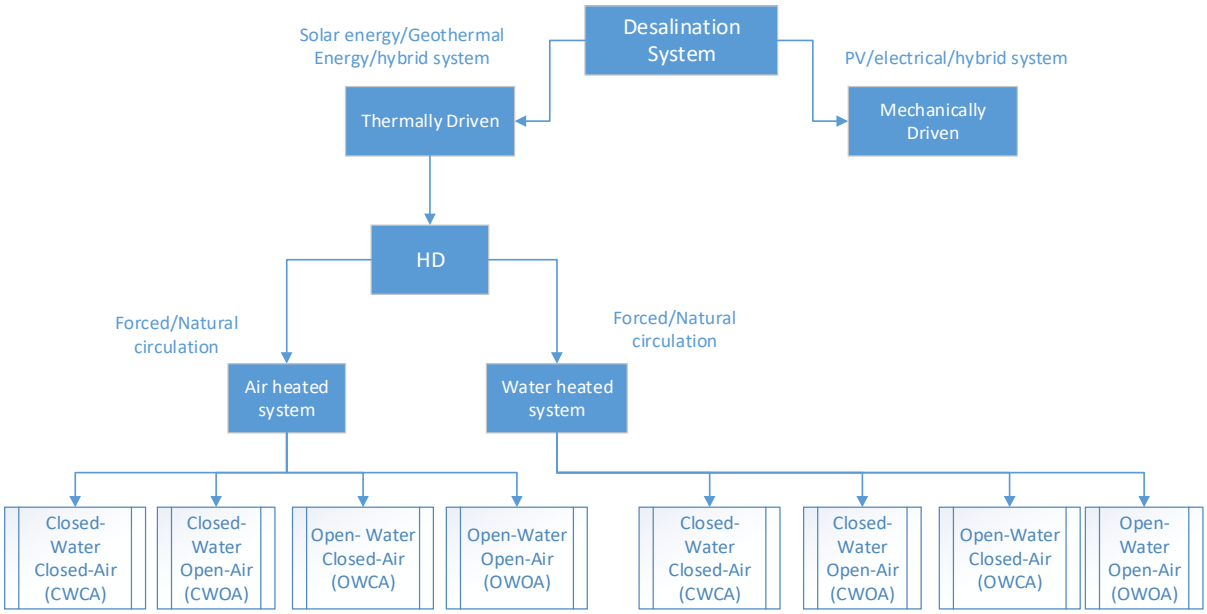


Figure 6. HD system classification based on cycle configurations.

The HD has attracted particular attention from thermal-driven desalination cycles because of its simplicity, operational stability, cheap cost, low-grade thermally driven, and integration flexibility with other systems such as heat pumps, adsorption, and absorption cycles [154–156]. Therefore, extensive research has been undertaken to optimise the HD cycle's performance via different configurations and integrations (i.e., fresh water productivity and efficiency). In terms of mixing HD with another cycle, He et al. [147] generated both electricity and fresh water by combining an organic Rankine cycle with an air-heated HD cycle. At its peak, the combined system generated 19.53 kg/h of fresh water at a GOR of 2.82. Fouda et al. [157] evaluated the transient performance of single-stage, double-stage, and modified double-stage HDH systems that were driven by solar energy. The improved two-stage HD cycle generated 350 kg/d of fresh water with a GOR of 1.63.

By combining the HD cycle with a silica gel adsorption cooling cycle, Qasem and Zubair [158] showed that the HD cycle may be used in conjunction with a silica gel adsorption cooling cycle. For USD 6.4/m^3, this system could produce 20–30 kg/h and may provide GOR levels that are higher than 7.5. Elbassoussi et al. [156] evaluated the effectiveness of combining water-heated HD with an adsorption cycle to provide fresh water and cooling. Fresh water was generated for USD 11.5/m^3 with a GOR of 2.5. Ali et al. [154] established a connection between HD, two ejectors, and the desalination cycle through adsorption. Theoretical studies indicated that the system could produce 98.41 m^3/ton of silica gel daily at a GOR of 2.75. Rostamzadeh et al. [159] studied and optimised an HD system driven by an absorption–compression heat pump. With a GOR of 9, the hybrid cycle produced fresh water at a rate of 2329 kg/h.

The configuration of the water and air routes in the HD desalination cycle significantly affects its performance [160]. Ettouney [161] conducted research in this regard by examining the performance of different HD cycle topologies. For each arrangement, different governing equations were devised. According to studies, configurations must be tuned for maximum efficiency and the lowest possible water cost. Closed-air and closed-water HD cycles function equally well, according to Narayan et al. [34]. Sharqawy et al. [74] assessed the performance of a single humidifier equipped with a water- and air-heated HD cycle. The two cycles were compared in detail. It was found that increasing GOR might be accomplished by employing a more efficient humidifier and dehumidifier.

Zubair et al. [162] investigated an open-water open-air (OWOA) and a modified closed-water open-air (CWOA) HD desalination cycle using experimental and computational methods. The modified cycle outperforms the original cycle by a factor of 10, according to some sources. Garg et al. [163] developed a thorough heat and mass transport model for an open-water closed-air (OWCA) and water-heated desalination cycle using HD. The humidifier and dehumidifier were sized optimally to provide the required thermal cycle performance, as measured by GOR and recovery ratio. With parametric analysis, it was discovered that there was always a maximum GOR value and that the thermal performance of the system was more dependent on the dehumidifier's performance than on the humidifier's performance. Wu et al. [164] explored a single-effect OWCA-WH heated HD cycle that was driven by solar energy. The findings indicate that raising the operational temperature (i.e., the driving temperature) decreases the amount of effort needed. Muthusamy and Sridhar [165] presented an enhanced HD cycle that would boost fresh water production while using less energy. A 40% decrease in input power was obtained when compared to the traditional HD cycle. Müller-Holst [166] presented a multi-effect HD cycle for system performance optimisation. The OWCA water-heated system with multiple effects was claimed to have the maximum energy efficiency and the lowest water cost of around USD 3–7/m^3 [166]. Dave et al. [167] proposed and investigated a direct absorption solar humidifier in conjunction with the OWCA HD desalination system, characterising the effects of seawater and air flow rates on the HD desalination system's performance in order to determine the optimal operating state for solar thermal conditions. The suggested system outperformed the traditional system by 18.4%, and the anticipated cost of water production was between 0.007 and 0.035 USD/L. Additional past research is summarised in Table 4 [168].

Table 4. Previous studies on HD cycles.

Cycle Type	Yield	GOR	Cost	Remarks	Ref.
OWCA-WH OWCA-AH	10 L/h 10 L/h	1.93 2.19	– –	• The WH cycle was powered by a solar collector. • The optimal MR for the WH cycle was 2.04 and for the AH cycle was 0.66. • The surface area of the dehumidifiers was 11.7 m^2 for WH and 47.1 m^2 for AH, respectively. • GOR value rose proportionately to humidifier efficacy, at the expense of system size and capital cost.	[74]
OWCA-WH	–	3.8	–	• Theoretically, a two-stage HD system was investigated. • By distributing the heat evenly, the system's efficiency was increased. • Through thermodynamic balancing, entropy generation was minimised, and energy efficiency was maximised.	[169]
OWOA-WH	104 kg/m^2	1.2–1.58	3 USD/m^3	• Geothermal energy was used to supply more fresh water than solar energy since solar energy is not available 24 h a day. • Increasing the temperature of geothermal water resulted in the production of more fresh water. • Increasing the geothermal mass flow rate resulted in a reduction in performance.	[170]
OWOA-AH	6.1 kg/h	1.0	13.3 USD/m^3	• Biomass fuel was used to power the cycle. • We utilised a bubble column humidifier. • When compared to solar energy, employing biomass fuel reduces the cost of water. The solar energy cycle, on the other hand, has a greater GOR.	[171]
OWCA-WH	0.182 m^3/h	2.65	2.5 USD/m^3	• A three-stage cycle powered by an electric heater was investigated. • The isothermal heating mode increased productivity.	[172]
OWCA-WH	84.60 kg/h	1.44	6.2–13.41 USD/kg	• The cycle was fuelled by furnace exhaust gas. • A packed-bed dehumidifier was used to mitigate salt water corrosion. • When spraying salt water at a lower temperature and increasing the ambient temperature, the unit cost of water fell.	[146]
OWCA-W/AH	2–2.2 kg/h	1.28–3.3	2–41 USD/m^3	• Water heaters with evacuated tubes and air heaters with flat plates are utilised. • At sub-atmospheric pressure, the humidifier operated. • When the humidifier pressure was reduced from 0.9 to 0.1 bar, a 50% increase in fresh water output occurred.	[173]
OWCA-WH	99.05 kg/h	1.51	20 USD/m^3	• The cycle was powered by waste heat. • As the airflow rate and seawater temperature grew, the productivity improved as well. • The cycle was highly dependent on the dehumidifier's balancing settings.	[174]

Table 4. *Cont.*

Cycle Type	Yield	GOR	Cost	Remarks	Ref.
CWOA-WH	~21 kg/d	0.8	30 USD/m^3	• A flat plate collector propelled the cycle. • The dehumidifier was a shell and tube heat exchanger, whereas the humidifier was a Maisotsenko cycle-based air saturator, which saved 14% on the cost. • Environmental studies revealed a carbon footprint reduction of around 7%.	[175]
OWCA-A/WH	1.07 kg/h·m^2	3.43	4.1 USD/m^3	• The dehumidifier used a two-pipe heat exchanger; the humidifier utilised a packed-bed direct water spray. • By lowering the humidifier pressure, the cycle performed well. • Optimal operating conditions were determined using the response surface approach.	[176]
CWCA-WH	0.14 kg/h	12.24	8.59 USD/m^3	• A solar collector powered the cycle, and the humidifier and dehumidifier were evaporator condensers. • It was suggested to recover internal heat using mechanical vapour compression. • Improved system performance is achieved by increasing spraying seawater temperatures at 70 °C, with the maximum specific energy consumption (SEC) of 18.35 kg/kWh.	[177]
OWOA-WH	4.9 kg/h	0.65	–	• A gas burner powered the cycle. • The recirculation of brine was investigated. • The heat recovery was greatly improved in the cycle under investigation.	[80]
OWOA-WH	96.45 kg/h	1.7	0.00804 USD/kg	• Based on the first and second laws of thermodynamics, the optimum desalination performance is 0.38 kWh/kg for SEC. Due to the relevant negative entropy generation rates, situations with a mass flow rate ratio greater than 4.4 are not accessible.	[178]
OWOA-WH	22.3 kg/h	3.0	–	• Leverages the Maisotsenko cycle's key water evaporation process (M-cycle). Assessed the energetic and exergetic performance under a variety of operating circumstances. Recovery ratio (RR) of 0.223, SEC of 0.23 kWh/kg, and a 43.21% exergy efficiency	[179]
CWOA-WH	2.45 kg/h	0.35–0.55	0.047 USD/L	• Without heat recovery in the dehumidifier and electrical heater.	[180]

As previously indicated, the HD performance is mostly controlled by the arrangement of the water and air flow circuits. The presented investigations centred on a specific kind of HD system to be studied: thermodynamically balanced or hybrid systems. In addition, the research evaluated single humidifier air-heated vs. water-heated HD systems. There has not yet been a complete comparison and evaluation of alternative HD system configurations for single, double, and triple humidifier (water-heated and air-heated) HD systems. In the water-heated HD cycle, a higher amount of water is heated and sprayed into the humidifier. More hot water sprays from the humidifier result in higher water vapour and, therefore, more fresh water production. However, this large output does not suggest that the system GOR is high because of the considerable energy spent to increase the water temperature. As a consequence, the power consumption in the air-heated HD cycle is reduced, which may result in a higher GOR value.

4. Technological Advancements in Solar HD Systems

The numerous ways for improving the performance of solar HD systems are recognised and classified according to the working fluids of water and air. Selective coating absorber tubes, built-in channels, the use of risers in absorber tubes, the use of evacuated absorbers, the use of the thermosiphon effect, and the use of numerous heaters are all examples advances made in systems that use solar water heaters to heat HTF, water. In the case of systems that use air as the heat transfer fluid, the use of solar air heaters connected in series or parallel, the use of biomass or geothermal for preheating the air, the addition of an external reflector, and the use of baffles are some of the techniques used to improve the performance of solar air heaters. Enhancing the performance of solar water or air heaters would raise the temperature of HTF and the performance of solar HD systems, respectively, hence increasing fresh water output. All improvement techniques described in the literature are classified into broad categories according to the type of solar collector used, such as solar stills (SS), flat plate collectors (FPC), evacuated tube collectors (ETC), Fresnel lens collectors (FLC), and parabolic trough collectors (PTC) systems, for preheating the HTF (water and/or air), as illustrated in Figure 7.

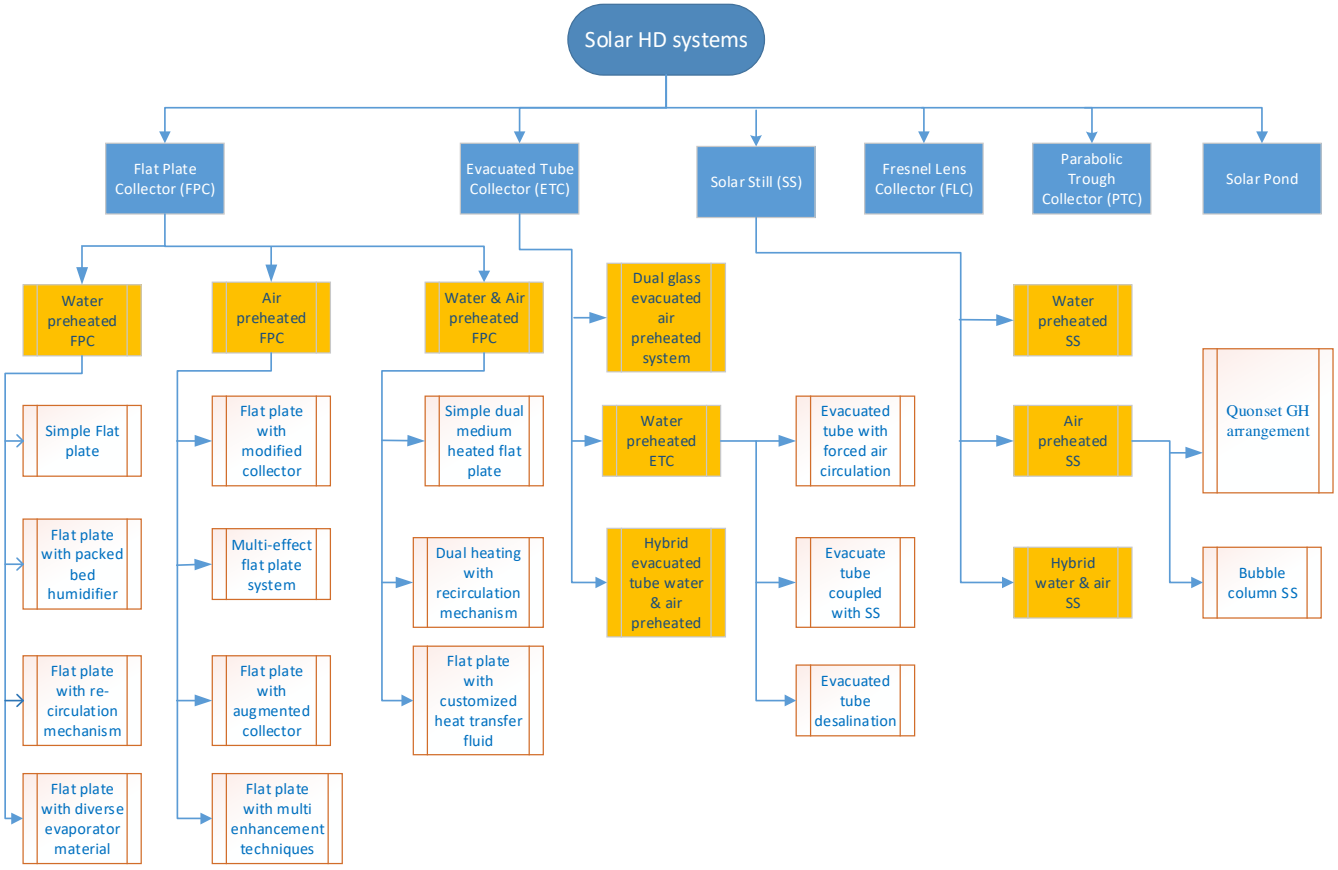


Figure 7. Classification of solar HD systems.

4.1. Flat Plate Collector (FPC)

FPC systems are a well-established technology for solar-powered hot water generation. These are also utilised in HD systems, where the operating water and/or air medium are warmed prior to entering the humidifier chamber. The FPC is a metallic box that is insulated on all sides except the top, which is coated with a glass layer. The water is conveyed in metallic absorber sheets that have been selectively coated, in conjunction with channels or riser tubes that are often painted black. The absorber absorbs the available solar energy and transfers the heat to the water, which serves as an HTF. Appropriate implementation of the stated improvement techniques enhances the effectiveness of the FPC system in heating the HTF [181–183]. The following section discusses the major advancements in HD systems driven by FPCs. Because the operational HTF utilises both water and air, the advancement approaches are classified into three major categories: water-preheated FPC systems, air-preheated FPC systems, and water and air-preheated FPC systems.

4.1.1. Water Preheated Flat Plate Collector Systems

The majority of HD systems use water as the working fluid because waste or salty water can be readily processed to produce fresh water. To increase the yield and efficiency of the HD process, modifications to the FPC HD system include the use of a packed bed humidifier, the implementation of a brine water recirculation mechanism, and the use of a variety of evaporator materials.

Simple Flat Plate Collector System

Previously, basic flat plate systems were used to investigate the influence of HD on yield improvement. Initially, the performance of a basic solar desalination unit using the multi-effect HD (MEHD) technology was examined [184]. An FPC was used to generate hot water, and the air was circulated using a forced circulation approach with a closed-

air/open-water cycle. It was discovered that by reducing the water flow rates, the system's efficiency increased, producing daily productivity of around 12 L/m^2/d. The scientists determined that the productivity of the HD system when combined with FPC is three times that of single basin solar still.

In a related study, A-hallaj et al. [94] investigated the performance of the MEHD desalination unit, which consists of two vertical rectangular ducts, for both indoor and outdoor operation. The experimental findings indicated that employing forced air circulation at temperatures above around 70 °C did not result in a substantial improvement. Additionally, it was discovered that the unit's water flow rate and mass had a significant influence on the production of fresh water during outdoor operations and that the productivity of fresh water from the saline warm water was greater than that of single basin solar stills.

Flat Plate Collector with Packed Bed Humidifier

Solar desalination of salt water through the HD cycle was tried by employing honeycomb packing material in the humidifier [138]. The honeycomb material was composed of porous and durable paper with a 45 and 60 °C wave line form for wetting, and the humidifier was incorporated into the system. The scientists found that the system operates effectively between 70 and 90 °C and can be powered by low-grade heat sources such as waste heat, coal, oil, and gas combustion. They also evaluated the impacts of humidifier input water mass flow rate, temperature, and fan rotation speed on the thermal efficiency of the system and water production, respectively.

MEHD solar desalination system was designed, simulated, and tested experimentally [185]. The utilisation of locally accessible packed bed materials and the functioning of the system as a self-contained unit without the need for a normal power source was the primary design and construction consideration for the complete system. The whole setup included a self-contained heat collecting device (solar collector and storage tank) and a distillation unit (distillation chamber). The findings show that when seawater is heated to around 55 °C by natural convection in a packed bed MEHD solar desalination system, a significant amount of fresh water may be generated.

Flat Plate Collector with Re-Circulation Mechanism

The impact of humidifier unit brine water recirculation has been investigated by Dayem and Fatouh [99] conducted a comparative experimental and computational examination of solar HD systems that used preheating to flash the saline water into the evaporator. Three systems with varying designs were investigated (Figure 8) to determine the most efficient one. The scientists determined from experimental and computational data that the solar open system with natural circulation (system III) was the most efficient and least expensive of the three systems.

Similarly, a unique solar diffusion-driven HD method was investigated for decentralised water production under dynamic operating circumstances [186]. After a thorough analytical and experimental evaluation of the system, the authors determined that it may produce up to 6.3 L/m^2/d of distilled water with a low average specific electric energy consumption of around 3.6 kWh/m^3 and minimal maintenance cost.

Flat Plate Collector with Diverse Evaporator Material

To increase the rate of heat transfer with a larger surface area contact in the humidifier unit (evaporator), efforts were made to evaluate the performance of HD systems with various evaporator materials [187]. Theoretical thermal performance research and practical validation of a solar energy-driven water HD unit were conducted. The evaporation tower was clad with naturally occurring thorn trees or palm tree leaves, while the condensation unit was constructed entirely of polypropylene condensation plates. The author determined that when the mass flow rate at the evaporation tower's entrance rose, the GOR increased as well. The GOR was determined to be greatest at a mass flow rate of 0.4 kg/s.

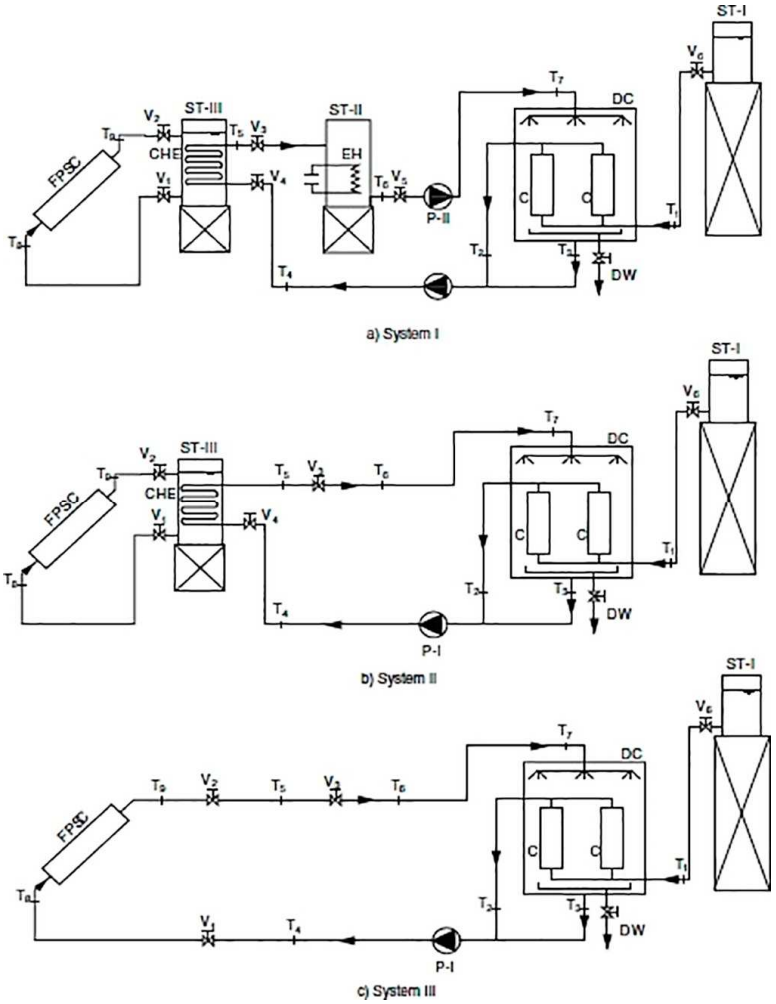


Figure 8. A study of solar saline water desalination systems. Reproduced with permission from Adel M. Abdel Dayem, M. Fatouh, Desalination Journal, published by Elsevier, 2009 [99].

Numerous novel system optimisation strategies have been developed to enhance the performance of solar HD systems using a variety of evaporator materials. Experiments were conducted to determine the operational and performance parameters of a solar HD system fitted with innovative packed porous plastic balls and finned heat exchangers [188]. As seen in Figure 9, the system is comprised of a solar loop for heating the salt water and two desalination loops with two heat exchangers (HEs). The highest output of about 63.6 kg/h was attained by increasing the water flow rate from 550 kg/h to 1000 kg/h. Additionally, experimental and numerical research was conducted on an expanded version of the aforesaid system with three desalination loops and three HE (Wu et al., 2016). In comparison to the previous system, the latter possessed the advantages of a compact structure, stable operation, ease of control, reduced space utilisation, residual heat recycling of saline water, and operation at atmospheric pressure within a very wide temperature range of approximately 60–95 °C. The results indicated that the upgraded version resulted in a yield increase of about 182.47 kg/h.

In another study by Zamenoop et al. [112], it was found that the two-stage solar HD technique is the most suitable alternative for increasing productivity and daily fresh water production while using less specific energy and incurring lower capital costs. The scientists discovered that when a two-stage solar HD pilot plant with an 80 m^2 solar collector area was compared to a single-stage unit, productivity rose by 20%.

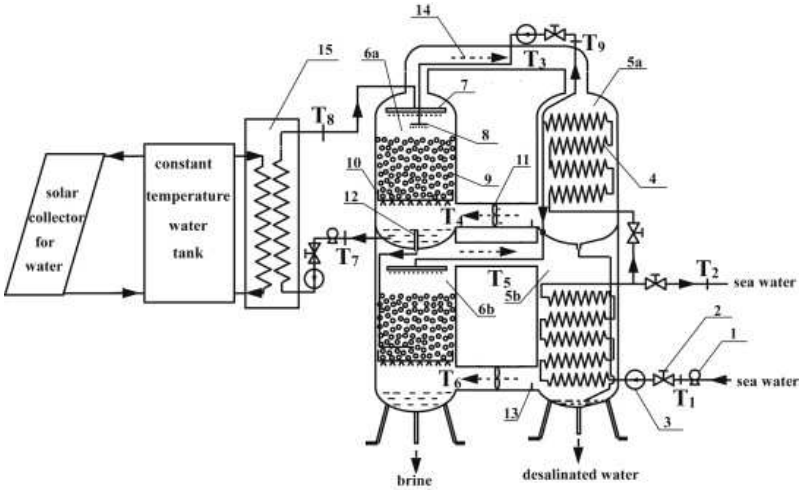


Figure 9. Schematic of two desalination and heat exchanger solar HD desalination systems. Reproduced with permission from Zehui Chang, Hongfei Zheng, Yingjun Yang, Yuehong Su, Zhanchun Duana, Renewable Energy Journal, published by Elsevier, 2014 [188].

Single-Stage HD System

Along with multi-stage solar HD systems [112,188,189], efforts have been made to improve the performance of single-stage systems. By way of example, an experimental investigation on the effect of water depth and condenser connection in a single-stage solar HD system was conducted by Ladouy and Khabbazi [190]. A laboratory-scale seawater desalination system consisting of a plate condenser cooled by salt water and a plastic envelope chilled by ambient air was tested, as seen in Figure 10. The scientists demonstrated the system's practicality for residential fresh water use by producing 11.5 L/d using solar energy and less electrical energy. Recently, an effort was made to conduct theoretical and practical research on a simple solar-based HD salt water desalination plant [191]. The system used an OWCA cycle, which included water evaporation and steam condensation from humid air. The authors employed a basic copper tube coil as a condenser and determined that the theoretical model's rate of distilled water production was in excellent accord with the practical data.

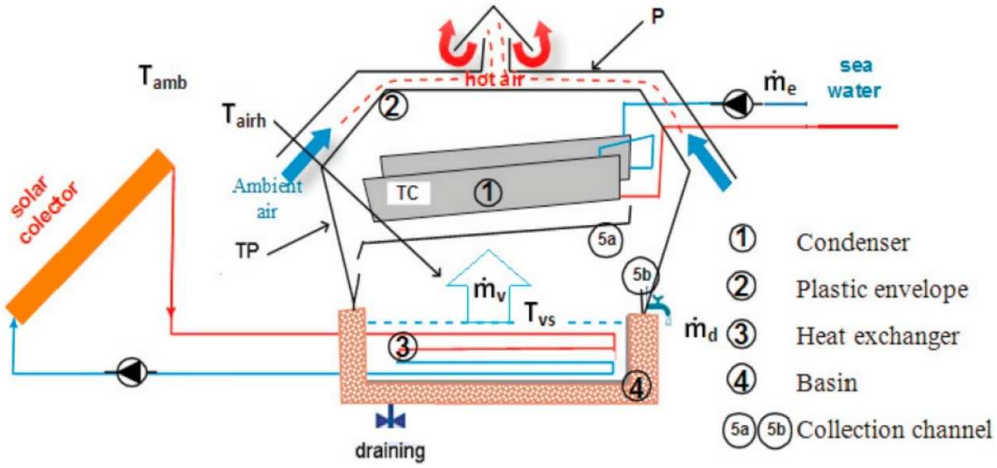


Figure 10. Schematics of a laboratory-size single-stage solar HD system [190].

4.1.2. Air-Preheated Flat Plate Collector Systems

A solar air heater is a module that utilises solar radiation to raise the temperature of HTF or air to an extremely high level [192]. Air-heated solar HD systems have the advantage of utilising locally and economically available materials for solar collectors,

pumps, humidifiers, and other system components, as the maximum heat carried by air is typically less than 80 °C [193]. Additionally, corrosion, scaling, and clogging issues may be prevented by using a solar air collecting system. As a result of these benefits, HD systems driven by solar air heaters are also often utilised to generate fresh water. As with water-heated HD systems, several technical advancements have been made in air-heated systems as well.

Modified Flat Plate Collector Structure

Modifications to the FPCs used to pre-heat the air medium were tried in order to achieve a higher HTF temperature at the collector outlet [194] creating a novel HD system for desalinating seawater that utilises low-cost solar air heaters and cost-effective polymers for construction. The system components and process optimisation were carried out first, followed by progressive heating and humidification of air utilising the newly created HD configuration comprised of fifteen parallel mounted polycarbonate multiple web FPCs. According to the presented findings, a four-stage pilot plant with a four-fold web plate collector can produce around 400 L/d of fresh water. Additionally, the study was expanded to include the design and optimisation of a solar desalination plant using the multi-stage HD approach [113]. The findings of the newly built desalination process and pilot plant were described in-depth, along with additional system parameter optimisation and economic analysis, utilising the TRNSYS simulation programme. An improved design for a small community desalination plant capable of producing 10 m^3/d of fresh water was given based on newly derived forecasts and calculations.

Multi-Effect Flat Plate Collector System

Based on the work of [103,194], the performance of a MEHD system employing FPCs to heat the air and a heat recovery system to heat the seawater through heat exchangers was studied. On the basis of an inquiry conducted in a one-stage experimental setup, an analysis of a system consisting of eight steps of air heating–humidification followed by final dehumidification to create fresh water was undertaken. The results indicated that the air humidity after the ninth stage of the heating–humidification process was around 140 g/kg of water of dry air, which was adequate for the final dehumidification process to produce fresh water. Based on the findings of the preceding research [103,194], the study was expanded to simulate and optimise an outdoor prototype desalination plant in Tunisia using the MEHD approach [136]. A one-stage heating humidification–dehumidification process was used to evaluate the procedure's performance using a solar four-fold web plate collector (FFWP) for heat recovery and condensation. The results indicated that the pilot plant produced about 355 kg/d of fresh water on an average basis throughout August 2003.

Augmented Flat Plate Collector Design

Improved solar air heater design may contribute significantly to the performance of air heated solar HD systems. Numerous strategies have been used by researchers to enhance the design of solar air heaters. Theoretical and practical analysis of the HD process was conducted utilising a double-pass solar air heater [90]. The operating concept was a closed-water open-air cycle. The effect of different operating circumstances and the use of the double-pass solar air heater on the desalination unit's performance was investigated. The results indicated that increasing the intake water temperature, feed water mass flow rate, and cooling water mass flow rate boosted the HD system's productivity. Additionally, the scientists discovered that when the system was run without a solar double-pass collector, the total production was reduced by around 15%.

In another study, Summers et al. [130] investigated the experimental and mathematical aspects of a solar air heater combined with phase change material (PCM) for use in the HD process. The redesigned solar air heater unit was constructed using PCM with folded aluminium mesh immediately underneath the absorber plate (Figure 11) to ensure that the HD system receives consistent air temperature and heat input throughout both day and

night hours. The scientists found that by modifying the solar air heater, they were able to raise the air temperature near the melting point of the PCM utilised and thus contribute effectively to the performance enhancement of the solar HD system.

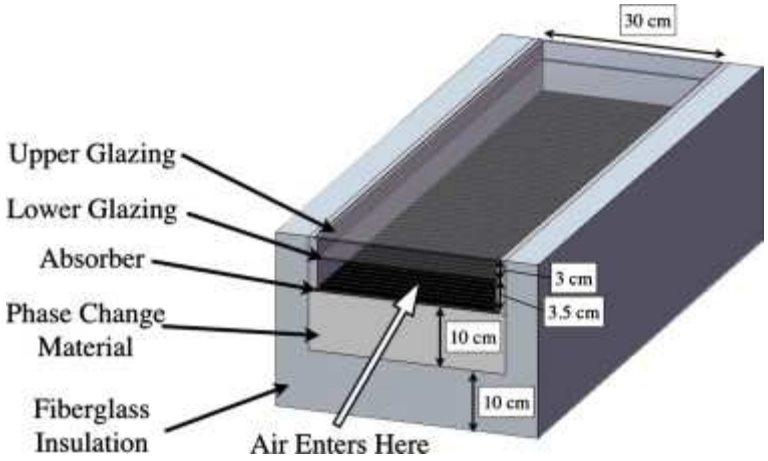


Figure 11. Shows the schematics and how to set up the solar air heater with PCM, Reproduced with permission from Edward K. Summers, Mohammed A. Antarb, John H. Lienhard V., Solar Energy Journal, published by Elsevier, 2012 [130].

Flat Plate Collector with Multi Enhancement Techniques

Additionally, other improvement techniques have been used or combined to further increase the performance of the solar flat plate air heater. Elminshawy et al. [195] conducted an experimental and analytical investigation on yield enhancement in an HD system by using a unique solar FPC water bath comprised of water heaters and an external reflector. The unique solar water bath functioned as a humidification unit, heating and humidifying the incoming ambient air as it passed over the heated water surface. The influence of water heaters and exterior reflectors on the performance and average daily production of solar flat plate humidification units was investigated in depth. The performance analysis revealed a significant improvement in system productivity when a revolutionary solar flat plate humidification device equipped with water heaters and an exterior reflector was used. The work was expanded by [196], who employed a solar air heater with a staggered arrangement of tiny cylindrical pipes to enhance the turbulence of the incoming air, hence increasing the desalination unit's overall performance. Two sets of experiments were conducted: set I used no solar air heater and two electric water heaters; set II used one electric water heater and one solar air heater to pre-heat the ambient air in the FPC water bath. The results indicated that the installation of a staggered solar air heater raised the entrance temperature of the air in the humidification unit by about 3–4 °C, hence, enhancing the desalination system's productivity. In another experiment using the same experimental design, hybrid energy (solar + geothermal) was employed to pre-heat the water and then the HTF, or solar collector air [170]. The solar air heater was unique in that it was connected to a geothermal tank with a consistent water temperature that heated the water in the collector through a heat exchanger. The combined influence of solar and geothermal energy significantly boosted the productivity of the system in which geothermal energy contribution surpassed solar energy contribution.

4.1.3. Water and Air Preheated Flat Plate Collector Systems

As previously stated, either water or air is warmed to increase the efficiency and performance of HD systems. This section will examine advancements in solar HD systems that use FPC to pre-heat both the water and air mediums to increase the system's output. It is worth noting that in the majority of solar HD systems that heat both water and air, FPC is the principal technology utilised to heat both mediums.

Simple Dual-Medium Heated Flat Plate Collector System

The authors conducted an experimental and theoretical analysis of a solar HD water desalination system with water and air being heated concurrently using water and air solar FPCs [104]. The system began by preheating salt water in the condenser chamber and then continued heating it in the solar collector. Additionally, it was passed through the evaporative chamber, where it was humidified by contact with hot air. The authors designed and built the system components using mathematical modelling to optimise the system's performance. The scientists observed that there is an optimal mass flow rate ratio between the air and water mediums for maximal fresh water production in any dual medium warmed system, and that performance degrades beyond that point.

Dual Heating System with Recirculation Mechanism

Zhani and Ben Bacha [197] investigated a novel solar HD prototype using solar water and air FPCs. Except for the installation of a solar air collector, the desalination system was constructed identically to that described in [187]. At the distillation unit's outlet, the dehumidified air and brine water were recirculated to corresponding solar flat plate air and water collectors for preheating. The inclusion of a solar air heater and recirculation mechanism boosted fresh water output (maximum—21.75 kg/d), and it was discovered that system performance was heavily dependent on the sun radiation component.

Additionally, modelling and experimental validation of the solar air and water FPCs employed in the aforementioned desalination system were performed [198]. Dynamic mathematical models were utilised to numerically simulate the behaviour of the system's air and water solar collectors in Sfax, Tunisia. Additionally, experimental validation was performed by measuring the temperature at different spots on the board and solar water collector using Pt100 sensors. The scientists determined that the performance of solar water and air collectors that contribute to the total system output is location-dependent and highly dependent on available solar radiation. In another endeavour, the study was expanded to explore the dynamic operation of all the components in the aforementioned desalination system, as well as to carry out a cost-benefit analysis of the system [199]. The author concluded through numerical prediction and experimental validation that the use of air and water recirculation mechanism in conjunction with an energy storage device enables the HD system to function 24 h a day with maximum output, even on overcast days.

Flat Plate Collector with Customised Heat Transfer Fluid

Apart from examining the collector design and operating medium circulation mechanism, researchers have tried to investigate the performance of HD systems employing customised HTF. The use of a nanofluid (Al_2O_3 H_2O) solar flat plate water heater in a single-stage HD system with solar water and air collectors has been tried [142]. The effect of several factors on the water productivity of the hybrid HD system was thoroughly investigated, including solar radiation, feed water and cooling water mass flow rates, intake cooling water temperature, and volume per cent nanoparticles. The experimental findings indicated that the system's maximum productivity with a nanofluid solar water collector was around 41.8 kg/d and that the solar water heater efficiency was substantially dependent on the volume percentage of nanoparticles.

Another attempt was made to boost desalination output by carrying out a two-stage HD process study [200]. Solar FPC was used to indirectly heat the saline water through a glycol-water combination, and it was also utilised to heat the humidifiers and air preheaters, which served as a HE in heating the air medium. Experiments and simulations demonstrated that using cold water in the dehumidifier unit increased the system's desalination output. In a separate endeavour, the inquiry was expanded by the development of a two-stage HD prototype plant for combined air conditioning and fresh water production with a solar FPC area of 16 m^2 [201]. We examined the influence of system performance characteristics such as the cooling effect, fresh water production, and energy usage factor (EUF). The findings of the experiments indicate that combined two-stage desalination and

the cooling plant have a greater EUF than standalone single-stage plants with a maximum fresh water output rate of around 2.5 L/h. Additional experimental research on FPC is presented in Table 5.

Table 5. A quick look at the research on HD plants with flat plate collectors (FPC).

Year	Brief Title	Major Conclusions	Refs.
2005	Efficiency assessment of a new-design air solar plate collector used in HD	Experimental testing was performed on a brand-new air heater design. In addition to irradiance and wind speed, researchers looked at the effects of the environment's temperature.	[202]
2009	Experimental validation of a solar HD unit	For a previously modelled device, researchers ran validation tests to make sure it worked properly. Optimizing the gadget resulted in a 2% increase in efficiency, according to the findings.	[203]
2010	Experimental testing of a solar HD plant	In the municipality of Geroskipou, Cyprus, a solar thermal HD was tried. The problems encountered throughout the installation and testing process were analysed.	[204]
2013	Effect of fixed bed characteristics on the performance of pulsed water flow HD	In Saudi Arabia's Jeddah, a pulsing water flow HD was put through its paces. Increased racing ring diameters were used in conjunction with decreased bed height to improve the overall performance. There was a variation in output capacity, from 10.4 L/d to 15.2 L/d	[205]
2014	Experimental study of a novel solar humidifier for HD	The addition of an external reflector to the bottom side of a humidifier resulted in a 3% increase in average air humidity.	[206]
2016	Investigating a multi-effect isothermal heat with tandem solar desalination based on HD	The device's performance was tested at different feeding water mass flow rates and heating temperatures. It was discovered that 508.8 L/d of fresh water could be created from an 8000 L/d salty water flow.	[189]
2017	Investigation of a solar HD incorporating a rotating surface	The movement of a revolving black surface within a desalination module was studied. Increases in cooling water and air volumetric flow rates, as well as a reduction in surface rotation velocity, were shown to increase productivity.	[207]
2017	Experimental investigation of a solar-powered HD unit	An HD module is being tested at Bizerte, Tunisia, for both forced and free convection modes of operation. The air velocity of 3.34 m/s was determined to be the optimal speed for maximum production.	[208]
2017	Investigation of different air heating methods	Pulse heating has been used in a triangle form close to the evaporation surface in the HD process. Compared to traditional air heating systems, the results of indoor shaded tests show an increase of 5% in efficiency.	[209]
2018	Experimental and numerical evaluation of an HD unit driven by solar energy	Experimental and numerical studies were conducted in Chile on a closed-air, open-water HD system. The most effective design features were derived via the use of experimental data.	[210]
2018	HD desalination system operated by a heat pump	It is possible to reach a maximum GOR of higher than 10 for humidifier and dehumidifier efficacy of 100%, which will result in systems that are more energy efficient.	[211]
2019	Studying a solar-assisted heat pump desalination	Experimental testing of an HD module using Honeycomb paper packing and polyhedron empty balls packing with a solar heat pump and internal heat recovery was carried out to determine its performance. Module productivity of 14.3 kg/kWh and GOR of 1.39 both increased by 15.51%, while fresh water prices declined by 17.36%.	[212]
2019	System for HD powered by heat pumps and has the potential for energy recovery	A new HD desalination system is built into a vapour compression (VC) heat pump. The price of fresh water made by the proposed systems ranges from 34.27 USD/m^3 to as low as 7.33 USD/m^3, depending on how the system works and how much it costs.	[213]
2020	Experimentation on a heat pump-powered HD with the dual goals of water purification and air conditioning	GOR may reach 4.07, RR 4.86%, COP 4.85, EUF 3.04, and productivity 287.8 L/day with the complete system. The system's minimum SEEC was 160.16 kWh/m^3 of fresh water. The system produces desalinated water and can cool 3.07 kW. Fresh water production cost USD 10.68–20.39/m^3.	[214]
2020	Investigation of a heat pump-driven open-air HD desalination system	System A (basic system with brine energy recovery for pre-heating salt water) and system B (basic system with brine energy recovery for pre-heating ambient air). Experiments show that system A has a maximum GOR of 5.06, an RR of 3.98%, water productivity of 11.46 kg/h, and a minimum cost of fresh water of 12.38 USD/m^3. In contrast, system B has a maximum GOR of 2.72, an RR of 2.56%, water productivity of 9.23 kg/h, and a minimum cost of fresh water of 15.14 USD/m^3.	[215]
2021	Research into a heat pump-driven HD desalination system with the option of energy recovery	Energy recovery HD using VC heat pumps. Two systems use recovered energy differently. System A preheats the heat pump condenser intake feed water, whereas system B preheats the humidifier inlet air. The suggested system's thermo-economic performance is compared to system "C" without energy recovery. Energy recovery in system A reduces fresh water costs for system C by 15.23%. System C improves its GOR by 23.1%, RR, productivity, and SEEC by 23.3% each. The data also reveal energy recovery conditions.	[216]

4.2. Evacuated Tube Collector (ETC)

As a result of the preceding discussion, it is obvious that researchers used a variety of enhancement approaches and ways to boost the performance of HD systems powered by FPCs that pre-heat the HTF. However, the better efficiency and reduced thermal losses of evacuated tube solar collectors make them a viable option for FPCs in HD systems [217]. ETCs are composed of evacuated double-layer borosilicate glass tubes with the outer layer of the inner tube coated with a selected absorbing substance for optimum solar energy absorption. Solar radiation absorbed heat is subsequently transmitted to the HTF flowing through the inner tube. Numerous studies have been conducted to increase the collector efficiency of ETCs by increasing the heating rate of the HTF with a precise enhancement approach [179,218–220]. As with FPC, the different sophisticated approaches used in HD systems powered by ETCs are classified as water-heated ETC systems, air-heated ETC systems, and hybrid evacuated tube water- and air-heated systems.

4.2.1. Water Preheated Evacuated Tube Collector Systems

As is the case with FPCs, the HD system with ETC is primarily provided with water as HTF. The ETC HD system has been modified to incorporate a forced air circulation mechanism, a system associated with solar stills, and the use of evacuated U-tube collectors and twin glass collectors to increase the yield and efficiency of the HD process, respectively.

Evacuated Tube Collector with Forced Air Circulation

In recent years, there have been attempts to analyse and evaluate the performance of water heated solar HD systems driven by ETCs. The authors conducted mathematical modelling and practical research on a solar HD system with forced air circulation and a treated cellulose paper substratum evaporator unit [92]. The system used a separate evaporator and condenser unit to circulate the salt water. The results indicated that when ETC was used for water heating, the output of fresh water was around 50–70% more than when solar was used with the same collector area.

Similarly, [221] investigated a solar HD system experimentally using two types of cellulose paper with varying wet surface areas as packing material in the evaporator unit. ETCs were included in a desalination system based on OWCA, as seen in Figure 12. The effects of natural and forced air circulation, namely from up, down, and up-down, were investigated in-depth, and the findings indicated that forced down air circulation performed better than the other two. The identical setup was investigated with just one fan for air circulation at the bottom of the dehumidifier [222]. For each component of the system, an experimental study and a theoretical simulation model were produced. The system's productivity was determined with and without preheating. The findings indicated that operating the desalination system for four hours per day with preheating resulted in an increase in productivity of around 22 L/d.

Evacuated Tube Collector Coupled with Solar Still

While ETC-integrated solar HD systems create an impressive amount of fresh water, there is a significant loss of warm water at the humidifier unit's outflow. To compensate for this loss, the authors studied a hybrid desalination system for continuous fresh water production employing HD and solar still methods with ETCs [223]. As with previous systems, fresh water was originally generated by the solar HD system, and the rejected warm water from the humidifier unit was re-circulated to a solar still to increase the overall productivity of the hybrid system (Figure 13). Daily fresh water production with a hybrid solar HD system (HD + solar still with condensate water from the HD) was approximately 37 L/d, according to performance analysis. To further increase the system's total yield, the setup was upgraded by the addition of four solar stills linked in parallel at the humidifier unit's outflow [224]. The results indicated that the inclusion of solar stills increased fresh water output by about 66.3 kg/d.

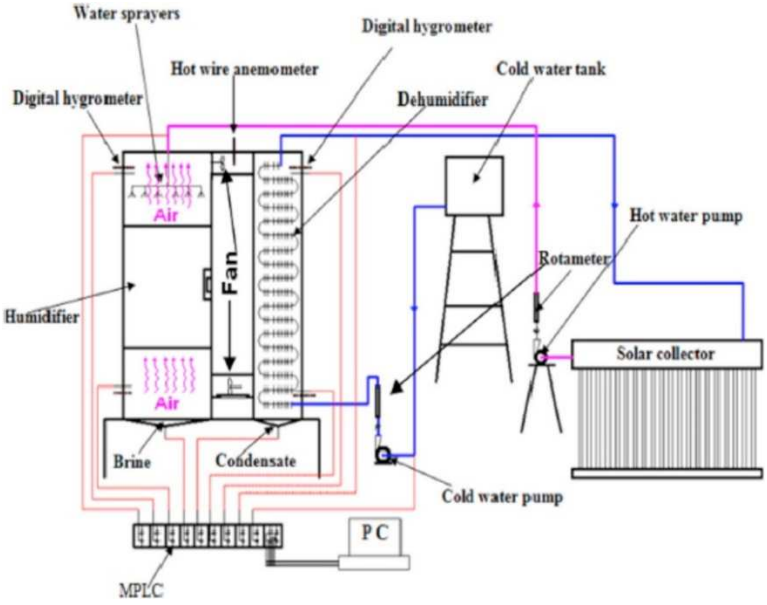


Figure 12. Desalination system based on OWCA including ETC. Reproduced with permission from A. E. Kabeel, Mofreh H. Hamed, Z. M. Omarab, S. W. Sharshirb, Eenergy Journal, published by Elsevier, 2014 [221].

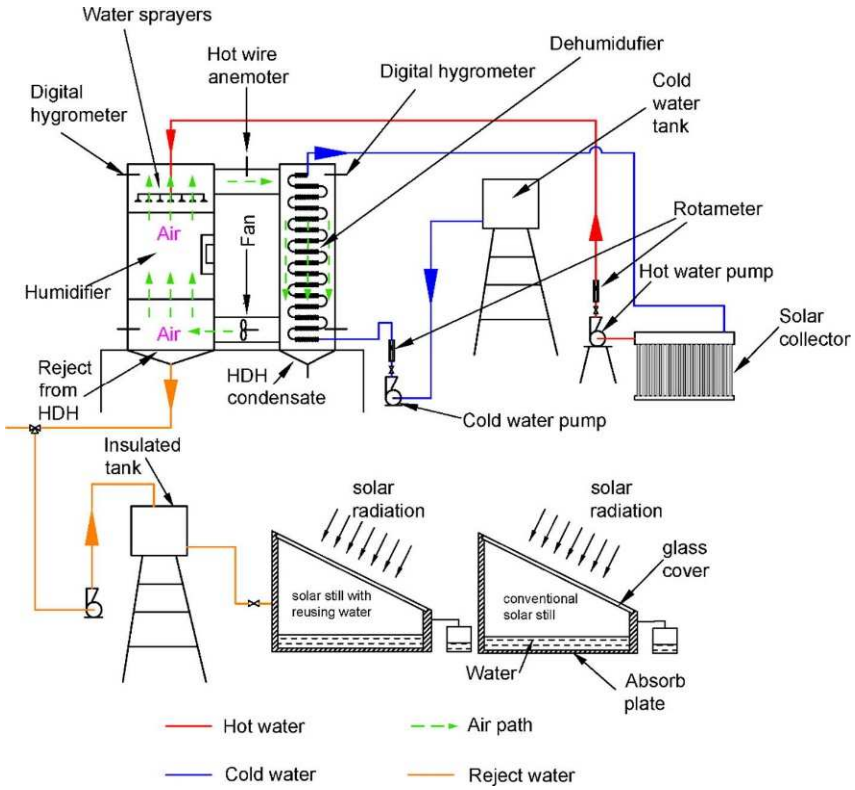


Figure 13. Diagrammatic representation of a hybrid solar HD desalination system with a single still and a traditional solar still. Reproduced with permission from S. W. Sharshir, Guilong Peng, Nuo Yang. M. O. A. El-Samadony, A. E. Kabeel, Applied Thermal Engineering Journal, published by Elsevier, 2016 [223].

Evacuated U-Tube Desalination System

In a hollow fibre membrane-based HD system, the use of an evacuated U-tube solar collector was investigated [225]. Solar heating, humidification, and dehumidification were

all tested in the same test rig that included a crossflow hollow fibre membrane unit, a fin and tube heat exchanger, and a dehumidifier (fin and tube heat exchanger). About 92% of the total energy consumption of the full system was accounted for by the use of U-tube evacuated solar collectors.

4.2.2. Dual Glass Evacuated Tube Collector Air Preheated System

A limited number of studies tried to examine the performance of ETC-driven air warmed HD systems. Dual glass evacuated tube array solar air collectors were shown to have greater thermal and energy performance than conventional evacuated solar air collectors in tests conducted by Xu et al. [226]. To power a small-scale HD system, all-glass evacuated tubes were employed [140]. Parallel connections of 20 vacuum-enhanced dual-wall glass tubes with vacuum were used in the new collectors. In addition, a pad humidifier made of cellulose material was used to humidify the air. Researchers discovered that a unique desalination system with dual-wall glass ETC performed better than standard ETC, and the findings might be used to construct and optimise a 1000 L/d solar HD system.

4.2.3. Hybrid Evacuated Tube Collector Water and Air Preheated Systems

ETC powered air warmed HD systems have a greater performance potential than FPC-powered HD systems, according to the preceding data. As a result, in a hybrid HD system (which preheats both air and water HTFs), an effort was made to use ETC and FPC to preheat the air medium and water medium, respectively. At the same time, an experimental investigation was carried out on a 1000 L/d solar HD system [227]. Each of the three components of the desalination system comprised a honeycomb structure pad humidifier, an evacuated tube solar air warmer, and a solar water collector with an area of around 12 m^2. The findings of the experiments showed that a solar radiation intensity of 550 W/m^2 may provide a fresh water production of up to 1200 L/d. Table 6 lists other experimental studies on ETC.

Table 6. A brief assessment of the experimental literature on the HD technique based on solar ETC.

Year	Brief Title	Major Conclusions	Refs.
2013	Investigating the operation of an air heated HD	The obtained findings indicated that when a two-stage approach is used instead of a single-stage method, the fresh water production capacity may be increased by 2.5 L/d.	[228]
2015	Mathematical and experimental investigation of a solar HD	Two time periods are examined to determine the system's productivity. When the system began at 1:00 p.m. and concluded at 5:00 p.m. with the water warmed, productivity increased by 6 L/d over when it began at 9:00 a.m. and ended at 5:00 p.m.	[222]
2016	Investigating hollow fibre membrane-based HD	The humidifier was a hollow fibre membrane module. While solar energy provided 92% of total energy usage, the COP was determined to be 0.75.	[225]
2020	HD ETC solar water system using wick as Packing Material.	Solar-powered HD machine for brackish water desalination was designed, built, and tested. 16 layers of wick were employed as packing material to improve mass and heat transmission between feed water and circulating air. The findings indicated that when the wick was employed, daily productivity rose by 28.3%. There was a very significant positive relationship between production and feed water flow rate. Additionally, the findings indicated that the greatest value of productivity was obtained at an air flowrate of 0.0075 kg/s. Furthermore, it was shown that increasing the feed water flow rate from 0.114 to 0.171 kg/s boosted daily production by 31.3% when the air flow rate was 0.0075 kg/s.	[229]
2022	Performance and economic feasibility of a GH dryer aided by ETC	The dryer's thermal efficiency is 18.5% for batch drying and 22.5% for semi-continuous drying. The energy payback time was projected to be 2.95 years and the cost payback period to be 1.10 years. CO_2 mitigation was determined to be 209.21 tonnes throughout its lifespan, demonstrating its appropriateness.	[230]
2022	GH integrated with a SS for arid climates	The full system comprises an evacuated tube collector, a GH unit connected with a solar still, a thermal energy storage system, and an absorption cooling cycle. Solar still decreases the cooling burden by over 20%. Additionally, the GH maintains an optimal temperature and relative humidity level throughout the year while using 1437.95 kW of electricity and 4.03–5.20 m^3/d of water.	[231]

4.3. Fresnel Lens Collector (FLC) System

Concentric grooves form a flat solar optical concentrator that serves as an individual prism by reflecting sun rays that fall on the curvature at any given place. There are some drawbacks to using FLC in solar HD despite its high concentration of solar energy, including the high level of complexity and expense associated with making Fresnel lenses without flaws on the facet edges [232]. Solar radiation is not properly focused on the receiver because of a misalignment of the facet edges. The performance of HD systems driven by FLC has been tested in a few studies. Mahmoud et al. [233] examined the performance of an HD system with FLC. The Fresnel lens' ability to heat the HD system's salty feed water and increase the system's fresh water production was both investigated experimentally and theoretically. The HD system's salty input water reached a temperature of roughly 90 °C when FLC was used, and the maximum yield with the closed-loop system was greater (112 $L/d/m^2$) than with the open-loop system (60 $L/d/m^2$).

Analysis of a cylindrical FLC-powered MEHD desalination system was carried out in a separate effort [234]. Thermal energy from a cylindrical FLC was used to heat both air and water within a single chamber, where evaporators and condensers were located. The system's highest yield was 3.4 kg/h with a maximum GOR of 2.1, according to the findings of the experiments. To their surprise, they found that FLC-based systems were capable of greater GORs even with their small design.

Xiao et al. [235] studied an HD system based on a bubbling humidifier–dehumidifier that was driven by a cylindrical FLC. Using an FLC with a 90% optical efficiency, the air and water were heated directly in the bubbling humidifier across the top and bottom parts. It was determined that when the heat input to the bubbling HD chamber increased, the water and air temperatures rose. When the maximum solar irradiation of 980 W/m^2 is present at midday, the maximum fresh water productivity is around 1.24 $L/h/m^2$. The total yield may reach 5.61 $L/d/m^2$ with an average thermal efficiency of around 69%.

4.4. Parabolic trough Collector (PTC) System

Work on the HD process using PTC, such as with FLC, has been restricted. The complexity of the PTC operation may be due to the need for a bigger collection area and tracking system. Using concentrated PTC for water heating and FPC for air heating, Fernández-García et al. [236] conducted an experimental examination of the HD process. The dehumidifier's cooling water flow rate and the influence of the weather on various operational parameters were thoroughly examined. Results from the experiments agreed well with those derived numerically [237]. Wind speed and temperature were shown to have the least impact on system performance, according to the authors. Factors such as humidifier water intake temperature, cool water flow rate, air flow rate, and sun intensity had a significant impact on the system's output.

HD systems with solar wick stills have recently been tested to see how they work [238]. It was necessary to connect two PTCs in series to pre-heat the water HTF entering the humidification chamber. With the use of two alternative humidifier materials, the system's performance was examined. With an increase in solar radiation, results showed that the PTC's warmed water temperature and system performance improved as a result.

When compared to fresh water produced just from the HD unit, the productivity of this system increased by almost double when using the hybrid system (HD + wicked solar stills). Table 7 summarises more experimental studies on the concentrating solar collector-HD approach.

Table 7. A concise assessment of the experimental literature on the concentrating solar collector-HD technique.

Year	Brief Title	Major Conclusions	Refs.
2011	Enhancement of solar desalination by HD	Saline water was misted with an air stream, increasing the surface area of contact. Additionally, the water was heated using a parabolic trough. Maximum output of 31.7 L/d was attained with a solar water heater set to 85 °C.	[239]
2013	Performance evaluation of v-trough solar concentrator in HD	When compared to a typical parabolic trough, the highest overall efficiency might reach up to 38% at 100 °C of operating temperature when using the unique V-trough collector in the HD device.	[240]
2015	HD desalination system using PTC solar air collector	To heat the humid air in the open-air, open-water HD desalination system, a PTC is used. The thermodynamic performance of two distinct particular schemes was estimated and compared to determine their impact on the overall performance of the HD. It was discovered that PTC was well-suited for air-heated HD systems in areas with strong radiation and that the scheme with the air heater situated between the humidifier and dehumidifier had a greater energy efficiency and produced more fresh water.	[144]
2016	Investigation of a novel design air humidifier using direct solar heating	Daily humidity levels in the three-stage bubble column were found to be around 23% higher than in a single stage bubble column. Additionally, the use of Fresnel lenses raised the absolute humidity by around 25%.	[241]
2018	CA comprehensive study of a solar-driven HD system	In Saudi Arabia, an HD unit with a PTC was tested, modelled, and adjusted. The cost of fresh water has been assessed to be 0.01254 USD/L. Additionally, it has been shown that raising the temperature of the flowing water improves the module's efficiency.	[242]
2020	The design, development, and operational circumstances affecting the effectiveness of a concentrated solar collector-based desalination system in Iraq	In Iraq, a study of the performance of a solar-powered brackish water distillation apparatus in the open created a comprehensive mathematical model of the multi-stage desalination system. Numerical findings indicate that three phases are the optimal number. In May, a noteworthy distillate production of 31 L/d was achieved. A cost savings of more than 40% when daily output exceeded 25 L was achieved	[243]
2022	Experimental analysis of an HD system of desalination operating with PTC	In Baghdad, Iraq, the HD system is comprised of six PTC with a combined aperture area of 8.772 m^2, a humidifier, a dehumidifier, and a tracking system. The findings indicate that the maximum daily fresh water production is about 6.37 L/d (6 h per day); the average daily productivity is 1.062 L/h when the salty water flow rate is 1 L/min. The OWCA circuit is the optimal arrangement.	[244]

4.5. Photovoltaic Module

A PV panel is a photovoltaic device that converts light into energy without the need for a moving motor. The photovoltaic thermal system might be created by using these modules to generate energy and heat [245]. This section examines the research on solar HDs that have been fitted with photovoltaic (PV) cells. There are a variety of ways to make PV cells, which are formed from a semiconductor thin film (mainly silicon and Gallium arsenide). Silicon cells have a potential efficiency of roughly 22%. Practical efficiency, on the other hand, is somewhere between 15 and 18%. Wang et al. [131] demonstrated that the desalination process in rural areas may be economically supported by a PV-driven HD, which uses solar radiation to provide power both directly and indirectly. In addition, they observed that this design performed better with forced convection than free convection under identical operating circumstances. Figure 14 depicts a schematic of the device developed by the authors. Using a PV-driven HD, Wang et al. [246] investigated the effects of various factors on evaporation and condensation rates. With forced convection and an evaporator temperature of 64.3 °C, the maximum fresh water output is estimated to be about 0.873 L/m^2/d compared to the free convection process with 0.789 kg/m^2/d.

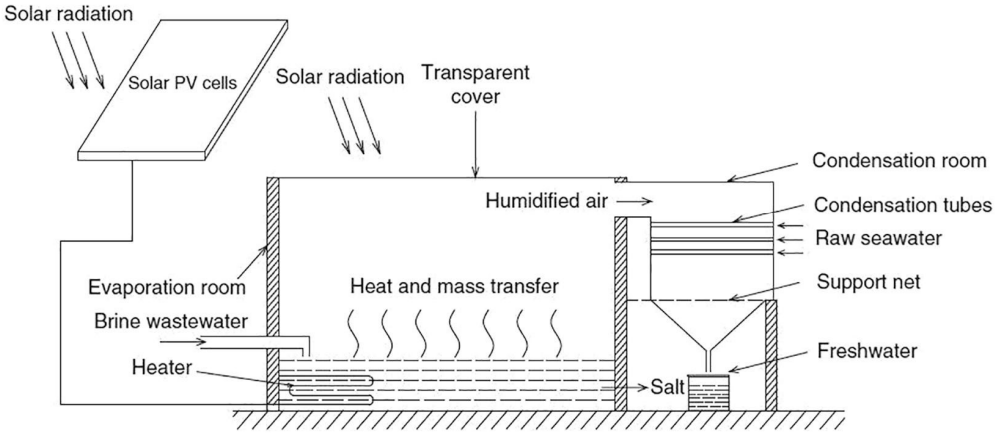


Figure 14. A photovoltaic-driven HD technique had been investigated in [131].

As a result of the PV's increased output power, the pump's efficiency decreases. Small-scale HD plants are more suited to using PV cells than large-scale ones. Consider the possibility of using extra power to develop a cogeneration facility. This is especially beneficial in distant areas where there are no major power distribution networks. Using this design process, desalination projects in distant areas may be more economically viable in competition with other desalination methods. Several notable studies on PV-driven HD systems are included in Table 8.

Table 8. A brief survey of the experimental literature on the photovoltaic-based HD process.

Year	Brief Title	Major Conclusions	Refs.
2019	HD process integrated with PV-thermal module	The findings demonstrated that for a maximum humidifier height of 6.4 m, a greater yield (0.21 kg/h.m^2) was obtained, demonstrating improved humidification at an increased wetted area.	[247]
2022	Parametric analysis of HD desalination driven by photovoltaic/thermal (PV/T) system	A unique packed dehumidifier-based PV/T-driven HD was presented to produce both fresh water and electricity cleanly and efficiently. The thermodynamic and economic performance is determined.	[248]

4.6. Hybrid Systems

4.6.1. Solar Still (SS)

The use of solar stills for the generation of fresh water has been widely accepted as a traditional and customary approach for many years. SSs play a significant role in fresh water production in distant and desert places when solar intensity is high and fresh water shortage persists [249,250]. The solar capability has been enhanced further by reducing the water depth, decreasing the inclination angle [144], installing reflectors in conjunction with solar collectors, increasing the surface area [251], and recovering latent heat for preheating saline water [252].

Pin-finned wicks [253], wet wicks [254], and vertical fins [255] were used to increase the heat transfer rate and hence the distillate rate in the SS. Energy-storing materials boost the thermal capacity of the basin by collecting heat during the day and releasing it during the evening or gloomy hours. SS has been improved by the addition of materials such as sand, black rubber, gravels [256], phase change material (PCM) [257], and mild steel pieces to the basin [258]. SS production was increased by integrating it with a parabolic dish concentrator [259], ETC [260], and a parabolic concentrator with cover cooling [261].

Condensation's latent heat was effectively used to heat the upper basin water, hence increasing solar still production [262]. The distillate yield of a twin basin SS was boosted by

reducing the water mass in the top basin [263]. By incorporating a thermoelectric module into a SS, the temperature differential between the evaporation and condensation surfaces is enhanced. This results in a greater condensation rate and increased distillate yield [264]. An SS equipped with a thermoelectric module produced 3.2 times more energy than a regular one [265]. A solar still with separate evaporation and condensation portion was tried, as well as a thermoelectric module to boost the condensation rate [266]. A CFD study was performed in a tubular SS and the findings were compared to those obtained experimentally [267]. By adding a divider in the basin and a glass cover, an effort was made to increase the performance of a single basin SS [268]. A stepped SS in conjunction with an HD process demonstrated enhanced performance and distillate yield [269]. By linking an HD system to a cascade SS, the performance of the system was revealed [270,271].

El-Said et al. [272] and Kabeel et al. [273] showed how to improve SS through the development of several approaches using porous material (PM). The findings indicated that the addition of PM improved both convection and conduction heat transfer coefficients. Rashidi et al. [274] provided an overview of porous material PM methods utilised in solar desalination systems. The findings indicated that the addition of PMs increased the system's performance and distillate production. Sharshir et al. [275] conducted a comprehensive analysis of the solar system's performance while still applying enhancement strategies. The findings indicated that sponge cubes increased distillate output by about 273% as compared to conventional cubes. Additionally, by using cuprous oxide nanoparticles, the distillation yield was raised by 133.6%. Kandeal et al. [276] investigated the economic performance of a SS desalination system combined with copper chips, nanofluid, and nano-based PCM. The results showed that all instances had significant performance gains and an increase in energy and exergy efficiency of around 112.5% and 190%, respectively, when compared to SS. Peng et al. [277] and Sharshir et al. [278] demonstrated the effects of PM on the performance of SS systems, including floating coal, cotton fabric, and carbon black nanoparticles. Sharshir et al. [279] demonstrated the performance of tubular solar still combined with mushrooms and nanofluid carbon paint in an experimental setting. The findings indicated that when nano-coated mushrooms were used instead of a conventional tubular solar still, productivity improved by 59.05% and manufacturing costs decreased by 33.85%. The performance of tubular solar was boosted by utilising nano-enhanced PCM combined with a v-corrugated aluminium basin, wick, and nanofluid. The findings indicate that the suggested approach increases daily fresh water consumption by about 88.8%. The performance of tubular SS was boosted by utilising nano-enhanced PCM combined with a v-corrugated aluminium basin, wick, and nanofluid [280]. The findings indicate that the suggested approach increases daily fresh water consumption by about 88.84%. Thermal energy efficiency was increased by roughly 82.16% while exergy efficiency was increased by approximately 221.8%. When compared to a traditional tubular SS, the cost per litre of fresh water was lowered by 22.47%. The performance of SSs can also increase using a revolving wick belt and quantum dots nanofluid [281].

The pyramid solar still [282] is an efficient way of purifying brackish water. The top surface of the pyramid SS is formed by triangular glass coverings. Two different styles of glass cover are used to create the top surface of the pyramid SS that is above the basin. One is still a three-sided triangle form, while the other is a four-sided triangular shape. The majority of researchers concentrated on enhancing the still's performance with the addition of fins, heat pipes, and wick material. Several others focused on phase change materials, nanoparticles, and nanotubes as a means of increasing distillate yield. Pyramid solar still performance is affected by design, operational, and environmental conditions [140].

Water Preheated Solar Still Systems

The production of the vast majority of these solar stills is subpar [283]. Research has been carried out to increase the amount of fresh water produced by solar stills [284]. The use of a solar still (SS) in conjunction with the HD system allows the HD system's feed water to be heated by the SS.

Recently, Farshchi et al. [270] conducted experimental research on a unique HD-SS system with cascaded SS. The HD system received hot feed water from the inclined SS as well as distilled water. As a result, the daily output of the HD system increased by 28%, while its overall productivity and efficiency were increased by 9–20%.

Air Preheated Solar Still Systems

In order to increase the overall productivity of the system, researchers have used unique enhancing strategies to increase the productivity of SS systems paired with HD systems [285,286].

- Quonset Greenhouse Arrangement

Perret and Sablani [287] built and studied a unique prototype HD system in a Quonset GH layout to deliver fresh water for irrigation from saline/brackish water. There were two condenser units, two evaporative cooling pads, and a modified SS structure that worked as humidifiers. Because the condenser temperature was constantly lower than the air dew point temperature, condensation occurred on the condensers, even if the amount of fresh water generated was negligible.

- Bubble Column Solar Still

Other researchers evaluated the efficacy of a new solar bubble column HD system, which used a humidifier comparable to a single-slope solar still [108]. Direct and warmed air supply (using a solar air heater with various turbulators) were studied to see how they affected the productivity of the modified HD system. Results showed that the system linked to a concave-baffled solar air heater produced the most output when compared to other setups. The research was expanded to include the operation of a bubble column HD system powered by biomass energy [171]. With and without air preheating utilising biomass energy, the humidifier and system performance were evaluated in an experiment. Bubble column HD systems with warmed air yielded 6.1 kg/h, whereas the usage of waste heat recovery systems resulted in less use of fuel, according to the study results. Table 9 summarises more experimental studies on the bubble column-HD approach.

Table 9. A brief assessment of the experimental literature on the desalination method based on bubble columns.

Year	Brief Title	Major Conclusions	Refs.
2016	A bubble column evaporator with a basic flat-plate condenser	A bubble evaporator was used in combination with a conventional flat plate collector. The innovative desalination plant presented in this study functioned efficiently at temperatures below the boiling point.	[105]
2016	Combined probation of bubble column HD using solar collectors	Three studies involving the integration of a bubble column with different collector configurations were completed. The overall efficiency of 78% was achieved when the bubble column HD was combined with a solar air heater equipped with turbulators.	[106]
2017	Analysis of multi-stage stepped bubble humidifier for HD	Pressure drop was explored as a function of water column height for different air superficial velocities in three single-stage, two-stage, and three-stage setups. The latter demonstrated the greatest gain in humidifier performance, with a 23% improvement over the single stage.	[107]
2017	Investigation of a heated bubble column humidifier	We looked at the impact of factors such as intake water temperature and humidity as well as air velocity. Fresnel lenses were reported to boost absolute humidity by 9–11%.	[288]
2020	investigation of bubble column humidification and thermoelectric cooler dehumidification	The bubble column humidification promotes a larger interfacial area, which increases the heat–mass transfer rate and hence the humidification efficiency.	[289]

Hybrid Water and Air Solar Still Systems

A hybrid dual-medium warmed HD system with SSs and FPCs was similar to ETCs. In a bubble column HD system, the combined impact of several solar collectors (FPC + SS) was examined by Rajaseenivasan et al. [106]. For the HD system with conventional solar air heater (case I), solar air heater featuring turbulators (case II) and dual-purpose turbulators (case III) correspondingly, the performance of the HD system was thoroughly examined. Figure 7 shows how the DPSC was constructed such that both the absorber plate and the riser tube are heated simultaneously, allowing both air and water to be heated at the same time. Case III was shown to be the most productive, producing 16.32 kg/m^2 day, 20.61 kg/m^2 day, and 23.92 kg/m^2 day, respectively, from the data.

In addition, the desalination system was modified such that jute fabric was used to fill the humidification chamber. DPSC-heated air and water were also circulated via the humidifier unit's bottom and top [271]. DPSC systems with, without, and with convex and semi-circular turbulators were all evaluated for their performance. The DPSC system with concave semi-circular turbulators had the highest production (15.23 kg/m^2) and the highest overall efficiency (67.6%) in the experiments.

4.6.2. Solar Pond

Solar ponds (SPs) are darkened pools of water designed to enhance light absorption. They are intended to increase in salinity with depth, so producing a density gradient that hinders natural convection currents. The absorption of solar energy by water causes its temperature to increase. As indicated in Table 10, the shorter the wavelength of sunlight, the deeper it may enter the water column [290,291]. The quantity of energy absorbed rises with depth, resulting in a vertical temperature gradient and a decreasing density gradient with depth. In contrast, salinity rises with depth, resulting in a vertical salinity gradient and an increasing density gradient with depth. As seen in Figure 15, the eventual result of these contradictory occurrences is a stratified pond with rising temperature and salinity with depth. Solar ponds serve as solar collectors as well as a thermal energy storage medium. The salinity-gradient solar pond (SGSP), which was proposed as a solar collector by Bloch in 1948, is one of the most basic methods for directly collecting solar energy and converting it to thermal heat [292]. Almost all lakes and natural ponds create thermal heat from incoming solar radiation; however, the majority of this energy is lost in the surrounding environment mostly as a result of evaporation and convection. Based on the convection behaviour of the saline solution in solar ponds, these ponds are classified as convective or non-convective. SGSPs are cost-effective, non-convective solar ponds that may generate heat for industrial or residential power or cooling subsystems [293]. Several characteristics influence the behaviour of a solar pond, including top insulation, side wall shading, starting pond conditions, sun incidence angle, non-convective zone thickness, and storage zone thickness [294]. In recent years, the possibility of merging an SGSP with other systems has been examined. Thermal desalination systems, such as HD desalination systems run on SGSP, are the optimal option. In semi-arid and dry countries, such as North Africa and the Middle East, the use of a solar HD desalination system becomes an intriguing situation.

Due to the tremendous potential of HD desalination technologies in extracting heat from salinity-gradient solar ponds, Rostamzadeh et al. [295] investigated the possibility of designing an SGSP-HD system for providing potable water. For this objective, a CAOW-WH/HD desalination system is employed to produce fresh water, and the spring and summer results for Iran's Lake Urmia are provided. In addition, a thermoelectric generator is utilised to utilise the thermal heat of UCZ, generated fresh water, and brine to create energy for the provision of pumps' power consumption and small-scale needs prior to their discharge. The findings of the case study indicate that maximum fresh water production (1562 m^3/h) occurs between 22 June and 22 July, whereas maximum electricity output (4.95 kW) occurs between 21 April and 21 May.

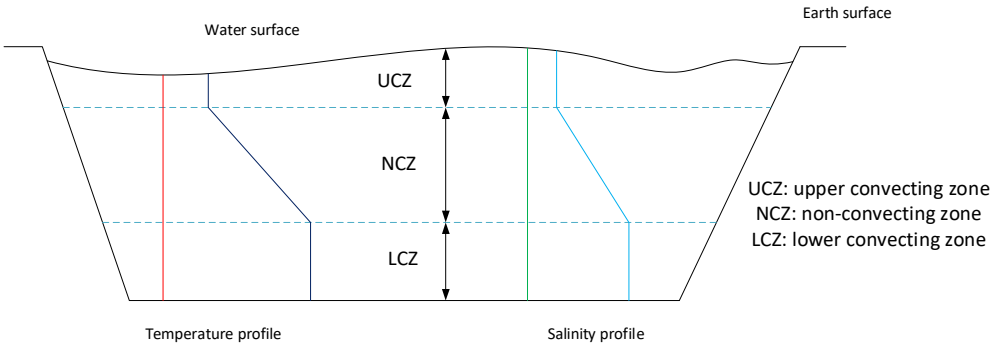


Figure 15. Vertical cross-section of a solar pond.

Table 10. Spectral absorption of solar radiation in water [296].

Wavelength (μm)	Layer Depth				
	0	1 cm	10 cm	1 m	10 m
0.2–0.6	23.7	23.7	23.6	22.9	17.2
0.6–0.9	36.0	35.3	36.0	12.9	0.9
0.9–1.2	17.9	12.3	0.8	0.0	0.0
>1.2	22.4	1.7	0.0	0.0	0.0
Total	100.0	73.0	54.9	35.8	18.1

A theoretical evaluation of the SP greenhouse heating unit was established by Badran et al. [297]. The results demonstrate that SP has the capacity to supply 30% of its heat to the greenhouse effect. For shallow SP (SSP), mathematical analysis was undertaken. It demonstrates that between May and September, shallow SP was the dominant greenhouse heating method. In addition to economic analyses, SSP was also the most cost-effective [298]. Due to the greenhouse effect, the glazed cover pond has achieved its highest level of efficiency. Ruskowitz et al. [299] advocated the use of floating discs, floating hemispheres, and a continuous sheet in order to reduce evaporation loss. The heat transfer behaviour of the composite phase change materials (PCM) of paraffin and steel wires was investigated by Wang et al. [300]. Initially, the findings demonstrate that the addition of steel wires to paraffin significantly increases the heat transfer performance. The greatest heat transfer coefficient during the melting phase is 18.17 W/m^2 $°C^{-1}$ with an increase of 18.84%, while the maximum during the freezing process is 21.59 W/m^2 $°C^{-1}$ with an increase of 20.88%. Secondly, an experimental investigation was done in an experimental SP with the addition of 20 PCM capsule tubes. The addition of RT 50 and RT 60 reduced the day-night temperature variations by 2.87 °C and 2.50 °C, respectively, compared to the circumstances without PCM. Adding RT 50 and RT 60 to the solar pond results in exergy increases of 9.34% and 14.13%, respectively. The research indicated that adding PCM to solar ponds increases the quality of the heat energy produced by SPs and expands the solar pond's heat application range.

4.6.3. Others

Cogeneration has the potential to dramatically improve the efficiency of the desalination process, which consumes a large amount of energy. For example, recent years have seen an increase in interest in hybrid systems that generate both energy and heat while desalinating seawater. Hybrid desalination units are examined in this part to conduct experiments.

Using a nanofluid solar water heater, Kabeel and El-Said [142] studied a hybrid HD device that combined an HD unit and single-stage flashing evaporation. Solar radiation, air mass flow rate, and water temperature were shown to have a positive effect on production. Solar air heater and solar water heater collector efficiency were 56% and 55%, respectively, with a maximum output of 41 L/d. Eliminshawy et al. [170] conducted economic and

technical feasibility studies for a hybrid solar-geothermal energy source in a solar HD unit. The experimental daily cumulative productivity reached 192 L/d, whereas the daily average GOR was found to be 1.2–1.58 L/d. In addition, the cost of water produced by the new unit was 0.003 USD/L. The hybrid solar-geothermal desalination system outperformed traditional solar modules in a side-by-side comparison.

Zhang et al. [301] investigated an HD device connected to a heat pump unit as an example of efforts relating to cogeneration. As seen in Figure 16, their experimental setup was comprised of a humidifier, heat pump unit, first stage dehumidifier, and plate heat exchanger. The plate heat exchanger allows heat from the heat pump to be transferred to salt water, while the second stage dehumidifier absorbs heat from the air and transfers it to the heat pump. The influence of seawater temperature on total production was found to be significantly greater than the effect of air temperature. Additionally, it was shown that productivity rises as the air flow rate increases. Measured and computed fresh water costs were 178.08 L/d and 0.051 USD/L, respectively, for the optimal production value. Kabeel and Abdelgaid [302] attempted to combine desalination and sun drying. An HD module was connected to an indirect solar dryer with reheating that was in a two-step stage. At 1.24 to 1.79, it was more than twice as high as the GOR of a system simply using an HD, which was 0.97–1.38. Increasing air flow from 50 m^3/h to 70 m^3/h enhanced the fresh water productivity and moisture removal from 29.55 L/d to 42.31 and from 8.33 L/d to 12.37 L/d, respectively, over the operating time of 8:00 am to 7:00 pm.

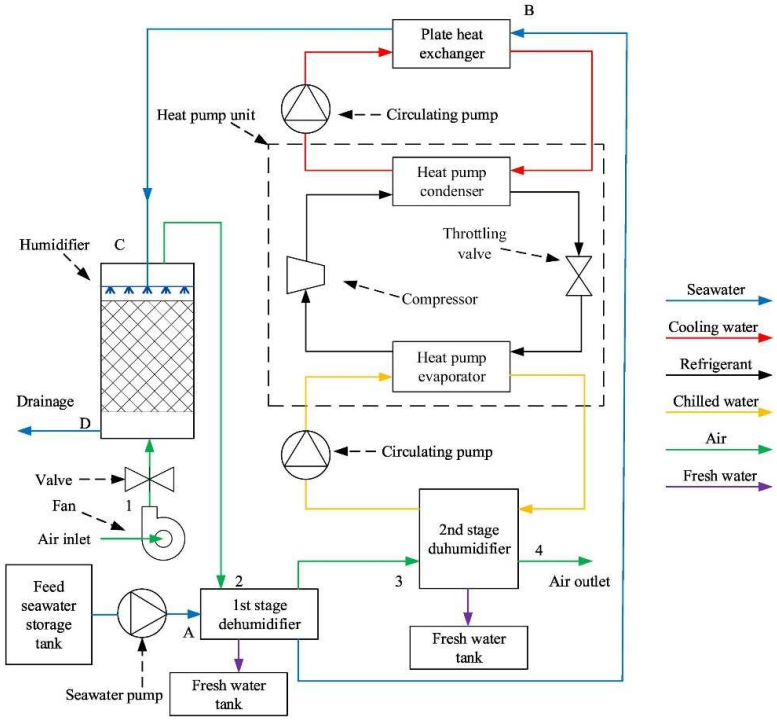


Figure 16. Diagrammatic representation of the suggested system by [301]. Reproduced with permission from Yin Zhang, Chunguang Zhua, Huan Zhang, Wandong, Zheng, Shijun You, Yuhan Zhenac, Desalination Journal, published by Elsevier, 2018 [301].

Overall, the research shows that merging different generating methods improves efficiency. With desalination, the total efficiency of the device is substantially better, making it an excellent alternative for small-scale rural places. In addition, a hybrid system might make use of solar and geothermal energy sources. Even fossil fuels may be used with renewable energy sources in some kind of energy hybridisation. Regional and climatic factors have a large role in determining the ideal arrangement. For places where solar power is not always accessible, this is a considerable benefit. The price of produced water for hybrid renewable energy-HD systems has been estimated as follows: HD with geothermal energy at 0.0276 USD/L, HD

with a heat pump at 0.0114 USD/L, SS with PV at 0.0095 USD/L, SS with ultrasound wave at 0.012 USD/L, HD with hot air steam at 0.03006 USD/L, HD with SS and solar water heater at 0.034 USD/L, HD with low-grade waste heat at 0.014 USD/L [303,304]. Table 11 outlines the most significant efforts in this very wide-ranging subject.

Table 11. A concise summary of the experimental literature pertaining to the hybrid HD method.

Year	Brief Title	Major Conclusions	Refs.
2010	Analysing an HD module embedded into a GH	In AL-Hail, Muscat, a prototype was tested. The obtained data indicated that increasing sun radiation enhanced condensate flow. For 800 W/m^2 solar radiation, a flow condensate speed of 65 L/h was reported.	[305]
2015	Using small scale HD in a bubble- GH	The distilled water created was used to hydrate a bubble GH. The humid atmosphere resulted in a significant decrease in plant water consumption. Additionally, it may benefit isolated places' social, economic, and environmental well-being.	[306]
2018	Assessing an HD system with a heat pump unit	A heat pump unit and a plate heat exchanger were used to test an HD module. The predicted maximum productivity and price of fresh water were 178.08 L/d and 0.051 USD/L, respectively.	[301]
2018	Evaluation of a modified solar hybrid desalination system	An HD module was connected to the solar still and the air–water heater, resulting in increased efficiency. Among other characteristics, air mass flow rate was shown to have a significant influence. The total efficiency was determined to be 21–39%, while the GOR was determined to be 2.57.	[141]
2018	Hybridizing an indirect evaporative air cooler with an HD	A solar HD module was used to test an indirect evaporative air cooler with baffles. The produced cooling load and created distilled water were determined to be 253.26–417.4 W and 38.651 L/d, respectively, with the average daily COP rising from 1.78 to 2.26.	[307]
2018	Evaluation of an HD unit integrated with wick solar stills	An HD module was tested in conjunction with six wick solar stills. For the humidifier, several packing materials and water flow rates were explored. The hybrid architecture was found to be twice as productive as traditional HD units, with a GOR increase of 5.1 to 5.7.	[238]
2018	Studying a two-stage indirect solar dryer	We explored an integrated solution for rural places that consists of an HD module and a two-stage indirect sun dryer with reheat. The gadget's overall GOR was increased by a factor of 29% when compared to an HD-only device.	[302]
2019	An HD desalination system using waste heat from a domestic air conditioning unit.	The performance of a hybrid HD desalination system was evaluated for hot and moderate climatic conditions using waste heat recovered from a vapour compression refrigeration (VCR) based home air-conditioning unit. The greatest average production of fresh water was 4.63 kg/h. The output of fresh water was greatly reliant on the temperature and relative humidity of the surrounding air. The cost of producing fresh water from waste heat was USD 0.1658/kg.	[67]
2021	exergoeconomic assessment of a novel combined ejector cooling with HD	The research includes experimenting with numerous changes in generator, condenser, and evaporator temperatures, as well as solar irradiation intensities. According to the findings, replacing solar collectors with free waste heat recovery may cut the cost of generated fresh water from 3.84 USD/m^3 to 2.39 USD/m^3.	[308]
2021	Highly saline water desalination using an integrated hybrid solar HD system	The hybrid HD has been put to the test in desalination experiments using water that was exceedingly salty. When the input temperature is below 60 °C, the HD is unable to considerably generate fresh water. With a reflector saves 16.5% of daily electricity usage. When very saline water was utilised instead of brackish water, the electrical energy consumption was lowered by 65%. Saline water at a temperature of 85 °C may produce 72 kg/day.	[309]
2022	HD using a high-frequency ultrasonic humidifier and a solar-heated air stream	As a humidification device, a high-frequency ultrasonic wave atomiser was employed. The greatest daily production is 7.72 kg. The efficiency of the system was 27.29%. The projected cost of water was around 0.03437 USD/L.	[310]

In this context, a wide range of setups and technologies are put to the test and examined. Nonetheless, the current study trend in this area has yielded some significant results, as the following list illustrates:

- Arid and semi-arid nations, particularly those in the Middle East and North Africa, host the majority of the trials. Since these nations are dealing with fresh water scarcity issues more often than other places, it is easy to see why this is the case;
- Bubble columns and other flat plate collectors are among the most studied and researched collectors;
- While the PTC, and ETC may give a greater temperature than the FPC, their high cost and intricate design have restricted their use, particularly with the HD. Various configurations are examined, and reliable productivity and GOR measures have been created for various systems and configurations;
- PV-based HD modules seem to be under-researched. For HD plants, PV panels have been shown to be a dependable source of energy, particularly in distant places where solar insolation is considerable. Future work is needed in this field;
- HD units may be included in a variety of various plant layouts to increase overall plant efficiency. Approaching cogeneration by combining the production of fresh water with the production of electricity, heating, or cooling is highly recommended for places with coverable utility needs, particularly for small-scale applications of this kind.

5. Humidification Dehumidification Greenhouses

Conventional agricultural techniques contribute significantly to greenhouse gas (GHG) emissions [311], which have a detrimental impact on the environment. As a result, it is critical to establish sustainable and low-carbon food production systems that save resources and boost crop output by enabling year-round agriculture [312]. With this context in mind, agricultural GHs provide a realistic alternative; they minimise fossil fuel usage while increasing crop output by 10–20% [313].

5.1. Greenhouse Design

Components of the GH design include the cladding material, the form, and the orientation, as well as the technological equipment required to regulate the microclimate inside the GH (Figure 17). The optimal covering material must have maximum photosynthetically active radiation (PAR) spectrum transmission and minimum longwave band transmission. Low-density polyethylene films (LDPE) are the most often used material for greenhouse cladding because of their strong mechanical performance, appropriate optical qualities, and affordable pricing [314,315]. The downsides are that it is readily damaged by strong winds and that the colour deteriorates with time owing to UV penetration, which may partly restrict solar energy from entering the plant zone. Because glass coverings such as fibreglass and polycarbonate manufactured configurations are more costly than polyethylene plastic covers, they are employed for high grade items such as fragrances and medicinal plants. Glass-encased GHs do not reflect the infrared rays that keep the GH warm at night [12].

Sethi [316] researched the five most common types of single-span greenhouses: even span, uneven span, vinery, modified arch, and Quonset type (Figure 18). For an exact comparison, the primary geometrical features of each shape, such as length, breadth, and height, were maintained. As seen in Figure 16, any form may be broken into several pieces based on their orientations.

It has been established that a greenhouse with an uneven–span shape catches the most solar energy regardless of the latitude evaluated, but the Quonset design is the poorest for solar radiation collecting. In addition, the maximum inside air temperature was recorded with an uneven-span shape and the minimum with a Quonset shape. East-west (E–W) orientation is the optimal orientation for all latitudes since it requires less energy and collects more solar radiation.

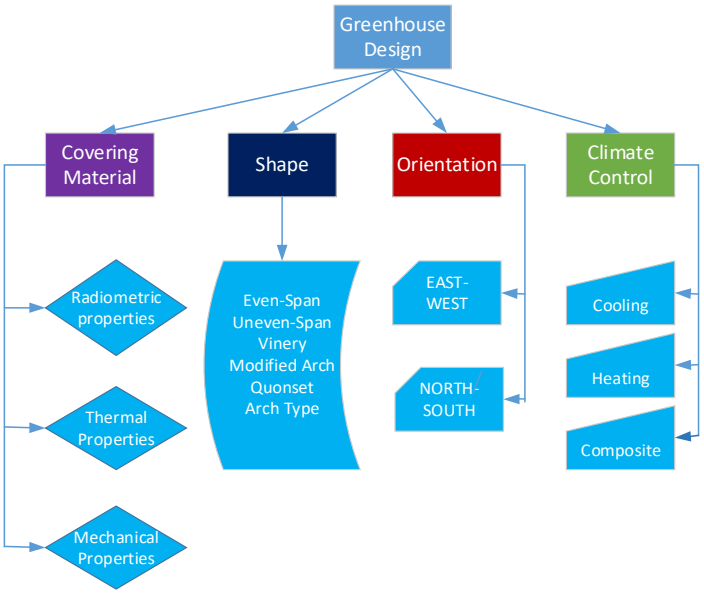


Figure 17. Greenhouse design components.

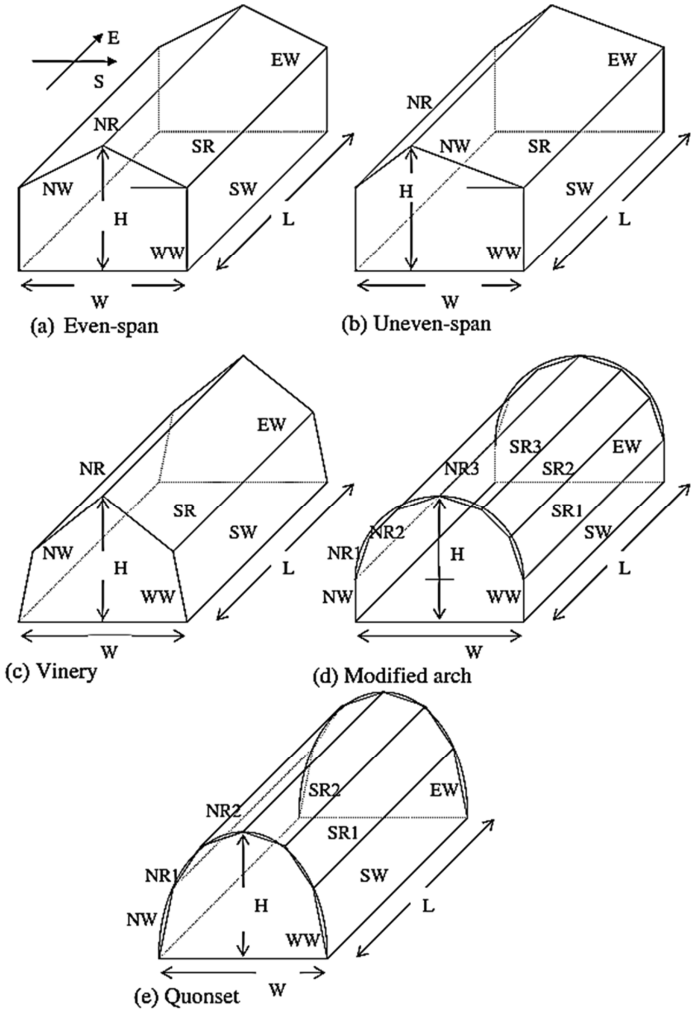


Figure 18. View of several greenhouse shapes. Reproduced with permission from V. P. Sethi, Solar Energy Journal, published by Elsevier, 2009 [316].

5.2. Greenhouse Microclimate

The microclimate inside a covered structure is mostly determined by physical processes including mass/vapour and energy/heat transmission between the air, plants, plastic cover, and growth medium. Varied crops need different growth circumstances [317], mostly in terms of air temperature, relative humidity, and CO_2 level, hence the greenhouse's microclimate has a direct impact on crop development and production. Microclimatic and other key elements, such as solar radiation, air temperature, RH, ventilation/CO_2, nutrients, and water, inhibit the metabolic processes of plants. Therefore, it is crucial to maintain the microclimatic parameters within the appropriate range for enhanced plant development, yield, and product quality. This may be accomplished using a variety of passive/natural or active/forced microclimate management approaches, including ventilation (natural or forced) [318]. In addition, the microclimate is highly dependent on greenhouse ventilation performance concerning numerous ventilation characteristics such as air exchange rate, vent opening area or vent ratio [319], wind speed [320], wind direction, the distance between the roof and side vents [320], roof slope, use of insect-proof screens, number of spans, and greenhouse size. Therefore, optimising the aforementioned ventilation parameters is essential for achieving enhanced microclimatic conditions and energy efficiency. Understanding the microclimate and features of a greenhouse is essential for maintaining optimal operating conditions throughout different phases of plant development. It is essential to have an accurate estimate of solar radiation, mass transfer coefficients, and heat transfer coefficients in order to construct a realistic physical model, since these factors greatly affect the greenhouse energy and mass balance [321,322]. By maintaining the ideal temperature at each stage of crop development, the greenhouse can provide a greater yield outside of the crop's growing season. An appropriate method of heating or cooling must be used for this purpose [323,324]. In cold weather, optimal plant development requires higher interior air temperatures, which may be achieved by preserving the greenhouse effect or by deploying any suitable heating device. In contrast, in very hot areas, the greenhouse effect is only required for a brief period of two to three months, while other adequate cooling technologies are required for the remaining months [325,326].

5.3. Seawater Greenhouse

A seawater GH (SWGH) is a type of desalination unit that uses sunlight and seawater, humidifies the air in the interior of the GH, and produces fresh water. This fresh water can be used for irrigating and drinking. Since seawater GHs use solar energy and employ fewer mechanical parts, they greatly reduce costs of energy consumption and construction, repair, and maintenance compared to other desalination units. GHs are built to create suitable environmental conditions for plant growth where these conditions do not exist outside the GH. Irrigation efficiency in GHs improves considerably compared to traditional methods. The solar GH can be used for brackish or seawater via a desalination process. This type of GHs was first introduced by the English inventor Charlie Paton in the early 1990s. Their success depends largely on the environmental conditions surrounding them and they are more suitable for warm, sunny, and dry coastal areas with steady wind blow. A seawater GH is self-sufficient in fresh water production for crops grown within or around it. Therefore, it can be employed as a suitable method for agriculture in warm and arid regions with low rainfall. A simple seawater GH consists of two evaporative coolers (evaporators), a condenser and fans, pipes carrying seawater and distilled water, and crops growing between the two evaporators.

The humidification process is often followed by the dehumidification process in industrial applications, particularly desalination facilities. However, this innovative method combines these two processes in a GH [327–329]. The objective of HD GHs is not to lower humidity for the benefit of plant development, but rather to create fresh water for agricultural needs by collecting water vapour inside the GH. In recent years, research has been performed on combining these two processes in GHs. However, as will be described later, this concept was not always used in the same manner. In certain GHs, water

evaporation and condensation occur inside the space between two layers of GH glazing material [330,331]. These GHs use the so-called 'solar still' principle (Figure 19).

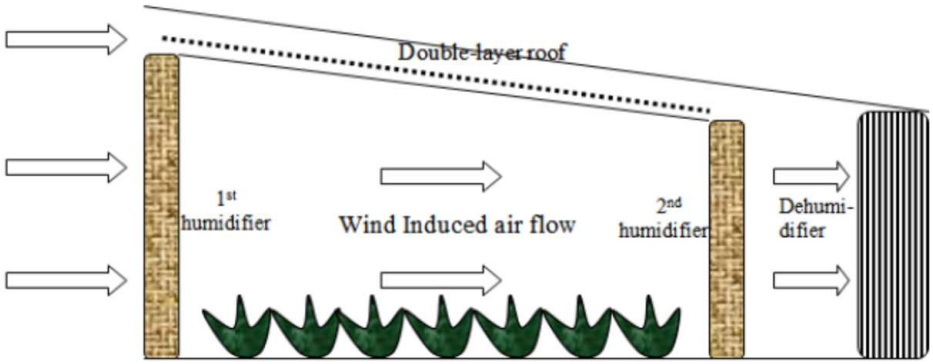


Figure 19. A sketch of combined solar still and a GH [332].

Other greenhouses humidify the air using standard evaporative cooling pads. As air circulates throughout the GH, its temperature rises owing mostly to solar heat uptake. This temperature rise may be attributed to the sensible heat extracted from plants [333], soil, and cover. As air temperature rises, RH falls, which may be read as a rise in the air's ability to store more water vapour [287,332]. Before the fans, a second humidifier is positioned to provide more moisture to the air. Then, towards the conclusion of the GH, a dehumidifier situated between the second humidifier and the fans dehumidifies the moisture [329,334–337]. As a coolant, somewhat cold water is first circulated through the dehumidifier. This water acquires some heat as a consequence of the dehumidification process occurring on the exterior surface of the dehumidifier releasing the latent heat of vaporisation (L_v). The warmed water is then pumped to the first humidifier, where it contacts the warm air going via the first humidifier. As a consequence, water evaporates, causing the air and water temperatures to decrease.

5.4. Commercial Humidification Dehumidification Greenhouses–Desalination Systems

In 1994, a seawater HD GH was manufactured and studied in Tenerife's southern region using the same approach described above [337,338]. The GH consisted of two humidifiers; the first humidifier was located on one side of the GH and the second humidifier was located on the other side of the GH before the fans. In addition, this prototype GH's dehumidifier was chilled with cold deep salt water. Figure 20 depicts the air and water circulation in this GH.

More than twice as much water was generated as was necessary to irrigate an identical greenhouse ground area. In the absence of cold feed salt water, the water going through the first humidifier may be used as a cooler if its temperature has lowered enough due to evaporation [287,332,339]. The authors indicated that the use of this water as the dehumidifier's coolant is viable since its temperature is always lower than the saturation temperature of the moist air flowing through the dehumidifier throughout their testing (see Figure 21).

During their studies, this temperature difference was produced by night-time evaporation in the first humidifier owing to the dry, warm air conditions. Several adjustments to the parameters of the seawater HD greenhouse in Tenerife were subsequently implemented in a second greenhouse built in the United Arab Emirates in 2000 [336,338]. Modifications included using water from the first humidifier as a coolant in the second humidifier. The water output was less than anticipated. With further adjustment, however, the GH was able to satisfy its fresh water needs. This improvement consisted of running the water used to moisten the second humidifier via a 'solar heater' to increase evaporation. The solar heater was just an array of black polyethylene hose tubes exposed to the sun.

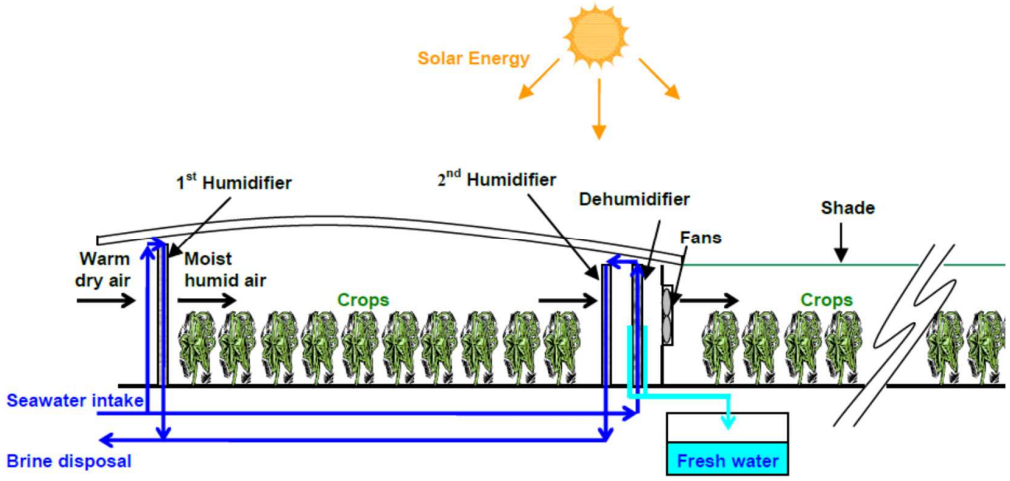


Figure 20. Schematic of the seawater HD GH. Reproduced with permission from M. F. A. Goosen, S. S. Sablani, C. Paton, J. Perret, A. Al-Nuaimi, I. Haffar, H. Al-Hinai, W. H. Shayya, Solar Energy Journal, published by Elsevier, 2003 [334,335].

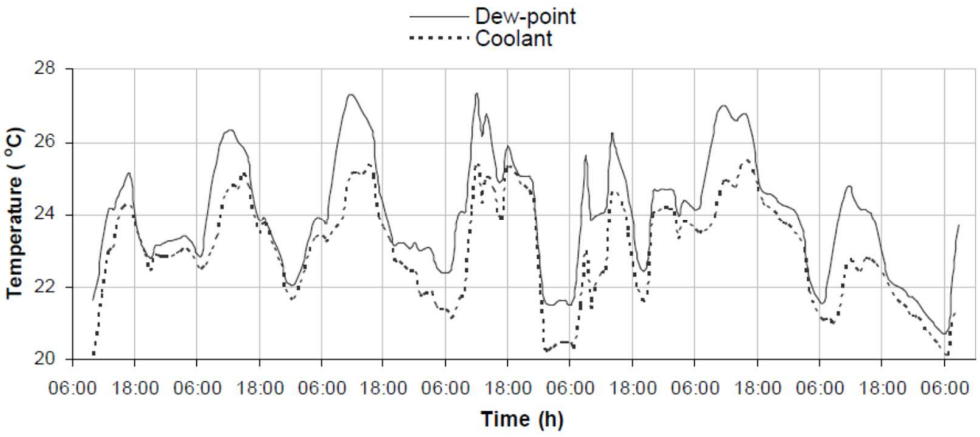


Figure 21. Changes in the dew-point temperature of the air and the coolant temperature with time. Reproduced with permission from J. S. Perret, A. M. Al-Ismaili, S. S. Sablani, Biosystems Engineering Journal, published by Elsevier, 2005 [287,332].

The third seawater HD greenhouse was built in Oman using the expertise gathered from the previous two GHs. This GH has two water circuits. The first circuit connected the first humidifier to the dehumidifier, while the second circuit connected the tube array (i.e., the solar heater) to the second humidifier (see Figure 22). The tube array was installed inside the GH, right under the cover. The dehumidifier material was changed from the previously utilised tube-and-fin dehumidifier consisting of cupronickel and aluminium to a plastic-tube dehumidifier [64]. Based on visual inspection, the greenhouse seemed to be generating enough condensate.

The Australia project, which started in 2010, was the first with a commercial emphasis. Falling input costs and rising efficiency, notably of solar PV and RO desalination technologies, as well as the global deepening of water scarcity and drought, created a one-of-a-kind commercial opportunity for Seawater GH. The initiative started as a 2000 m^2 trial plant near Port Augusta and has since been built up 100-fold to 20 ha under new owners.

The Sahara Forest Project [46], situated in Qatar, is a large commercial trial project for seawater GHs. Seawater GHs are supposed to provide perfect growing conditions for the year-round cultivation of high-value food crops in the harsh Qatari desert. The GH structure consists of three bays for horticultural production. The cooling system is provided by an evaporative cooler located at one end of the GH. The cold air is supplied underneath the plants through polythene ducts, providing consistent and low-level distribution along

the GH. As the temperature increases, the air rises and exits via high-level openings in the end wall.

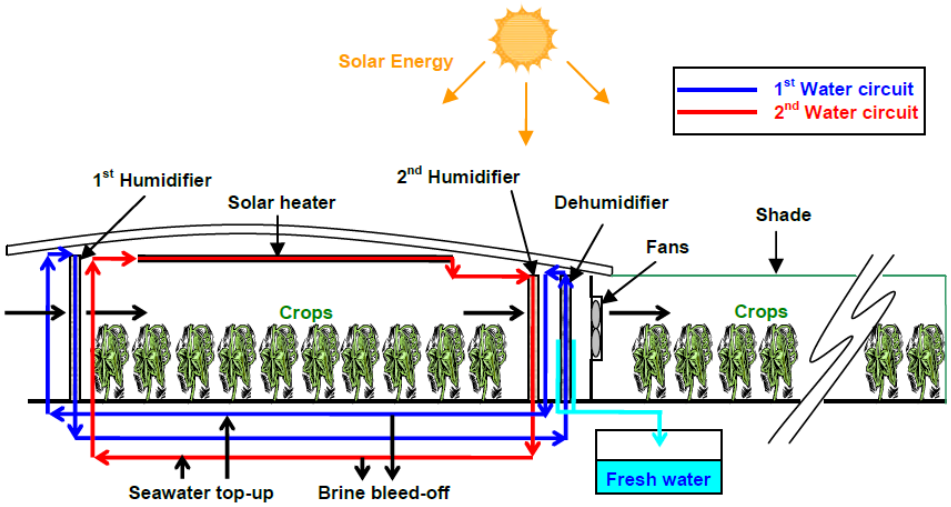


Figure 22. Illustration of the two water circuits of the HD GH in Oman [332].

In Oman, Al-Ismaili [332] explored the HD thought in a Quonset GH (Figure 23). He explored the achievability of using such innovation to make water systems water utilizing GHs around the country. The examination's discoveries were significant. The shortfall of critical build-up was ascribed to the moderately high air speed (more than 2.4 m/s) through the little cross-sectional space of the dehumidifiers because the coolant temperature (for example water from the cooling cushions) was consistently underneath the dew-point temperature (for example build-up was hypothetically conceivable) (0.9 m × 0.9 m) [287,332].

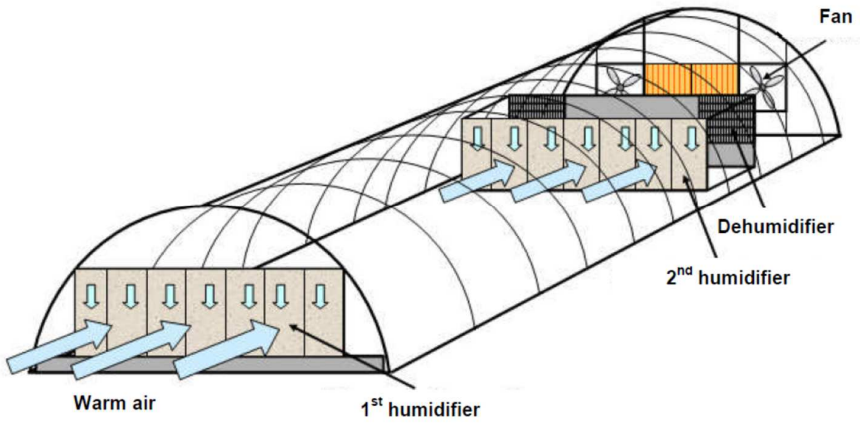


Figure 23. Illustration of the GH. Reproduced with permission from J. S. Perret, A. M. Al-Ismaili, S. S. Sablani, Biosystems Engineering Journal, published by Elsevier, 2005 [287].

However, GHs built on the HD concept can have certain drawbacks. When the outside RH is high (in a given area), evaporative cooling becomes inefficient because the ambient air's wet-bulb temperature rises [340]. As a result, the high temperatures and solar gains result in heightened temperatures within the GH, particularly during the summer. These traditional GHs must shut down for 3–4 months, which makes them economically unviable [24]. As a result, many solutions for reducing the GH cooling demand have been developed, including radiation filters and fluid roof coverings [341].

In this context, decreasing the GH's cooling burden by pumping fluid through the roof while allowing some radiation to pass provides a potential solution to the GH's high temperatures. Chaibi and Jilar [342] investigated the impact of water passing through the

GH cover's double glass sheet. The double glass roof minimised transmission by partly absorbing solar energy that was used to evaporate salty water. Condensate was collected from the evaporated water and used to irrigate the crops. Abdel-Ghany et al. [341] used a thermodynamic model to investigate the influence of the fluid roof on GH temperature. The model's results indicated that the fluid roof might lower the GH's temperature by up to 5 °C when compared to the ambient temperature. Another option for filtering incident irradiance is to employ SSs, which use solar energy to generate fresh water. Other researchers [343–345] investigated solar stills running under comparable circumstances and found exergy efficiencies of around 5%. However, few studies have combined an SS with an HD system and a GH unit to provide optimal growth conditions and adequate irrigation water for crops. Mamouri et al. [346] designed a GH equipped with light-splitting solar panels in order to lower GH's cooling demand. The HD unit was filled with heated water from the SS since the system provided 85% of the water necessary for tomato cultivation. Rabhy et al. [347] created a greenhouse with an integrated transparent solar distiller. The solar distiller used the absorbed energy to generate 37.5% of the required water and lowered GH cooling power usage by 60%.

Mahmood and Al-Ansari [348] created a solar-powered HD-based GH system for dry locations. The GH maintained an optimal temperature and RH, while the HD system-generated water at a rate of 17.5–27.3 m^3/day. Sajid and Bicer [349] designed a sustainable GH system that consisted primarily of an ETC, a multistage desalination unit, an absorption cooling cycle (ACS), thermal energy storage (TES), and PV thermal (PV/T). The PV/T reduced cooling demand by using spectrum selective nanofluids in the GH roof. The results indicated that by feeding the selective nanofluid through the GH's roof, the cooling demand was lowered by roughly 26%. Mahmood et al. [350] designed a solar-powered integrated system for an off-grid GH in a similar manner. The system generated power, water, space cooling, and oxygen as outputs with a 41.0% energy and 28.4% exergy efficiency.

El-Awady et al. [248] constructed a GH with a width of 4 m, a length of 10 m, and a height of 2 m. The evaporator was built domestically in Egypt using water-absorbent polymers that created a wet thin layer that could be evaporated using hot and dry air. The condenser was composed of one horizontal copper header tube and ten vertical risers finished with a metal sheet. Desalinated water was used to irrigate 40 m^2 GH areas at a rate of 100 L/d. In Egypt, HD productivity was around 2.5 L/d/m^2 [248].

When creating natural administration frameworks for yields and creatures, horticultural specialists should comprehend the physical and thermodynamic attributes of sodden air, as per Mangold et al. [351]. Goosen et al. [328] underlined the need of knowing GH thermodynamics to further develop HD activities. Therefore, by having careful information on the thermodynamic cycles that happen in the HD GH, the analyst might set aside both cash and time before continuing with real forms and examinations. Numerical re-enactment models might be incredibly valuable in measuring the basic boundaries engaged with the HD GH's thermodynamic cycles.

Zarei et al. [352] used artificial neural networks to study the influence of the width and length of GH, the height of the first evaporator and the transparency of the roof on the water production and the energy consumption of a GH water method. An appropriate structure was obtained for this method, and the statistics RE, RMSE, and R2 were used to evaluate the performance of the network. The method and the experimental data show a good corresponding relationship. Using the prepared optimisation network, the influence of each parameter on water production and energy consumption was checked because the parameter values vary widely. Finally, a 125 m wide and 200 m long GH with a 4 m high evaporator and a permeability of 0.6 was found to be the best configuration, providing 161.6 cubic meters of daily water production, and each cubic meter of water produced consumed 1558 kWh of Energy.

Zarei and Behyad [353] used artificial neural networks to test the effective parameters of GH for fresh water production, such as the width, length, and height of the front evaporator and the transparency of the roof. A suitable structure was obtained for the

multilayer perceptron method (MLP) and mathematical statistics RE, RMSE, and R2 were used to evaluate the performance of the network. This method agrees with the experimental data. Using the optimised network, the impact of each parameter on the fresh water produced was evaluated. Finally, a GH with a width of 125 m and a length of 200 m was introduced. The front evaporator height was 4 m and the roof transparency was 0.6, which can produce 161.6 m^3/day of fresh water as the best GH of seawater.

Various types of controlled climate systems offer appropriate conditions for heating, cooling, lighting, irrigation, dehumidification, and CO_2 concentration, depending on the temperature of a specific area, the kind of crop being grown, and the GH structure [354,355]. Tropical and dry locations, for example, offer significant solar resources for agricultural cultivation. However, because of the severe temperatures and RH, cooling measures such as forced ventilation, evaporative cooling, fogging, screening, shade, and heat pumps are necessary to maintain optimum growth conditions [356,357]. On the other hand, colder areas acquire less sunlight and have lower ambient temperatures, necessitating heating to maintain optimal growth conditions [356]. In the majority of circumstances, the energy needed to heat cold climate GHs is proportional to latitude: the higher the latitude, the greater the energy demand [355]. Additionally, supplemental illumination is sometimes necessary for crops cultivated in northern GHs where sun radiation is inadequate for photosynthesis [357].

6. By-Product Treatment Subsystem

During the desalination process, a by-product known as brine is created [358]. This concentrated solution contains seawater with salt levels 1.6 to 2 times greater than seawater (36 g/L NaCl), as well as any chemicals employed in the pre-treatment and post-treatment stages (NaOCl, $FeCl_3$, $AlCl_3$, H_2SO_4, HCl, $NaHSO_3$, and scale inhibitors). Even though all desalination methods have a negative environmental effect, brine saltiness tends to be greater with the MSF and MED techniques. In MSF and MED, brine is blended with cool water before discharge to minimise salt concentrations [359]. In addition, the temperature of the ejected liquid must be taken into account as well. A rise in discharge temperature of up to 1.82 times greater than the MD technology may be achieved with the MSF and MED procedures by contacting the brine with the surrounding environment.

According to a United Nations-sponsored study, Jones et al. [360] published a report in 2019 titled 'The state of desalination and brine production: a global outlook,' in which they highlight the advantages of providing drinking water from desalination plants while also pointing out the numerous drawbacks. Economic and technological challenges in brine management are also highlighted in the report. Most desalination facilities (80% of them globally) dump untreated concentrate straight into nature. According to Jones and colleagues, there are several ways to overcome these difficulties, such as using brine to grow fish that are resistant to salinity, as well as commercially recovering salt and metals from brine. Using any of the aforementioned treatment procedures may generate revenue from these ancillary activities.

Brine removal is a major source of environmental concern since it raises soil salinity, affects marine life at its discharge point, and contains chemical products and corrosion metals including Copper (Cu), Nickel (Ni), Chromium (Cr), Ferrous (Fe), and molybdenum (Mo). In contrast to saline from a single desalination plant, which would have little influence on the marine ecosystem, brine from several plants running nearby for extended periods might have negative effects [361]. It was for this reason that research conducted in 2015 [361] by Gall and Thompson, and more recently in 2018 [362] by Al-Shammari and Ali, proved the negative impact seawater salinity increases have on marine life. Brine discharge into the ocean is avoided by copious marine currents and is of an acceptable magnitude, resulting in little consequences on marine animals [363].

In light of the foregoing, a variety of disposal strategies have been suggested and developed in this research. Desalination's environmental effect must be minimised, thus it's critical to figure out the best way to do it. These include the amount, quality and

composition of brine in the desalination plant as well as other criteria such as geographic location, the availability of space for discharge, public acceptability, operational costs, and the capability for future expansions [364]. The dilution approach involves adding another liquid to the brine to dilute its salt content, while the concentration method makes use of direct solar radiation to remove the brine or turn it into another by-product (see Table 12) [365].

Table 12. Classification of current brine disposal techniques.

Method Family	Technique
Dilute	Surface water discharge Sewer discharge Deep-well injection Land application
Concentrate	Evaporation ponds Zero liquid discharge (ZLD)

Costs to remove brine range from 5% to 33% of the entire process cost and rely on a variety of factors, such as the technology used, volume, and properties of brine, treatment level, and disposal location [366]. The desalination process may employ any kind of water as long as the brine composition is appropriate to prevent pollution of the receiving body of water [367]. Although the various salt disposal methods minimise their effect, they do not totally solve the issue until the by-product of the brine disposal process can be reintegrated into the economic cycle.

In sum, pumping systems are required to dilute brine in desalination plants, and the size of these systems depends on how much salt they remove from water. The evaporation points concentration systems, on the other hand, use solar radiation as a power source, whereas the zero liquid discharge (ZLD) method has a high energy consumption, ranging from 5.1 kWh/m^3 to 67 kWh/m^3 of treated water depending on the technology used [368]. Finally, Table 13 summarises the implementation costs [369] associated with the various brine treatment procedures.

Table 13. Illustrates the cost ranges associated with the installation of various brine treatment procedures. Reproduced with permission from Shefaa Mansour, Hassan A. Arafat, Shadi W. Hasan, Desalination Sustainability Journal, published by Elsevier, 2017 [370].

Method	Implementation Cost Range
Surface water discharge	0.05 to 0.3 USD/m^3
Sewer discharge	0.32 to 0.66 USD/m^3
Deep-well injection	0.54 to 2.65 USD/m^3
Evaporation ponds	3.28 to 10.04 USD/m^3
Land application	0.74 to 1.95 USD/m^3

7. Recent Advancements in HD Desalination Systems

The use of the fogging nozzles technique with a droplet size of 20-μ in an HD desalination system was investigated experimentally by Alrbai et al. [371]. The technology of fogging nozzles was able to significantly minimise entropy generation and energy consumption. With a minimal entropy generation of 0.235 kJ/kg K, a maximum GOR of 3.4 was achieved. Energy and exergy analyses were used to determine the system's performance.

El-Said et al. [372] conducted experiments to explore the integration of solar water desalination using HD methods with a cooling system and a hot air flow rate. Where the relative humidity approached 100%, a porous activated carbon tube was employed as a humidifier, and the cooling system was used as a dehumidifier. The highest daily output of fresh water is 6.12 kg/d. Energy and exergy efficiency, as well as the GOR, were 26.73%

and 1.57%, and 1.24, respectively. According to economic calculations, the cost of fresh water is USD 0.01386/L.

An HD-vapour compression refrigeration (HD-VCR) cycle has been combined to fulfil fresh water, space cooling, and hot water requirements while using the least amount of floor space possible [373]. The intended outputs of the refrigeration and heat pump cycles are heat absorption and heat rejection, respectively. To create the appropriate outputs in the proposed HD-VCR, a water-cooled condenser for humidification and an evaporator for dehumidification are utilised concurrently. Through parametric analysis, the evaporator temperature was tuned to maximise the energy performance ratio (EPR) of the cycle and plant. Maximum cycle EPR requires a lower evaporator temperature than maximum plant EPR. The optimal evaporator temperature increases as the temperature of the hot water, the temperature of the ambient air, and the RH of the ambient air rise. At 100 m^3/h and a hot water supply temperature of 50 °C, the area of the solar PV plant and the area of the SWH are practically identical at 14.23 m^2 and 11.74 m^2, respectively. In these circumstances, the EPR of the HDH-VCR cycle is 1.80.

Rafiei [374] performed an HD combined with a thermal PV system for the purpose of producing fresh water and power. They developed a novel sort of solar collector: a dish concentrator with a conical cavity receiver as the primary source of heat. Additionally, solar PV thermal was employed as a supplementary thermal energy source to pre-heat salt water. They also investigated the impact of several nanofluids as working fluids for the heating process, including Cu/oil, CuO/oil, Al_2O_3/oil, TiO_2/oil, and MWCNT/oil. Kolahi et al. [375] combined an organic Rankin cycle with an HD desalination system in a series and parallel arrangement to generate both fresh water and electricity. The hybrid system generated fresh water at a rate of 3.93 L/s and a total work output of 5.72 MW through parallel and series arrangements, respectively.

There is a novel arrangement for the cogeneration of electricity and distilled water by using thermal energy stored in the lower convective zone (LCZ) of a solar pond with a salinity gradient (SGSP) [376]. A Kalina cycle (KC), an HD unit, and two thermoelectric generators (TEGs) are included in the proposed system. The findings of multi-objective optimisation indicate that the energy utilisation factor (EUF), exergy efficiency, and total unit cost of the product (TUCP) may all be increased by 14.09%, 5.5%, and 27.93%, respectively, over the base case. The optimal EUF, exergy efficiency, and TUCP values were 0.756, 27.7%, and 30.54 USD/GJ, respectively, when the proposed power/desalination system was designed with the following design parameters: solar pond area of 15,326 m^2, LCZ thickness of 1.65 m, NCZ thickness of 1.35 m, UCZ thickness of 0.35 m, LCZ temperature of 370 K, figure of merit of 2.45, desalination flow ratio of 2.45 The example study determined that between 20 March and 20 April, the system generates the least amount of fresh water, 0.152 m^3/h. On the contrary, between 21 June and 21 July, the greatest volume of distilled water is available. Additionally, the optimal period to operate the system to create distilled water and power simultaneously is from 21 May to 21 August.

Qasem et al. [155] investigated the HD in combination with a double-effect absorption refrigeration cycle that was fuelled by a low heat energy source (solar collector and waste heat), while the heat outlet/rejected from this system was utilised to heat the salt water. In comparison to the traditional HD, the hybrid system improved performance by about 2.21 times in terms of fresh water productivity, 2.20 times in terms of GOR, and 8.24 times in terms of fresh water cost reduction. Sachdev et al. [377] heated the air in their HD using a double-pass solar collector. The system was linked with the wind tower system in this research to generate fresh water and air inside the comfort zone. In comparison to alternative heat sources, employing a heat pump cycle to heat HD desalination systems significantly enhanced GOR (GOR = 4.17) [378].

8. Suggestions for Further Work

Examining the contributions of prior research in the area of HD desalination reveals some recommendations for future research.

- When it comes to humidification, the potential for cost-effective, superior hydrophilic packing materials such as cotton (water absorption capacity of 27 times) [379,380] and polyvinyl alcohol (PVA) (water absorption capacity of 12 times) [381] has not been fully explored;
- Optimising the baffle arrangement and roughening the surface of PV waste heat-powered HD systems may increase the heat recovery rate due to the increased surface area [382]. As a result, the HD efficiency is increased;
- When economic, structural, and manufacturing considerations are made, wall condensation dehumidifiers may be a more efficient alternative to traditional dehumidifiers; nevertheless, their performance in HD systems has not been evaluated [383]. Similarly, adsorptive dehumidification of desiccant material may lead to an energy-efficient yield [384];
- A hybrid waste heat-powered solar PV–HVAC–HD system might be constructed to operate throughout the day and night. Additionally, leftover thermal energy might be retained and used via the use of an efficient thermal energy storage (TES) unit equipped with fins and nano/microparticles [385,386];
- In terms of thermal performance, nanocoating the dehumidifier tube surface with efficient thermally conductive materials such as TiO_2, CuO, and CNTs improves surface heat transfer, hence increasing the dehumidifier's efficacy [387];
- Extensive research on HD desalination systems in combination with PV panels that can be cooled with either air or water reveals that the heat rejected by the solar panels is utilised to heat the water in this arrangement;
- When HD is combined with hybrid energy, both GOR and the cost of fresh water production improve. As a result, research into such systems must be broadened;
- HD powered by geothermal, or biomass energy sources may have a beneficial effect on the environment and increase the performance of desalination systems;
- Water desalination may become economically viable by using waste heat from power plants or industrial activities as a source of heat for HD;
- To achieve saturated air following the humidifier, the contact duration between water and air must be enhanced by adding packing to the bubble column humidifier during the humidification process;
- Exergy analysis is necessary for the proposed HD desalination systems that include external energy sources and multi-effect desalination plants;
- Nuclear energy is used to desalinate salt water;
- The majority of successful implementations used solar collectors to heat salt water before adding it to the humidification chamber, whereas minimal research was conducted on air heating before adding it to the humidifier. As a result, more research into the HD system powered by solar energy for air heating is necessary.

9. Conclusions

Green desalination has built a dependable business utilising fewer chemicals and cleaning chemicals. Concerning low-cost renewable energy, solar energy in particular is now accessible to tackle renewable energy-related challenges [388]. The seawater greenhouse (SWGH) configuration is a novel concept in the agricultural field for the production of fresh water that has recently been developed for irrigation and drinking purposes. The SWGH desalination technology is a sort of desalination plant that reproduces the water cycle through seawater evaporation and condensation into fresh water (the HD concept). The SWGH system is the most suitable technology for arid and remote regions, especially in the coastal zones of the Middle East and Northern Africa.

Meanwhile, the FPC for WH is the most often utilised device in the HD system, accounting for 61% of this desalination system [389]. The FPC's low temperature may be readily enhanced by employing reflectors [390], which increase absorbed solar radiation by up to 80% when top, bottom, right, and lift reflectors are utilised.

One of HD's primary disadvantages is the limited mass and heat transmission between the salty water and the surrounding air. Numerous ways have been explored to address this issue, including the humidifier's use of wick, treated cellulose paper, corrugated cellulosic material, and wooden slates. Additionally, the air bubble basin humidifier demonstrated effective performance due to its wide surface area for heat transmission between water and air [391].

HD heated with FPC has the potential to provide an ideal worldwide solution for the disposal of high salinity industrial water. This visibility is based on four HD characteristics: it is capable of operating in excessively salty water, has a basic design, and is free of biological fouling or silt [309].

There are few active SWGHs around the world, but considering the global climatic conditions, global warming, reduced fresh water resources, and increased world population growth, their applications will be extended.

HD can be used for seawater or brackish water desalination to obtain sustainable GH and can also aid recirculation to partially restore excess moisture in the GH cavity, especially in hot and dry countries. Thus, proper circumstances are critical in guaranteeing a greenhouse's outstanding functioning.

Author Contributions: Conceptualization, N.G. and M.M.E.; methodology, M.M.E. and A.A.E.-B.; validation, N.G., N.B., M.M.E. and G.E.H.; formal analysis, M.M.E. and N.G.; investigation, M.M.E. and N.G.; resources, A.B.; data curation, M.M.E. and A.B.; writing—original draft preparation, M.M.E. and N.G.; writing—review and editing, A.B. and A.A.E.-B.; visualization, M.M.E.; supervision, M.M.E. and A.A.E.-B.; project administration, N.G. and M.M.E.; funding acquisition, N.G. and A.B. All authors have read and agreed to the published version of the manuscript.

Funding: This research is funded by Deputyship for Research & Innovation, Ministry of Education in Saudi Arabia, grant/project number RDO-503.

Data Availability Statement: All the data generated or analysed is contained in this article.

Acknowledgments: The authors extend their appreciation to the Deputy of Research & Innovation, Ministry of Education in Saudi Arabia for funding this research work through project number RDO-503.

Conflicts of Interest: The authors declare no conflict of interest. The funders had no role in the design of the study; in the collection, analyses, or interpretation of data; in the writing of the manuscript, or in the decision to publish the results.

Abbreviations

ACS	Absorption cooling cycle
AH	Air-heated
CDI	Capacitive deionisation
CWCA	Closed-water closed-air
CWOA	Closed-water open-air
DPSC	Dual purpose solar collector
EDI	Electrodeionisation
ED	Electrodialysis
EDR	Electrodialysis reversal
EPR	energy performance ratio
F	Energy reuse factor
EUF	Energy usage factor
ETC	Evacuated tube collectors
FTHE	Finned tube heat exchanger
FPC	Flat plate collector
FO	Forward osmosis

FFWP	four-fold web plate collector
FLC	Fresnel lens collector
GOR	Gain output ratio
GH	Greenhouse
GHG	Greenhouse gases
HD-VCR	HD-vapour compression refrigeration
HE	Heat exchanger
HTF	Heat transfer fluid
HVAC	Heating, ventilation, and air conditioning
HD	Humidification–dehumidification
KC	Kalina cycle
LDPE	Low-density polyethylene
LCZ	Lower convective zone
MR	Mass flow rate ratio
MD	Membrane distillation
MED	Multi-effect distillation
MEHD	Multi-effect HD
MLP	Multilayer perceptron method
MSF	Multi-stage flash
NF	Nanofiltration
NIR	Near-infrared
NCZ	Non-convecting zone
OWCA	Open-water closed-air
OWOA	Open-water open-air
PTC	Parabolic trough collectors
ppm	Parts per million
PCM	Phase change material
PAR	Photosynthetically active radiation
PV/T	Photovoltaic/thermal
PM	Porous material
RR	Recovery ratio
RH	Relative humidity
RO	Reverse osmosis
SEEC	Specific electrical energy consumption (kWh/m^3)
SGSP	Salinity gradient solar pond
SWGH	Seawater greenhouse
SSP	shallow SP
STHE	Shell and tube heat exchanger
SMCE	Solar multiple condensation evaporation cycle (SMCEC)
SP	Solar pond
SS	Solar still
SEC	Specific energy consumption
S_{gen}	Specific entropy generation.
TES	Thermal energy storage
TEGs	Thermoelectric generators
TDS	Total dissolved solids
TUCP	Total unit cost of the product
UV	Ultraviolet
UCZ	Upper convecting zone
VC	Vapour compression
VCR	Vapour compression refrigeration
WH	Water-heated
ZLD	Zero liquid discharge

References

1. Eltawil, M.A.; Zhengming, Z.; Yuan, L. A review of renewable energy technologies integrated with desalination systems. *Renew. Sustain. Energy Rev.* **2009**, *13*, 2245–2262. [CrossRef]
2. UN-Water. UN-Water Annual Report 2021. Available online: https://www.unwater.org/publications/un-water-annual-report-2021/ (accessed on 17 July 2022).
3. Hamoda, M.F. Desalination and water resource management in Kuwait. *Desalination* **2001**, *138*, 385–393. [CrossRef]
4. Ayoub, J.; Alward, R. Water requirements and remote arid areas: The need for small-scale desalination. *Desalination* **1996**, *107*, 131–147. [CrossRef]
5. Arnell, N.W. Climate change and global water resources: SRES emissions and socio-economic scenarios. *Glob. Environ. Chang.* **2004**, *14*, 31–52. [CrossRef]
6. Kalogirou, S.A. Seawater desalination using renewable energy sources. *Prog. Energy Combust. Sci.* **2005**, *31*, 242–281. [CrossRef]
7. AltEnergyMag. Advancements in Desalination Using Solar Energy. Available online: https://www.altenergymag.com/article/2021/02/advancements-in-desalination-using-solar-energy/34562 (accessed on 16 July 2022).
8. Hürdoğan, E.; Kara, O. Performance assessment of a desalination system integrated with ground heat exchanger for hydrogen and fresh water production. *Environ. Prog. Sustain. Energy* **2022**, *41*, e13745. [CrossRef]
9. El-Ghonemy, A.M.K. Water desalination systems powered by renewable energy sources: Review. *Renew. Sustain. Energy Rev.* **2012**, *16*, 1537–1556. [CrossRef]
10. Ahmed, F.E.; Hashaikeh, R.; Hilal, N. Solar powered desalination—Technology, energy and future outlook. *Desalination* **2019**, *453*, 54–76. [CrossRef]
11. Ghiat, I.; Mahmood, F.; Govindan, R.; Al-Ansari, T. CO_2 utilisation in agricultural greenhouses: A novel 'plant to plant' approach driven by bioenergy with carbon capture systems within the energy, water and food Nexus. *Energy Convers. Manag.* **2021**, *228*, 113668. [CrossRef]
12. Fath, H.E.B.S. Desalination and Greenhouses. In *Handbook of Environmental Chemistry*; Negm, A.M., Ed.; Springer International Publishing: Cham, Switzerland, 2019; Volume 75, pp. 455–483, ISBN 978-3-319-95071-6.
13. Mahmood, F.; Govindan, R.; Bermak, A.; Yang, D.; Khadra, C.; Al-Ansari, T. Energy utilization assessment of a semi-closed greenhouse using data-driven model predictive control. *J. Clean. Prod.* **2021**, *324*, 129172. [CrossRef]
14. Kumar, K.S.; Tiwari, K.N.; Jha, M.K. Design and technology for greenhouse cooling in tropical and subtropical regions: A review. *Energy Build.* **2009**, *41*, 1269–1275. [CrossRef]
15. Chand Singh, M.; Singh, J.P.; Kumar Pandey, S.; Gladwin Cutting, N.; Sharma, P.; Shrivastav, V.; Sharma, P. A Review of Three Commonly Used Techniques of Controlling Greenhouse Microclimate. *Int. J. Curr. Microbiol. Appl. Sci.* **2018**, *7*, 3491–3505. [CrossRef]
16. Taiz, L.; Zeiger, E.; Møller, I.M.; Murphy, A. *Plant Physiology and Development*, 5th ed.; Taiz, L., Zeiger, E., Møller, I.M., Murphy, A., Eds.; Sinauer Associates Incorporated: Sunderland, MA, USA, 2010; Volume 1, ISBN 9780878938667.
17. Chalabi, Z.S.; Bailey, B.J.; Wilkinson, D.J. A real-time optimal control algorithm for greenhouse heating. *Comput. Electron. Agric.* **1996**, *15*, 1–13. [CrossRef]
18. Paulsen, G.M. High Temperature Responses of Crop Plants. In *Physiology and Determination of Crop Yield*; American Society of Agronomy: Madison WI, USA, 1994; pp. 365–389.
19. Guzman-Plazola, R.A.; Davis, R.M.; Marois, J.J. Effects of relative humidity and high temperature on spore germination and development of tomato powdery mildew (*Leveillula taurica*). *Crop Prot.* **2003**, *22*, 1157–1168. [CrossRef]
20. Burn, S.; Hoang, M.; Zarzo, D.; Olewniak, F.; Campos, E.; Bolto, B.; Barron, O. Desalination techniques—A review of the opportunities for desalination in agriculture. *Desalination* **2015**, *364*, 2–16. [CrossRef]
21. Sethi, V.P.; Sharma, S.K. Survey and evaluation of heating technologies for worldwide agricultural greenhouse applications. *Sol. Energy* **2008**, *82*, 832–859. [CrossRef]
22. Soussi, M.; Chaibi, M.T.; Buchholz, M.; Saghrouni, Z. Comprehensive Review on Climate Control and Cooling Systems in Greenhouses under Hot and Arid Conditions. *Agronomy* **2022**, *12*, 626.
23. Wang, H.; Li, W.; Yue, Y.; Zhao, H. Distributed Economic Control for AC/DC Hybrid Microgrid. *Electronics* **2021**, *11*, 13. [CrossRef]
24. Linker, R.; Kacira, M.; Arbel, A. Robust climate control of a greenhouse equipped with variable-speed fans and a variable-pressure fogging system. *Biosyst. Eng.* **2011**, *110*, 153–167. [CrossRef]
25. Mahmood, A.; Hu, Y.; Tanny, J.; Asante, E.A. Effects of shading and insect-proof screens on crop microclimate and production: A review of recent advances. *Sci. Hortic.* **2018**, *241*, 241–251. [CrossRef]
26. Heidari, A.; Roshandel, R.; Vakiloroaya, V. An innovative solar assisted desiccant-based evaporative cooling system for co-production of water and cooling in hot and humid climates. *Energy Convers. Manag.* **2019**, *185*, 396–409. [CrossRef]
27. Mahmood, F.; Govindan, R.; Yang, D.; Bermak, A.; Al-Ansari, T. Forecasting cooling load and water demand of a semi-closed greenhouse using a hybrid modelling approach. *Int. J. Ambient Energy* **2022**, 1–50. [CrossRef]
28. Paton, C.; Davies, P. The Seawater Greenhouse Cooling, Fresh Water and Fresh Produce from Seawater. In Proceedings of the 2nd Internatioanl Conference on Water Resources & Arid Environment, Riyadh, Saudi Arabia, 26–29 November 2006; pp. 1–16.
29. Mahmoudi, H.; Spahis, N.; Abdul-Wahab, S.A.; Sablani, S.S.; Goosen, M.F.A. Improving the performance of a Seawater Greenhouse desalination system by assessment of simulation models for different condensers. *Renew. Sustain. Energy Rev.* **2010**, *14*, 2182–2188. [CrossRef]

30. Ghazi, Z.M.; Rizvi, S.W.F.; Shahid, W.M.; Abdulhameed, A.M.; Saleem, H.; Zaidi, S.J. An overview of water desalination systems integrated with renewable energy sources. *Desalination* **2022**, *542*, 116063. [CrossRef]
31. Al-Ismaili, A.M.; Jayasuriya, H. Seawater greenhouse in Oman: A sustainable technique for freshwater conservation and production. *Renew. Sustain. Energy Rev.* **2016**, *54*, 653–664. [CrossRef]
32. Ali, M.T.; Fath, H.E.S.; Armstrong, P.R. A comprehensive techno-economical review of indirect solar desalination. *Renew. Sustain. Energy Rev.* **2011**, *15*, 4187–4199. [CrossRef]
33. Eltawil, M.A.; Zhengming, Z. Wind turbine-inclined still collector integration with solar still for brackish water desalination. *Desalination* **2009**, *249*, 490–497. [CrossRef]
34. Narayan, G.P.; Sharqawy, M.H.; Summers, E.K.; Lienhard, J.H.; Zubair, S.M.; Antar, M.A. The potential of solar-driven humidification–dehumidification desalination for small-scale decentralized water production. *Renew. Sustain. Energy Rev.* **2010**, *14*, 1187–1201. [CrossRef]
35. Parekh, S.; Farid, M.M.; Selman, J.R.; Al-Hallaj, S. Solar desalination with a humidification-dehumidification technique—A comprehensive technical review. *Desalination* **2004**, *160*, 167–186. [CrossRef]
36. Maia, C.B.; Silva, F.V.M.; Oliveira, V.L.C.; Kazmerski, L.L. An overview of the use of solar chimneys for desalination. *Sol. Energy* **2019**, *183*, 83–95. [CrossRef]
37. Zuo, L.; Zheng, Y.; Li, Z.; Sha, Y. Solar chimneys integrated with sea water desalination. *Desalination* **2011**, *276*, 207–213. [CrossRef]
38. Mezher, T.; Fath, H.; Abbas, Z.; Khaled, A. Techno-economic assessment and environmental impacts of desalination technologies. *Desalination* **2011**, *266*, 263–273. [CrossRef]
39. Midilli, A.; Ayhan, T. Natural vacuum distillation technique—Part I: Theory and Basics. *Int. J. Energy Res.* **2004**, *28*, 355–371. [CrossRef]
40. Kasaeian, A.; Rajaee, F.; Yan, W.-M. Osmotic desalination by solar energy: A critical review. *Renew. Energy* **2019**, *134*, 1473–1490. [CrossRef]
41. Shalaby, S.M. Reverse osmosis desalination powered by photovoltaic and solar Rankine cycle power systems: A review. *Renew. Sustain. Energy Rev.* **2017**, *73*, 789–797. [CrossRef]
42. Colangelo, A.; Marano, D.; Spagna, G.; Sharma, V.K. Photovoltaic powered reverse osmosis sea-water desalination systems. *Appl. Energy* **1999**, *64*, 289–305. [CrossRef]
43. Herold, D.; Neskakis, A. A small PV-driven reverse osmosis desalination plant on the island of Gran Canaria. *Desalination* **2001**, *137*, 285–292. [CrossRef]
44. Peñate, B.; García-Rodríguez, L. Current trends and future prospects in the design of seawater reverse osmosis desalination technology. *Desalination* **2012**, *284*, 1–8. [CrossRef]
45. Reif, J.H.; Alhalabi, W. Solar-thermal powered desalination: Its significant challenges and potential. *Renew. Sustain. Energy Rev.* **2015**, *48*, 152–165. [CrossRef]
46. Manolakos, D.; Papadakis, G.; Mohamed, E.S.; Kyritsis, S.; Bouzianas, K. Design of an autonomous low-temperature solar Rankine cycle system for reverse osmosis desalination. *Desalination* **2005**, *183*, 73–80. [CrossRef]
47. El Batouti, M.; Alharby, N.F.; Elewa, M.M. Review of New Approaches for Fouling Mitigation in Membrane Separation Processes in Water Treatment Applications. *Separations* **2021**, *9*, 1. [CrossRef]
48. Ortiz, J.M.; Expósito, E.; Gallud, F.; García-García, V.; Montiel, V.; Aldaz, A. Electrodialysis of brackish water powered by photovoltaic energy without batteries: Direct connection behaviour. *Desalination* **2007**, *208*, 89–100. [CrossRef]
49. Naim, M.M.; El Batouti, M.; Elewa, M.M. Novel heterogeneous cellulose-based ion-exchange membranes for electrodialysis. *Polym. Bull.* **2022**, *79*, 9753–9777. [CrossRef]
50. Byrne, P.; Fournaison, L.; Delahaye, A.; Ait Oumeziane, Y.; Serres, L.; Loulergue, P.; Szymczyk, A.; Mugnier, D.; Malaval, J.L.; Bourdais, R.; et al. A review on the coupling of cooling, desalination and solar photovoltaic systems. *Renew. Sustain. Energy Rev.* **2015**, *47*, 703–717. [CrossRef]
51. Qtaishat, M.R.; Banat, F. Desalination by solar powered membrane distillation systems. *Desalination* **2013**, *308*, 186–197. [CrossRef]
52. Alkhudhiri, A.; Darwish, N.; Hilal, N. Membrane distillation: A comprehensive review. *Desalination* **2012**, *287*, 2–18. [CrossRef]
53. Blanco Gálvez, J.; García-Rodríguez, L.; Martín-Mateos, I. Seawater desalination by an innovative solar-powered membrane distillation system: The MEDESOL project. *Desalination* **2009**, *246*, 567–576. [CrossRef]
54. Koschikowski, J.; Wieghaus, M.; Rommel, M. Solar thermal driven desalination plants based on membrane distillation. *Water Supply* **2003**, *3*, 49–55. [CrossRef]
55. El Batouti, M.; Al-Harby, N.F.; Elewa, M.M. A Review on Promising Membrane Technology Approaches for Heavy Metal Removal from Water and Wastewater to Solve Water Crisis. *Water* **2021**, *13*, 3241. [CrossRef]
56. Elsheniti, M.B.; Elbessomy, M.O.; Wagdy, K.; Elsamni, O.A.; Elewa, M.M. Augmenting the distillate water flux of sweeping gas membrane distillation using turbulators: A numerical investigation. *Case Stud. Therm. Eng.* **2021**, *26*, 101180. [CrossRef]
57. Naim, M.M.; Elewa, M.M.; Moneer, A.A.; El-Shafei, A.A. Desalination by directional freezing: An experimental investigation. *Desalin. Water Treat.* **2017**, *73*, 185–197. [CrossRef]
58. Attia, A.A.A. New proposed system for freeze water desalination using auto reversed R-22 vapor compression heat pump. *Desalination* **2010**, *254*, 179–184. [CrossRef]
59. DesalData. Available online: https://www.desaldata.com/forecasts/market-report (accessed on 18 July 2022).

60. Kabeel, A.E.; Hamed, M.H.; Omara, Z.M.; Sharshir, S.W. Water Desalination Using a Humidification-Dehumidification Technique—A Detailed Review. *Nat. Resour.* **2013**, *4*, 286–305. [CrossRef]
61. Patel, A.M.; Chokshi, H.S.; Sumant, M.M. A Review of Circular Solar Collector for Close-Water, Open-air (CWOA) air Heated Humidification and Dehumidification Process. *J. Basic Appl. Eng. Res.* **2014**, *1*, 10–16.
62. Bourouni, K.; Chaibi, M.T.; Tadrist, L. Water desalination by humidification and dehumidification of air: State of the art. *Desalination* **2001**, *137*, 167–176. [CrossRef]
63. Moumouh, J.; Tahiri, M.; Balli, L. Solar Desalination by Humidification-Dehumidification of Air. *MATEC Web Conf.* **2018**, *149*, 02092. [CrossRef]
64. Lawal, D.U.; Antar, M.A.; Aburub, A.; Aliyu, M. Performance assessment of a cross-flow packed-bed humidification–dehumidification (HDH) desalination system—The effect of mass extraction. *Desalin. Water Treat.* **2018**, *104*, 28–37. [CrossRef]
65. Abdel Dayem, A.M.; AlZahrani, A. Psychometric study and performance investigation of an efficient evaporative solar HDH water desalination system. *Sustain. Energy Technol. Assess.* **2022**, *52*, 102030. [CrossRef]
66. Rahimi-Ahar, Z.; Hatamipour, M.S.; Ahar, L.R. Air Humidification-Dehumidification Process for Desalination: A review. *Prog. Energy Combust. Sci.* **2020**, *80*, 100850. [CrossRef]
67. Santosh, R.; Kumaresan, G.; Selvaraj, S.; Arunkumar, T.; Velraj, R. Investigation of humidification-dehumidification desalination system through waste heat recovery from household air conditioning unit. *Desalination* **2019**, *467*, 1–11. [CrossRef]
68. Cao, F.; Liu, Q.; Xiao, H. Experimental Study of a Humidification-Dehumidification Seawater Desalination System Combined with the Chimney. *Int. J. Photoenergy* **2020**, *2020*, 1937040. [CrossRef]
69. Abutayeh, M.; Li, C.; Yogi Goswami, D.; Stefanakos, E.K. Solar Desalination. In *Desalination: Water from Water*; Kurchea, J., Ed.; John Wiley & Sons: Hoboken, NY, USA; Scrivener Publishing: Salem, MA, USA, 2014; pp. 549–581, ISBN 9781118904855.
70. Mohamed, A.S.A.; Ahmed, M.S.; Maghrabie, H.M.; Shahdy, A.G. Desalination process using humidification–dehumidification technique: A detailed review. *Int. J. Energy Res.* **2021**, *45*, 3698–3749. [CrossRef]
71. Mistry, K.H.; Mitsos, A.; Lienhard, J.H. Optimal operating conditions and configurations for humidification–dehumidification desalination cycles. *Int. J. Therm. Sci.* **2011**, *50*, 779–789. [CrossRef]
72. Chafik, E. A new type of seawater desalination plants using solar energy. *Desalination* **2003**, *156*, 333–348. [CrossRef]
73. Ghaffour, N.; Missimer, T.M.; Amy, G.L. Technical review and evaluation of the economics of water desalination: Current and future challenges for better water supply sustainability. *Desalination* **2013**, *309*, 197–207. [CrossRef]
74. Sharqawy, M.H.; Antar, M.A.; Zubair, S.M.; Elbashir, A.M. Optimum thermal design of humidification dehumidification desalination systems. *Desalination* **2014**, *349*, 10–21. [CrossRef]
75. Soufari, S.M.; Zamen, M.; Amidpour, M. Performance optimization of the humidification-dehumidification desalination process using mathematical programming. *Desalination* **2009**, *237*, 305–317. [CrossRef]
76. Siddiqui, O.K.; Sharqawy, M.H.; Antar, M.A.; Zubair, S.M. Performance evaluation of variable pressure humidification-dehumidification systems. *Desalination* **2017**, *409*, 171–182. [CrossRef]
77. Hamieh, B.M.; Beckman, J.R. Seawater desalination using Dewvaporation technique: Theoretical development and design evolution. *Desalination* **2006**, *195*, 1–13. [CrossRef]
78. Mistry, K.H.; Lienhard, J.H.; Zubair, S.M. Effect of entropy generation on the performance of humidification-dehumidification desalination cycles. *Int. J. Therm. Sci.* **2010**, *49*, 1837–1847. [CrossRef]
79. McGovern, R.K.; Thiel, G.P.; Prakash Narayan, G.; Zubair, S.M.; Lienhard, V.J. H. Performance limits of zero and single extraction humidification-dehumidification desalination systems. *Appl. Energy* **2013**, *102*, 1081–1090. [CrossRef]
80. Dehghani, S.; Date, A.; Akbarzadeh, A. An experimental study of brine recirculation in humidification-dehumidification desalination of seawater. *Case Stud. Therm. Eng.* **2019**, *14*, 100463. [CrossRef]
81. Hamed, M.H.; Kabeel, A.E.; El-Said, E.M.S. Enhancement of heat and mass transfer performance on humidification tower using injection of different carrier gases into water bed. *Appl. Therm. Eng.* **2017**, *111*, 455–476. [CrossRef]
82. Abu Arabi, M.K.; Reddy, K.V. Performance evaluation of desalination processes based on the humidification/dehumidification cycle with different carrier gases. *Desalination* **2003**, *156*, 281–293. [CrossRef]
83. Miller, J.A.; Lienhard, V.J.H. Impact of extraction on a humidification-dehumidification desalination system. *Desalination* **2013**, *313*, 87–96. [CrossRef]
84. Thanaiah, K.; Gumtapure, V.; Mitiku Tadesse, G. Experimental analysis on humidification-dehumidification desalination system using different packing materials with baffle plates. *Therm. Sci. Eng. Prog.* **2021**, *22*, 100831. [CrossRef]
85. Zarei, T.; Miroliaei, M.R. Performance evaluation of an HDH desalination system using direct contact packed towers: Experimental and mathematical modeling study. *J. Water Reuse Desalin.* **2022**, *12*, 92–110. [CrossRef]
86. El-Ashtoukhy, E.S.Z.; Abdel-Aziz, M.H.; Farag, H.A.; El Azab, I.H.; Sh. Zoromba, M.; Naim, M.M. An innovative unit for water desalination based on humidification dehumidification technique. *Alex. Eng. J.* **2022**, *61*, 8729–8742. [CrossRef]
87. He, W.F.; Yang, H.X.; Han, D. Thermodynamic analysis of a novel humidification dehumidification desalination system driven by heat pump. *Energy Procedia* **2019**, *158*, 6030–6037. [CrossRef]
88. Faegh, M.; Behnam, P.; Shafii, M.B. A review on recent advances in humidification-dehumidification (HDH) desalination systems integrated with refrigeration, power and desalination technologies. *Energy Convers. Manag.* **2019**, *196*, 1002–1036. [CrossRef]
89. Yuan, G.; Zhang, H. Mathematical modeling of a closed circulation solar desalination unit with humidification-dehumidification. *Desalination* **2007**, *205*, 156–162. [CrossRef]

90. Yamalı, C.; Solmus, İ. A solar desalination system using humidification–dehumidification process: Experimental study and comparison with the theoretical results. *Desalination* **2008**, *220*, 538–551. [CrossRef]
91. Amer, E.H.; Kotb, H.; Mostafa, G.H.; El-Ghalban, A.R. Theoretical and experimental investigation of humidification-dehumidification desalination unit. *Desalination* **2009**, *249*, 949–959. [CrossRef]
92. Hermosillo, J.-J.; Arancibia-Bulnes, C.A.; Estrada, C.A. Water desalination by air humidification: Mathematical model and experimental study. *Sol. Energy* **2012**, *86*, 1070–1076. [CrossRef]
93. Muthusamy, C.; Srithar, K. Energy and exergy analysis for a humidification-dehumidification desalination system integrated with multiple inserts. *Desalination* **2015**, *367*, 49–59. [CrossRef]
94. Al-Hallaj, S.; Farid, M.M.; Rahman Tamimi, A. Solar desalination with a humidification-dehumidification cycle: Performance of the unit. *Desalination* **1998**, *120*, 273–280. [CrossRef]
95. Nematollahi, F.; Rahimi, A.; Gheinani, T.T. Experimental and theoretical energy and exergy analysis for a solar desalination system. *Desalination* **2013**, *317*, 23–31. [CrossRef]
96. Nafey, A.S.; Fath, H.E.S.; El-Helaby, S.O.; Soliman, A. Solar desalination using humidification–dehumidification processes. Part II. An experimental investigation. *Energy Convers. Manag.* **2004**, *45*, 1263–1277. [CrossRef]
97. Bacha, H.B.; Damak, T.; Bouzguenda, M.; Maalej, A.Y. Experimental validation of the distillation module of a desalination station using the SMCEC principle. *Renew. Energy* **2003**, *28*, 2335–2354. [CrossRef]
98. Abdel Dayem, A.M. Experimental and numerical performance of a multi-effect condensation-evaporation solar water distillation system. *Energy* **2006**, *31*, 2710–2727. [CrossRef]
99. Abdel Dayem, A.M.; Fatouh, M. Experimental and numerical investigation of humidification/dehumidification solar water desalination systems. *Desalination* **2009**, *247*, 594–609. [CrossRef]
100. Abdel Dayem, A.M. Efficient solar desalination system using humidification/dehumidification process. *J. Sol. Energy Eng. Trans. ASME* **2014**, *136*, 41014. [CrossRef]
101. Boehm, R.F.; Kreith, F. Direct-Contact Heat Transfer Processes. In *Direct-Contact Heat Transfer*; Kreith, F., Boehm, R.F., Eds.; Springer: Berlin/Heidelberg, Germany, 1988; pp. 1–24.
102. Younis, M.A.; Darwish, M.A.; Juwayhel, F. Experimental and theoretical study of a humidification-dehumidification desalting system. *Desalination* **1993**, *94*, 11–24. [CrossRef]
103. Ben Amara, M.; Houcine, I.; Guizani, A.; Mâalej, M. Experimental study of a multiple-effect humidification solar desalination technique. *Desalination* **2004**, *170*, 209–221. [CrossRef]
104. Orfi, J.; Laplante, M.; Marmouch, H.; Galanis, N.; Benhamou, B.; Nasrallah, S.B.; Nguyen, C.T. Experimental and theoretical study of a humidification-dehumidification water desalination system using solar energy. *Desalination* **2004**, *168*, 151–159. [CrossRef]
105. Schmack, M.; Ho, G.; Anda, M. A bubble column evaporator with basic flat-plate condenser for brackish and seawater desalination. *Environ. Technol.* **2016**, *37*, 74–85. [CrossRef] [PubMed]
106. Rajaseenivasan, T.; Shanmugam, R.K.; Hareesh, V.M.; Srithar, K. Combined probation of bubble column humidification dehumidification desalination system using solar collectors. *Energy* **2016**, *116*, 459–469. [CrossRef]
107. Abd-Ur-rehman, H.M.; Al-Sulaiman, F.A.; Antar, M.A. Experimental analysis of solar driven multi-stage stepped bubbler humidifier for humidification-dehumidification (HDH) water desalination system. In Proceedings of the ASME 2016 10th International Conference on Energy Sustainability collocated with the ASME 2016 Power Conference and the ASME 2016 14th International Conference on Fuel Cell Science, Engineering and Technology, Charlotte, NC, USA, 26–30 June 2016; Volume 1.
108. Srithar, K.; Rajaseenivasan, T. Performance analysis on a solar bubble column humidification dehumidification desalination system. *Process Saf. Environ. Prot.* **2017**, *105*, 41–50. [CrossRef]
109. El-Agouz, S.A.; Abugderah, M. Experimental analysis of humidification process by air passing through seawater. *Energy Convers. Manag.* **2008**, *49*, 3698–3703. [CrossRef]
110. Khalil, A.; El-Agouz, S.A.; El-Samadony, Y.A.F.; Abdo, A. Solar water desalination using an air bubble column humidifier. *Desalination* **2015**, *372*, 7–16. [CrossRef]
111. Müller-Holst, H.; Engelhardt, M.; Herve, M.; Schölkopf, W. Solarthermal seawater desalination systems for decentralised use. *Renew. Energy* **1998**, *14*, 311–318. [CrossRef]
112. Zamen, M.; Soufari, S.M.; Vahdat, S.A.; Amidpour, M.; Zeinali, M.A.; Izanloo, H.; Aghababaie, H. Experimental investigation of a two-stage solar humidification-dehumidification desalination process. *Desalination* **2014**, *332*, 1–6. [CrossRef]
113. Chafik, E. Design of plants for solar desalination using the multi-stag heating/humidifying technique. *Desalination* **2004**, *168*, 55–71. [CrossRef]
114. Farid, M.M.; Parekh, S.; Selman, J.R.; Al-Hallaj, S. Solar desalination with a humidification-dehumidification cycle: Mathematical modeling of the unit. *Desalination* **2003**, *151*, 153–164. [CrossRef]
115. Nawayseh, N.K.; Farid, M.M.; Al-Hallaj, S.; Al-Timimi, A.R. Solar desalination based on humidification process—I. Evaluating the heat and mass transfer coefficients. *Energy Convers. Manag.* **1999**, *40*, 1423–1439. [CrossRef]
116. Bourouni, K.; Martin, R.; Tadrist, L.; Chaibi, M.T. Heat transfer and evaporation in geothermal desalination units. *Appl. Energy* **1999**, *64*, 129–147. [CrossRef]
117. Klausner, J.F.; Li, Y.; Darwish, M.; Mei, R. Innovative diffusion driven desalination process. *J. Energy Resour. Technol.* **2004**, *126*, 219–225. [CrossRef]

118. Zhang, G.; Wang, B.; Li, X.; Shi, W.; Cao, Y. Review of experimentation and modeling of heat and mass transfer performance of fin-and-tube heat exchangers with dehumidification. *Appl. Therm. Eng.* **2019**, *146*, 701–717. [CrossRef]
119. Kim, N.-H.; Lee, K.-J.; Jeong, Y.-B. Airside performance of oval tube heat exchangers having sine wave fins under wet condition. *Appl. Therm. Eng.* **2014**, *66*, 580–589. [CrossRef]
120. Wang, C.-C.; Liaw, J.-S.; Yang, B.-C. Airside performance of herringbone wavy fin-and-tube heat exchangers—Data with larger diameter tube. *Int. J. Heat Mass Transf.* **2011**, *54*, 1024–1029. [CrossRef]
121. Ma, X.; Ding, G.; Zhang, Y.; Wang, K. Airside heat transfer and friction characteristics for enhanced fin-and-tube heat exchanger with hydrophilic coating under wet conditions. *Int. J. Refrig.* **2007**, *30*, 1153–1167. [CrossRef]
122. Kim, M.-H.; Song, S.; Bullard, C.W. Effect of inlet humidity condition on the air-side performance of an inclined brazed aluminum evaporator. *Int. J. Refrig.* **2002**, *25*, 611–620. [CrossRef]
123. Kim, M.-H.; Bullard, C.W. Air-side performance of brazed aluminum heat exchangers under dehumidifying conditions. *Int. J. Refrig.* **2002**, *25*, 924–934. [CrossRef]
124. Howongsakun, T.; Theerakulpisut, S.; Sujumnongtokul, P.; Palasan, P. The behavior of lewis number in finned tube cooling coils under highly moist inlet air conditions. *Int. J. Technol* **2016**, *7*, 1253–1259. [CrossRef]
125. Wang, C.-C.; Lee, W.-S.; Sheu, W.-J.; Chang, Y.-J. A comparison of the airside performance of the fin-and-tube heat exchangers in wet conditions; with and without hydrophilic coating. *Appl. Therm. Eng.* **2002**, *22*, 267–278. [CrossRef]
126. Pirompugd, W.; Wang, C.-C.; Wongwises, S. Correlations for wet surface ratio of fin-and-tube heat exchangers. *Int. J. Heat Mass Transf.* **2010**, *53*, 568–573. [CrossRef]
127. Liang, S.Y.; Wong, T.N. Experimental validation of model predictions on evaporator coils with an emphasis on fin efficiency. *Int. J. Therm. Sci.* **2010**, *49*, 187–195. [CrossRef]
128. Yun, R.; Kim, Y.; Kim, Y. Air side heat transfer characteristics of plate finned tube heat exchangers with slit fin configuration under wet conditions. *Appl. Therm. Eng.* **2009**, *29*, 3014–3020. [CrossRef]
129. Lin, Y.-T.; Hwang, Y.-M.; Wang, C.-C. Performance of the herringbone wavy fin under dehumidifying conditions. *Int. J. Heat Mass Transf.* **2002**, *45*, 5035–5044. [CrossRef]
130. Summers, E.K.; Antar, M.A.; Lienhard, J.H. Design and optimization of an air heating solar collector with integrated phase change material energy storage for use in humidification-dehumidification desalination. *Sol. Energy* **2012**, *86*, 3417–3429. [CrossRef]
131. Wang, J.H.; Gao, N.Y.; Deng, Y.; Xia, S.J.; Qiao, J.L. Pv cell-driven humidification-dehumidification (h/d) process for brine treatment. *Desalin. Water Treat.* **2011**, *28*, 328–337. [CrossRef]
132. Hu, H.; Gao, J.; Ding, G.; Gao, Y.; Song, J. Fin design for an evaporator with small diameter microgroove tubes. *HVAC&R Res.* **2014**, *20*, 790–797.
133. Nuntaphan, A.; Kiatsiriroat, T.; Wang, C.-C. Heat transfer and friction characteristics of crimped spiral finned heat exchangers with dehumidification. *Appl. Therm. Eng.* **2005**, *25*, 327–340. [CrossRef]
134. Liu, L.; Jacobi, A.M. The Impact of Fin Surface Wettability on the Performance of Dehumidifying Heat Exchangers. *ASHRAE Trans.* **2014**, *120*, 1–8.
135. Wang, S.K.; Wang, S.K. *Handbook of Air Conditioning and Refrigeration*; McGraw-Hill: New York, NY, USA, 1993; Volume 2.
136. Houcine, I.; BenAmara, M.; Guizani, A.; Maâlej, M. Pilot plant testing of a new solar desalination process by a multiple-effect-humidification technique. *Desalination* **2006**, *196*, 105–124. [CrossRef]
137. Sievers, M.; Lienhard, V.J.H. Design of plate-fin tube dehumidifiers for humidification–dehumidification desalination systems. *Heat Transf. Eng.* **2015**, *36*, 223–243. [CrossRef]
138. Dai, Y.J.; Zhang, H.F. Experimental investigation of a solar desalination unit with humidification and dehumidification. *Desalination* **2000**, *130*, 169–175. [CrossRef]
139. Dai, Y.J.; Wang, R.Z.; Zhang, H.F. Parametric analysis to improve the performance of a solar desalination unit with humidification and dehumidification. *Desalination* **2002**, *142*, 107–118. [CrossRef]
140. Li, X.; Yuan, G.; Wang, Z.; Li, H.; Xu, Z. Experimental study on a humidification and dehumidification desalination system of solar air heater with evacuated tubes. *Desalination* **2014**, *351*, 1–8. [CrossRef]
141. Kabeel, A.E.; El-Said, E.M.S. A hybrid solar desalination system of air humidification-dehumidification and water flashing evaporation. Part I. A numerical investigation. *Desalination* **2013**, *320*, 56–72. [CrossRef]
142. Kabeel, A.E.; El-Said, E.M.S. A hybrid solar desalination system of air humidification, dehumidification and water flashing evaporation: Part II. Experimental investigation. *Desalination* **2014**, *341*, 50–60. [CrossRef]
143. Behnam, P.; Shafii, M.B. Examination of a solar desalination system equipped with an air bubble column humidifier, evacuated tube collectors and thermosyphon heat pipes. *Desalination* **2016**, *397*, 30–37. [CrossRef]
144. Al-Sulaiman, F.A.; Zubair, M.I.; Atif, M.; Gandhidasan, P.; Al-Dini, S.A.; Antar, M.A. Humidification dehumidification desalination system using parabolic trough solar air collector. *Appl. Therm. Eng.* **2015**, *75*, 809–816. [CrossRef]
145. He, W.F.; Xu, L.N.; Han, D. Parametric analysis of an air-heated humidification-dehumidification (HDH) desalination system with waste heat recovery. *Desalination* **2016**, *398*, 30–38. [CrossRef]
146. He, W.F.; Wu, F.; Wen, T.; Kong, Y.P.; Han, D. Cost analysis of a humidification dehumidification desalination system with a packed bed dehumidifier. *Energy Convers. Manag.* **2018**, *171*, 452–460. [CrossRef]
147. He, W.F.; Zhang, X.K.; Han, D.; Gao, L. Performance analysis of a water-power combined system with air-heated humidification dehumidification process. *Energy* **2017**, *130*, 218–227. [CrossRef]

148. Santosh, R.; Lee, H.S.; Kim, Y.D. A comprehensive review on humidifiers and dehumidifiers in solar and low-grade waste heat powered humidification-dehumidification desalination systems. *J. Clean. Prod.* **2022**, *347*, 131300. [CrossRef]
149. Kasaeian, A.; Babaei, S.; Jahanpanah, M.; Sarrafha, H.; Sulaiman Alsagri, A.; Ghaffarian, S.; Yan, W.M. Solar humidification-dehumidification desalination systems: A critical review. *Energy Convers. Manag.* **2019**, *201*, 112129. [CrossRef]
150. Tarazona-Romero, B.E.; Campos-Celador, A.; Maldonado-Muñoz, Y.A. Can solar desalination be small and beautiful? A critical review of existing technology under the appropriate technology paradigm. *Energy Res. Soc. Sci.* **2022**, *88*, 102510. [CrossRef]
151. Elsaid, K.; Kamil, M.; Sayed, E.T.; Abdelkareem, M.A.; Wilberforce, T.; Olabi, A. Environmental impact of desalination technologies: A review. *Sci. Total Environ.* **2020**, *748*, 141528. [CrossRef]
152. Belessiotis, V.; Kalogirou, S.; Delyannis, E.; Belessiotis, V.; Kalogirou, S.; Delyannis, E. Chapter 4—Membrane Distillation. In *Thermal Solar Desalination*; Belessiotis, V., Kalogirou, S., Delyannis, E., Eds.; Academic Press: Cambridge, MA, USA, 2016; pp. 191–251, ISBN 9780128096567.
153. Ghazouani, N.; Bawadekji, A.; El-Bary, A.A.; Becheikh, N.; Alassaf, Y.; Hassan, G.E.; Elewa, M.M. Greenhouse Desalination by Humidification–Dehumidification Using a Novel Green Packing Material. *Water* **2022**, *14*, 869. [CrossRef]
154. Ali, E.S.; Mohammed, R.H.; Qasem, N.A.A.; Zubair, S.M.; Askalany, A. Solar-powered ejector-based adsorption desalination system integrated with a humidification-dehumidification system. *Energy Convers. Manag.* **2021**, *238*, 114113. [CrossRef]
155. Qasem, N.A.A.; Zubair, S.M.; Abdallah, A.M.; Elbassoussi, M.H.; Ahmed, M.A. Novel and efficient integration of a humidification-dehumidification desalination system with an absorption refrigeration system. *Appl. Energy* **2020**, *263*, 114659. [CrossRef]
156. Elbassoussi, M.H.; Mohammed, R.H.; Zubair, S.M. Thermoeconomic assessment of an adsorption cooling/desalination cycle coupled with a water-heated humidification-dehumidification desalination unit. *Energy Convers. Manag.* **2020**, *223*, 113270. [CrossRef]
157. Fouda, A.; Nada, S.A.; Elattar, H.F.; Rubaiee, S.; Al-Zahrani, A. Performance analysis of proposed solar HDH water desalination systems for hot and humid climate cities. *Appl. Therm. Eng.* **2018**, *144*, 81–95. [CrossRef]
158. Qasem, N.A.A.; Zubair, S.M. Performance evaluation of a novel hybrid humidification-dehumidification (air-heated) system with an adsorption desalination system. *Desalination* **2019**, *461*, 37–54. [CrossRef]
159. Rostamzadeh, H.; Namin, A.S.; Ghaebi, H.; Amidpour, M. Performance assessment and optimization of a humidification dehumidification (HDH) system driven by absorption-compression heat pump cycle. *Desalination* **2018**, *447*, 84–101. [CrossRef]
160. Lawal, D.U.; Qasem, N.A.A. Humidification-dehumidification desalination systems driven by thermal-based renewable and low-grade energy sources: A critical review. *Renew. Sustain. Energy Rev.* **2020**, *125*, 109817. [CrossRef]
161. Ettouney, H. Design and analysis of humidification dehumidification desalination process. *Desalination* **2005**, *183*, 341–352. [CrossRef]
162. Zubair, S.M.; Antar, M.A.; Elmutasim, S.M.; Lawal, D.U. Performance evaluation of humidification-dehumidification (HDH) desalination systems with and without heat recovery options: An experimental and theoretical investigation. *Desalination* **2018**, *436*, 161–175. [CrossRef]
163. Garg, K.; Das, S.K.; Tyagi, H. Thermal design of a humidification-dehumidification desalination cycle consisting of packed-bed humidifier and finned-tube dehumidifier. *Int. J. Heat Mass Transf.* **2022**, *183*, 122153. [CrossRef]
164. Wu, G.; Kutlu, C.; Zheng, H.; Su, Y.; Cui, D. A study on the maximum gained output ratio of single-effect solar humidification-dehumidification desalination. *Sol. Energy* **2017**, *157*, 1–9. [CrossRef]
165. Muthusamy, C.; Srithar, K. Energy saving potential in humidification-dehumidification desalination system. *Energy* **2017**, *118*, 729–741. [CrossRef]
166. Müller-Holst, H. Solar thermal desalination using the multiple effect humidification (MEH)-method. In *NATO Security through Science Series C: Environmental Security*; Springer: Dordrecht, The Netherlands, 2007; pp. 215–225, ISBN 1402055064.
167. Dave, T.; Ahuja, V.; Krishnan, S. Economic analysis and experimental investigation of a direct absorption solar humidification-dehumidification system for decentralized water production. *Sustain. Energy Technol. Assess.* **2021**, *46*, 101306. [CrossRef]
168. Khass, T.M.; Mohammed, R.H.; Qasem, N.A.A.; Zubair, S.M. Different configurations of humidification-dehumidification desalination systems: Thermal and economic assessment. *Energy Convers. Manag.* **2022**, *258*, 115470. [CrossRef]
169. Chehayeb, K.M.; Narayan, G.P.; Zubair, S.M.; Lienhard, J.H. Thermodynamic balancing of a fixed-size two-stage humidification dehumidification desalination system. *Desalination* **2015**, *369*, 125–139. [CrossRef]
170. Elminshawy, N.A.S.; Siddiqui, F.R.; Addas, M.F. Development of an active solar humidification-dehumidification (HDH) desalination system integrated with geothermal energy. *Energy Convers. Manag.* **2016**, *126*, 608–621. [CrossRef]
171. Rajaseenivasan, T.; Srithar, K. An investigation into a laboratory scale bubble column humidification dehumidification desalination system powered by biomass energy. *Energy Convers. Manag.* **2017**, *139*, 232–244. [CrossRef]
172. Wu, G.; Zheng, H.F.; Wang, F.; Chang, Z.H. Parametric study of a tandem desalination system based on humidification-dehumidification process with 3-stage heat recovery. *Appl. Therm. Eng.* **2017**, *112*, 190–200. [CrossRef]
173. Rahimi-Ahar, Z.; Hatamipour, M.S.; Ghalavand, Y. Solar assisted modified variable pressure humidification-dehumidification desalination system. *Energy Convers. Manag.* **2018**, *162*, 321–330. [CrossRef]
174. He, W.F.; Han, D.; Zhu, W.P.; Ji, C. Thermo-economic analysis of a water-heated humidification-dehumidification desalination system with waste heat recovery. *Energy Convers. Manag.* **2018**, *160*, 182–190. [CrossRef]
175. Tariq, R.; Sheikh, N.A.; Xamán, J.; Bassam, A. An innovative air saturator for humidification-dehumidification desalination application. *Appl. Energy* **2018**, *228*, 789–807. [CrossRef]

176. Rahimi-Ahar, Z.; Hatamipour, M.S.; Ghalavand, Y. Experimental investigation of a solar vacuum humidification-dehumidification (VHDH) desalination system. *Desalination* **2018**, *437*, 73–80. [CrossRef]
177. Xu, H.; Sun, X.Y.; Dai, Y.J. Thermodynamic study on an enhanced humidification-dehumidification solar desalination system with weakly compressed air and internal heat recovery. *Energy Convers. Manag.* **2019**, *181*, 68–79. [CrossRef]
178. He, W.F.; Chen, J.J.; Han, D.; Luo, L.T.; Wang, X.C.; Zhang, Q.Y.; Yao, S.Y. Energetic, entropic and economic analysis of an open-air, open-water humidification dehumidification desalination system with a packing bed dehumidifier. *Energy Convers. Manag.* **2019**, *199*, 112016. [CrossRef]
179. Dehghan, M.; Ghasemizadeh, M.; Rashidi, S. Solar-driven water treatment: Generation II technologies. In *Solar-Driven Water Treatment*; Mahian, O., Wei, J., Taylor, R.A., Wongwises, S., Eds.; Academic Press: Cambridge, MA, USA, 2022; pp. 119–200, ISBN 978-0-323-90991-4.
180. Mohamed, A.S.A.; Ahmed, M.S.; Shahdy, A.G. Theoretical and experimental study of a seawater desalination system based on humidification-dehumidification technique. *Renew. Energy* **2020**, *152*, 823–834. [CrossRef]
181. Said, Z.; Sabiha, M.A.; Saidur, R.; Hepbasli, A.; Rahim, N.A.; Mekhilef, S.; Ward, T.A. Performance enhancement of a Flat Plate Solar collector using Titanium dioxide nanofluid and Polyethylene Glycol dispersant. *J. Clean. Prod.* **2015**, *92*, 343–353. [CrossRef]
182. Esen, M.; Esen, H. Experimental investigation of a two-phase closed thermosyphon solar water heater. *Sol. Energy* **2005**, *79*, 459–468. [CrossRef]
183. Balaji, K.; Iniyan, S.; Swami, M.V. Exergy, economic and environmental analysis of forced circulation flat plate solar collector using heat transfer enhancer in riser tube. *J. Clean. Prod.* **2018**, *171*, 1118–1127. [CrossRef]
184. Farid, M.; Al-Hajaj, A.W. Solar desalination with a humidification-dehumidification cycle. *Desalination* **1996**, *106*, 427–429. [CrossRef]
185. Garg, H.P.; Adhikari, R.S.; Kumar, R. Experimental design and computer simulation of multi-effect humidification (MEH)-dehumidification solar distillation. *Desalination* **2003**, *153*, 81–86. [CrossRef]
186. Alnaimat, F.; Klausner, J.F. Solar diffusion driven desalination for decentralized water production. *Desalination* **2012**, *289*, 35–44. [CrossRef]
187. Zhani, K. Solar desalination based on multiple effect humidification process: Thermal performance and experimental validation. *Renew. Sustain. Energy Rev.* **2013**, *24*, 406–417. [CrossRef]
188. Chang, Z.; Zheng, H.; Yang, Y.; Su, Y.; Duan, Z. Experimental investigation of a novel multi-effect solar desalination system based on humidification-dehumidification process. *Renew. Energy* **2014**, *69*, 253–259. [CrossRef]
189. Gang, W.; Zheng, H.; Kang, H.; Yang, Y.; Cheng, P.; Chang, Z. Experimental investigation of a multi-effect isothermal heat with tandem solar desalination system based on humidification-dehumidification processes. *Desalination* **2016**, *378*, 100–107. [CrossRef]
190. Ladouy, S.; Khabbazi, A. Experimental Study of the Water Depth Effect and the Impact of Condensers Connection in a New Desalination System by HDH Process, Using Solar Energy. *Energy Procedia* **2015**, *74*, 952–959. [CrossRef]
191. Moumouh, J.; Tahiri, M.; Salouhi, M.; Balli, L. Theoretical and experimental study of a solar desalination unit based on humidification–dehumidification of air. *Int. J. Hydrogen Energy* **2016**, *41*, 20818–20822. [CrossRef]
192. Kabeel, A.E.; Hamed, M.H.; Omara, Z.M.; Kandeal, A.W. Solar air heaters: Design configurations, improvement methods and applications—A detailed review. *Renew. Sustain. Energy Rev.* **2017**, *70*, 1189–1206. [CrossRef]
193. Ozgen, F.; Esen, M.; Esen, H. Experimental investigation of thermal performance of a double-flow solar air heater having aluminium cans. *Renew. Energy* **2009**, *34*, 2391–2398. [CrossRef]
194. Chafik, E. A new seawater desalination process using solar energy. *Desalination* **2003**, *153*, 25–37. [CrossRef]
195. Elminshawy, N.A.S.; Siddiqui, F.R.; Addas, M.F. Experimental and analytical study on productivity augmentation of a novel solar humidification-dehumidification (HDH) system. *Desalination* **2015**, *365*, 36–45. [CrossRef]
196. Siddiqui, F.R.; Elminshawy, N.A.S.; Addas, M.F. Design and performance improvement of a solar desalination system by using solar air heater: Experimental and theoretical approach. *Desalination* **2016**, *399*, 78–87. [CrossRef]
197. Zhani, K.; Ben Bacha, H. Experimental investigation of a new solar desalination prototype using the humidification dehumidification principle. *Renew. Energy* **2010**, *35*, 2610–2617. [CrossRef]
198. Zhani, K.; Ben Bacha, H.; Damak, T. Modeling and experimental validation of a humidification-dehumidification desalination unit solar part. *Energy* **2011**, *36*, 3159–3169. [CrossRef]
199. Ben Bacha, H. Dynamic modeling and experimental validation of a water desalination prototype by solar energy using humidification dehumidification process. *Desalination* **2013**, *322*, 182–208. [CrossRef]
200. Chiranjeevi, C.; Srinivas, T. Experimental and simulation studies on two stage humidification-dehumidification desalination and cooling plant. *Desalination* **2015**, *376*, 9–16. [CrossRef]
201. Chiranjeevi, C.; Srinivas, T. Experimental Analysis of Augmented Desalination by Cooling Integration. *Energy Procedia* **2016**, *90*, 283–291. [CrossRef]
202. Ben-Amara, M.; Houcine, I.; Guizani, A.A.; Maalej, M. Efficiency investigation of a new-design air solar plate collector used in a humidification-dehumidification desalination process. *Renew. Energy* **2005**, *30*, 1309–1327. [CrossRef]
203. Soufari, S.M.; Zamen, M.; Amidpour, M. Experimental validation of an optimized solar humidification-dehumidification desalination unit. *Desalin. Water Treat.* **2009**, *6*, 244–251. [CrossRef]

204. Mathioulakis, E.; Panaras, G.; Belessiotis, V. Experience gained through the implementation and operation of a solar humidification—Dehumidification desalination plant. *Desalin. Water Treat.* **2010**, *21*, 375–381. [CrossRef]
205. El-Shazly, A.H.; Al-Zahrani, A.A.; Al-Hamed, Y.A.; Nosier, S.A. Effect of fixed bed characteristics on the performance of pulsed water flow humidification-dehumidification solar desalination unit. *Desalin. Water Treat.* **2013**, *51*, 863–871. [CrossRef]
206. Ghazal, M.T.; Atikol, U.; Egelioglu, F. An experimental study of a solar humidifier for HDD systems. *Energy Convers. Manag.* **2014**, *82*, 250–258. [CrossRef]
207. Abu-Arabi, M.; Al-Harahsheh, M.; Tashtoush, R.; Mousa, H.; Al-Otoom, A. Experimental investigation of a solar desalination with humidification-dehumidification using a rotating surface. *Desalin. Water Treat.* **2017**, *73*, 101–106. [CrossRef]
208. Saidi, S.; Ben Rhadia, R.; Benhamou, B.; Nafiri, N.; Ben Jabrallah, S. Experimental investigation of a solar powered humidification-dehumidification desalination unit. *Desalin. Water Treat.* **2017**, *62*, 1–10. [CrossRef]
209. Ladouy, S.; Khabbazi, A. Experimental investigation of different air heating methods near to the evaporation surface in closed triangular shape unit powered by solar energy, one stage—Indoor experiment. *Appl. Therm. Eng.* **2017**, *127*, 203–211. [CrossRef]
210. Hernández, C.; Reyes, M.; Barraza, R.; Rheinschmidt, U.; Saldivia, D.; Vasquez-Padilla, R. Experimental and numerical evaluation of a humidification dehumidification desalination unit driven by solar energy. *AIP Conf. Proc.* **2018**, *2033*, 160003.
211. Lawal, D.; Antar, M.; Khalifa, A.; Zubair, S.; Al-Sulaiman, F. Humidification-dehumidification desalination system operated by a heat pump. *Energy Convers. Manag.* **2018**, *161*, 128–140. [CrossRef]
212. Xu, H.; Zhao, Y.; Dai, Y.J. Experimental study on a solar assisted heat pump desalination unit with internal heat recovery based on humidification-dehumidification process. *Desalination* **2019**, *452*, 247–257. [CrossRef]
213. Lawal, D.U.; Antar, M.A.; Khalifa, A.; Zubair, S.M. Heat pump operated humidification-dehumidification desalination system with option of energy recovery. *Sep. Sci. Technol.* **2020**, *55*, 3467–3486. [CrossRef]
214. Lawal, D.U.; Antar, M.A.; Khalifa, A.; Zubair, S.M.; Al-Sulaiman, F. Experımental investigation of heat pump driven humidification-dehumidification desalination system for water desalination and space conditioning. *Desalination* **2020**, *475*, 114199. [CrossRef]
215. Lawal, D.U.; Jawad, S.A.; Antar, M.A. Experimental and theoretical study on a heat pump driven open-air humidification dehumidification desalination system. *Energy* **2020**, *207*, 118252. [CrossRef]
216. Lawal, D.U.; Antar, M.A. Investigation of heat pump-driven humidification–dehumidification desalination system with energy recovery option. *J. Therm. Anal. Calorim.* **2021**, *145*, 3177–3194. [CrossRef]
217. Lu, L.; Liu, Z.H.; Xiao, H.S. Thermal performance of an open thermosyphon using nanofluids for high-temperature evacuated tubular solar collectors. Part 1: Indoor experiment. *Sol. Energy* **2011**, *85*, 379–387. [CrossRef]
218. Esen, M. Thermal performance of a solar cooker integrated vacuum-tube collector with heat pipes containing different refrigerants. *Sol. Energy* **2004**, *76*, 751–757. [CrossRef]
219. Sharafeldin, M.A.; Gróf, G. Evacuated tube solar collector performance using CeO_2/water nanofluid. *J. Clean. Prod.* **2018**, *185*, 347–356. [CrossRef]
220. Feliński, P.; Sekret, R. Effect of PCM application inside an evacuated tube collector on the thermal performance of a domestic hot water system. *Energy Build.* **2017**, *152*, 558–567. [CrossRef]
221. Kabeel, A.E.; Hamed, M.H.; Omara, Z.M.; Sharshir, S.W. Experimental study of a humidification-dehumidification solar technique by natural and forced air circulation. *Energy* **2014**, *68*, 218–228. [CrossRef]
222. Hamed, M.H.; Kabeel, A.E.; Omara, Z.M.; Sharshir, S.W. Mathematical and experimental investigation of a solar humidification-dehumidification desalination unit. *Desalination* **2015**, *358*, 9–17. [CrossRef]
223. Sharshir, S.W.; Peng, G.; Yang, N.; El-Samadony, M.O.A.; Kabeel, A.E. A continuous desalination system using humidification—Dehumidification and a solar still with an evacuated solar water heater. *Appl. Therm. Eng.* **2016**, *104*, 734–742. [CrossRef]
224. Sharshir, S.W.; Peng, G.; Yang, N.; Eltawil, M.A.; Ali, M.K.A.; Kabeel, A.E. A hybrid desalination system using humidification-dehumidification and solar stills integrated with evacuated solar water heater. *Energy Convers. Manag.* **2016**, *124*, 287–296. [CrossRef]
225. Li, G.P.; Zhang, L.Z. Investigation of a solar energy driven and hollow fiber membrane-based humidification-dehumidification desalination system. *Appl. Energy* **2016**, *177*, 393–408. [CrossRef]
226. Xu, L.; Wang, Z.; Yuan, G.; Li, X.; Ruan, Y. A new dynamic test method for thermal performance of all-glass evacuated solar air collectors. *Sol. Energy* **2012**, *86*, 1222–1231. [CrossRef]
227. Yuan, G.; Wang, Z.; Li, H.; Li, X. Experimental study of a solar desalination system based on humidification–dehumidification process. *Desalination* **2011**, *277*, 92–98. [CrossRef]
228. Antar, M.A.; Sharqawy, M.H. Experimental investigations on the performance of an air heated humidification-dehumidification desalination system. *Desalin. Water Treat.* **2013**, *51*, 837–843. [CrossRef]
229. Shalaby, S.M.; Kabeel, A.E.; El-Bialy, E. Investigation and improvement of the humidification–Dehumidification solar water desalination system implemented wick as packing material. *J. Sol. Energy Eng. Trans. ASME* **2020**, *142*, 011015. [CrossRef]
230. Singh, S.; Gill, R.S.; Hans, V.S.; Mittal, T.C. Experimental performance and economic viability of evacuated tube solar collector assisted greenhouse dryer for sustainable development. *Energy* **2022**, *241*, 122794. [CrossRef]
231. Mahmood, F.; Al-Ansari, T. Design and analysis of a renewable energy driven greenhouse integrated with a solar still for arid climates. *Energy Convers. Manag.* **2022**, *258*, 115512. [CrossRef]

232. Kumar, V.; Shrivastava, R.L.; Untawale, S.P. Fresnel lens: A promising alternative of reflectors in concentrated solar power. *Renew. Sustain. Energy Rev.* **2015**, *44*, 376–390. [CrossRef]
233. Mahmoud, M.S.; Farrag, T.E.; Mohamed, W.A. Experimental and Theoretical Model for Water Desalination by Humidification –Dehumidification (HDH). *Procedia Environ. Sci.* **2013**, *17*, 503–512. [CrossRef]
234. Wu, G.; Zheng, H.; Ma, X.; Kutlu, C.; Su, Y. Experimental investigation of a multi-stage humidification-dehumidification desalination system heated directly by a cylindrical Fresnel lens solar concentrator. *Energy Convers. Manag.* **2017**, *143*, 241–251. [CrossRef]
235. Xiao, J.; Zheng, H.; Jin, R.; Liang, S.; Wang, G.; Ma, X. Experimental investigation of a bubbling humidification-dehumidification desalination system directly heated by cylindrical Fresnel lens solar concentrator. *Sol. Energy* **2021**, *220*, 873–881. [CrossRef]
236. Fernández-García, A.; Zarza, E.; Valenzuela, L.; Pérez, M. Parabolic-trough solar collectors and their applications. *Renew. Sustain. Energy Rev.* **2010**, *14*, 1695–1721. [CrossRef]
237. Nafey, A.S.; Fath, H.E.S.; El-Helaby, S.O.; Soliman, A.M. Solar desalination using humidification dehumidification processes. Part I. A numerical investigation. *Energy Convers. Manag.* **2004**, *45*, 1243–1261. [CrossRef]
238. Abdullah, A.S.; Essa, F.A.; Omara, Z.M.; Bek, M.A. Performance evaluation of a humidification–dehumidification unit integrated with wick solar stills under different operating conditions. *Desalination* **2018**, *441*, 52–61. [CrossRef]
239. Mahmoud, M.S. Enhancement of solar desalination by humidification-dehumidification technique. *Desalin. Water Treat.* **2011**, *30*, 310–318. [CrossRef]
240. Riffat, S.; Mayere, A. Performance evaluation of v-trough solar concentrator for water desalination applications. *Appl. Therm. Eng.* **2013**, *50*, 234–244. [CrossRef]
241. Abd-ur-Rehman, H.M.; Al-Sulaiman, F.A. An experimental investigation of a novel design air humidifier using direct solar thermal heating. *Energy Convers. Manag.* **2016**, *127*, 667–678. [CrossRef]
242. Alghamdi, M.; Abdel-Hady, F.; Mazher, A.K.; Alzahrani, A. Integration of process modeling, design, and optimization with an experimental study of a solar-driven humidification and dehumidification desalination system. *Processes* **2018**, *6*, 163. [CrossRef]
243. Abed, F.M.; Eleiwi, M.A.; Hasanuzzaman, M.; Islam, M.M.; Mohammed, K.I. Design, development and effects of operational conditions on the performance of concentrated solar collector based desalination system operating in Iraq. *Sustain. Energy Technol. Assess.* **2020**, *42*, 100886. [CrossRef]
244. Hussain, Z.F.; Hamed, A.J.; Khalifa, A.H.N.; Hassan, M.F.; Najim, F.A. Experimental Investigation of a Humidification-Dehumidification Desalination Unit Working Under Baghdad Conditions. *Front. Heat Mass Transf.* **2022**, *18*, 14. [CrossRef]
245. Kasaeian, A.; Nouri, G.; Ranjbaran, P.; Wen, D. Solar collectors and photovoltaics as combined heat and power systems: A critical review. *Energy Convers. Manag.* **2018**, *156*, 688–705. [CrossRef]
246. Hong, W.-H.; Kim, K.-K. Design of Ultra Low-Voltage NCL Circuits in Nanoscale MOSFET Technology. *J. Korea Ind. Inf. Syst. Res.* **2012**, *17*, 17–23. [CrossRef]
247. Gabrielli, P.; Gazzani, M.; Novati, N.; Sutter, L.; Simonetti, R.; Molinaroli, L.; Manzolini, G.; Mazzotti, M. Combined water desalination and electricity generation through a humidification-dehumidification process integrated with photovoltaic-thermal modules: Design, performance analysis and techno-economic assessment. *Energy Convers. Manag. X* **2019**, *1*, 100004. [CrossRef]
248. El-Awady, M.H.; El-Ghetany, H.H.; Abdel Latif, M. Experimental investigation of an integrated solar green house for water desalination, plantation and wastewater treatment in remote arid Egyptian communities. *Energy Procedia* **2014**, *50*, 520–527. [CrossRef]
249. Yadav, S.; Sudhakar, K. Different domestic designs of solar stills: A review. *Renew. Sustain. Energy Rev.* **2015**, *47*, 718–731. [CrossRef]
250. Panchal, H.; Mohan, I. Various methods applied to solar still for enhancement of distillate output. *Desalination* **2017**, *415*, 76–89. [CrossRef]
251. Xiao, G.; Wang, X.; Ni, M.; Wang, F.; Zhu, W.; Luo, Z.; Cen, K. A review on solar stills for brine desalination. *Appl. Energy* **2013**, *103*, 642–652. [CrossRef]
252. Rajaseenivasan, T.; Murugavel, K.K.; Elango, T.; Hansen, R.S. A review of different methods to enhance the productivity of the multi-effect solar still. *Renew. Sustain. Energy Rev.* **2013**, *17*, 248–259. [CrossRef]
253. Alaian, W.M.; Elnegiry, E.A.; Hamed, A.M. Experimental investigation on the performance of solar still augmented with pin-finned wick. *Desalination* **2016**, *379*, 10–15. [CrossRef]
254. Sharshir, S.W.; Salman, M.; El-Behery, S.M.; Halim, M.A.; Abdelaziz, G.B. Enhancement of solar still performance via wet wick, different aspect ratios, cover cooling, and reflectors. *Int. J. Energy Environ. Eng.* **2021**, *12*, 517–530. [CrossRef]
255. Rajaseenivasan, T.; Tinnokesh, A.P.; Kumar, G.R.; Srithar, K. Glass basin solar still with integrated preheated water supply—Theoretical and experimental investigation. *Desalination* **2016**, *398*, 214–221. [CrossRef]
256. Kannan, R.; Selvaganesan, C.; Vignesh, M.; Babu, B.R.; Fuentes, M.; Vivar, M.; Skryabin, I.; Srithar, K. Solar still with vapor adsorption basin: Performance analysis. *Renew. Energy* **2014**, *62*, 258–264. [CrossRef]
257. Ansari, O.; Asbik, M.; Bah, A.; Arbaoui, A.; Khmou, A. Desalination of the brackish water using a passive solar still with a heat energy storage system. *Desalination* **2013**, *324*, 10–20. [CrossRef]
258. Rajaseenivasan, T.; Kalidasa Murugavel, K.; Elango, T. Performance and exergy analysis of a double-basin solar still with different materials in basin. *Desalin. Water Treat.* **2015**, *55*, 1786–1794. [CrossRef]

259. Omara, Z.M.; Eltawil, M.A. Hybrid of solar dish concentrator, new boiler and simple solar collector for brackish water desalination. *Desalination* **2013**, *326*, 62–68. [CrossRef]
260. Omara, Z.M.; Eltawil, M.A.; ElNashar, E.S.A. A new hybrid desalination system using wicks/solar still and evacuated solar water heater. *Desalination* **2013**, *325*, 56–64. [CrossRef]
261. Srithar, K.; Rajaseenivasan, T.; Karthik, N.; Periyannan, M.; Gowtham, M. Stand alone triple basin solar desalination system with cover cooling and parabolic dish concentrator. *Renew. Energy* **2016**, *90*, 157–165. [CrossRef]
262. Rajaseenivasan, T.; Elango, T.; Kalidasa Murugavel, K. Comparative study of double basin and single basin solar stills. *Desalination* **2013**, *309*, 27–31. [CrossRef]
263. Rajaseenivasan, T.; Kalidasa Murugavel, K. Theoretical and experimental investigation on double basin double slope solar still. *Desalination* **2013**, *319*, 25–32. [CrossRef]
264. Rahbar, N.; Esfahani, J.A. Experimental study of a novel portable solar still by utilizing the heatpipe and thermoelectric module. *Desalination* **2012**, *284*, 55–61. [CrossRef]
265. Rahbar, N.; Esfahani, J.A.; Asadi, A. An experimental investigation on productivity and performance of a new improved design portable asymmetrical solar still utilizing thermoelectric modules. *Energy Convers. Manag.* **2016**, *118*, 55–62. [CrossRef]
266. Esfahani, J.A.; Rahbar, N.; Lavvaf, M. Utilization of thermoelectric cooling in a portable active solar still—An experimental study on winter days. *Desalination* **2011**, *269*, 198–205. [CrossRef]
267. Rahbar, N.; Esfahani, J.A.; Fotouhi-Bafghi, E. Estimation of convective heat transfer coefficient and water-productivity in a tubular solar still—CFD simulation and theoretical analysis. *Sol. Energy* **2015**, *113*, 313–323. [CrossRef]
268. Rashidi, S.; Bovand, M.; Esfahani, J.A. Optimization of partitioning inside a single slope solar still for performance improvement. *Desalination* **2016**, *395*, 79–91. [CrossRef]
269. Mostafa, M.A.; El-Algouz, S.A. Enhancement of the Performance of Stepped Solar Still Using Humidification-Dehumidification Processes. *Nat. Sci.* **2013**, *11*, 88–98.
270. Farshchi Tabrizi, F.; Khosravi, M.; Shirzaei Sani, I. Experimental study of a cascade solar still coupled with a humidification-dehumidification system. *Energy Convers. Manag.* **2016**, *115*, 80–88. [CrossRef]
271. Rajaseenivasan, T.; Srithar, K. Potential of a dual purpose solar collector on humidification dehumidification desalination system. *Desalination* **2017**, *404*, 35–40. [CrossRef]
272. El-Said, E.M.S.; Elshamy, S.M.; Kabeel, A.E. Performance enhancement of a tubular solar still by utilizing wire mesh packing under harmonic motion. *Desalination* **2020**, *474*, 114165. [CrossRef]
273. Kabeel, A.E.; El-Said, E.M.S.; Abdulaziz, M. Computational fluid dynamic as a tool for solar still performance analysis and design development: A review. *Desalin. Water Treat.* **2019**, *159*, 200–213. [CrossRef]
274. Rashidi, S.; Esfahani, J.A.; Rashidi, A. A review on the applications of porous materials in solar energy systems. *Renew. Sustain. Energy Rev.* **2017**, *73*, 1198–1210. [CrossRef]
275. Sharshir, S.W.; Yang, N.; Peng, G.; Kabeel, A.E. Factors affecting solar stills productivity and improvement techniques: A detailed review. *Appl. Therm. Eng.* **2016**, *100*, 267–284. [CrossRef]
276. Kandeal, A.W.; El-Shafai, N.M.; Abdo, M.R.; Thakur, A.K.; El-Mehasseb, I.M.; Maher, I.; Rashad, M.; Kabeel, A.E.; Yang, N.; Sharshir, S.W. Improved thermo-economic performance of solar desalination via copper chips, nanofluid, and nano-based phase change material. *Sol. Energy* **2021**, *224*, 1313–1325. [CrossRef]
277. Peng, G.; Sharshir, S.W.; Wang, Y.; An, M.; Ma, D.; Zang, J.; Kabeel, A.E.; Yang, N. Potential and challenges of improving solar still by micro/nano-particles and porous materials—A review. *J. Clean. Prod.* **2021**, *311*, 127432. [CrossRef]
278. Sharshir, S.W.; Ismail, M.; Kandeal, A.W.; Baz, F.B.; Eldesoukey, A.; Younes, M.M. Improving thermal, economic, and environmental performance of solar still using floating coal, cotton fabric, and carbon black nanoparticles. *Sustain. Energy Technol. Assess.* **2021**, *48*, 101563. [CrossRef]
279. Sharshir, S.W.; Hamada, M.A.; Kandeal, A.W.; El-Said, E.M.S.; Mimi Elsaid, A.; Rashad, M.; Abdelaziz, G.B. Augmented performance of tubular solar still integrated with cost-effective nano-based mushrooms. *Sol. Energy* **2021**, *228*, 27–37. [CrossRef]
280. Abdelaziz, G.B.; Algazzar, A.M.; El-Said, E.M.S.; Elsaid, A.M.; Sharshir, S.W.; Kabeel, A.E.; El-Behery, S.M. Performance enhancement of tubular solar still using nano-enhanced energy storage material integrated with v-corrugated aluminum basin, wick, and nanofluid. *J. Energy Storage* **2021**, *41*, 102933. [CrossRef]
281. Essa, F.A.; Omara, Z.M.; Abdullah, A.S.; Kabeel, A.E.; Abdelaziz, G.B. Enhancing the solar still performance via rotating wick belt and quantum dots nanofluid. *Case Stud. Therm. Eng.* **2021**, *27*, 101222. [CrossRef]
282. Saravanavel, S.; Vijayakumar, K.; SathishKumar, G.B.; Meignanamoorthy, M.; Ravichandran, M. Performance on single basin square pyramid solar still. *Mater. Today Proc.* **2020**, in press. [CrossRef]
283. Kaushal, A.; Varun. Solar stills: A review. *Renew. Sustain. Energy Rev.* **2010**, *14*, 446–453. [CrossRef]
284. Dsilva Winfred Rufuss, D.; Iniyan, S.; Suganthi, L.; Davies, P.A. Solar stills: A comprehensive review of designs, performance and material advances. *Renew. Sustain. Energy Rev.* **2016**, *63*, 464–496. [CrossRef]
285. Tyagi, S.K.; Kamboj, S.; Himanshu; Tyagi, N.; Narayanan, R.; Tyagi, V.V. Technological advancements in jaggery-making processes and emission reduction potential via clean combustion for sustainable jaggery production: An overview. *J. Environ. Manag.* **2022**, *301*, 113792. [CrossRef] [PubMed]
286. Shanmugan, S.; Rajamohan, P.; Mutharasu, D.; Ibrahim, K. Performance evaluation of an acrylic mirror booster solar still for neera concentration in jaggery-making industry. *Int. J. Sustain. Energy* **2014**, *33*, 261–272. [CrossRef]

287. Perret, J.S.S.; Al-Ismaili, A.M.M.; Sablani, S.S. Development of a humidification-dehumidification system in a Quonset greenhouse for sustainable crop production in arid regions. *Biosyst. Eng.* **2005**, *91*, 349–359. [CrossRef]
288. Al-Sulaiman, F.A.; Abd-ur-Rehman, H.M.; Antar, M.A.; Munteshari, O. Experimental investigation of a bubble column humidifier heated through solar energy. *Desalin. Water Treat.* **2017**, *60*, 58–69. [CrossRef]
289. Patel, V.; Patel, R.; Patel, J. Theoretical and experimental investigation of bubble column humidification and thermoelectric cooler dehumidification water desalination system. *Int. J. Energy Res.* **2020**, *44*, 890–901. [CrossRef]
290. Goswami, D.Y. *Principles of Solar Engineering*; CRC Press: Boca Raton, FL, USA, 2015; ISBN 9780429100208.
291. El-Batouti, M.; Naim, M.M.; Al Harby, N.F.; Elewa, M.M. An Investigation into a Miniature Saltless Solar Pond. *Materials* **2022**, *15*, 5974. [CrossRef]
292. Velmurugan, V.; Srithar, K. Prospects and scopes of solar pond: A detailed review. *Renew. Sustain. Energy Rev.* **2008**, *12*, 2253–2263. [CrossRef]
293. Tabor, H.Z.; Doron, B. The Beith Ha'Arava 5 MW(e) Solar Pond Power Plant (SPPP)-Progress report. *Sol. Energy* **1990**, *45*, 247–253. [CrossRef]
294. Ali, H.M. Potential of solar ponds in hot climates. *Sol. Wind Technol.* **1989**, *6*, 137–141. [CrossRef]
295. Rostamzadeh, H.; Namin, A.S.; Nourani, P.; Amidpour, M.; Ghaebi, H. Feasibility investigation of a humidification-dehumidification (HDH) desalination system with thermoelectric generator operated by a salinity-gradient solar pond. *Desalination* **2019**, *462*, 1–18. [CrossRef]
296. Mericq, J.P.; Laborie, S.; Cabassud, C. Evaluation of systems coupling vacuum membrane distillation and solar energy for seawater desalination. *Chem. Eng. J.* **2011**, *166*, 596–606. [CrossRef]
297. Badran, A.A.; Jubran, B.A.; Qasem, E.M.; Hamdan, M.A. Numerical Model for the Behaviour of a Salt-Gradient Solar-Pond Greenhouse-Heating System. *Appl. Energy* **1997**, *58*, 57–72. [CrossRef]
298. Al-Hussaini, H.; Suen, K.O. Using shallow solar ponds as a heating source for greenhouses in cold climates. *Energy Convers. Manag.* **1998**, *39*, 1369–1376. [CrossRef]
299. Ruskowitz, J.A.; Suárez, F.; Tyler, S.W.; Childress, A.E. Evaporation suppression and solar energy collection in a salt-gradient solar pond. *Sol. Energy* **2014**, *99*, 36–46. [CrossRef]
300. Wang, H.; Zhang, C.Y.; Zhang, L.G. Effect of steel-wires and paraffin composite phase change materials on the heat exchange and exergetic performance of salt gradient solar pond. *Energy Rep.* **2022**, *8*, 5678–5687. [CrossRef]
301. Zhang, Y.; Zhu, C.; Zhang, H.; Zheng, W.; You, S.; Zhen, Y. Experimental study of a humidification-dehumidification desalination system with heat pump unit. *Desalination* **2018**, *442*, 108–117. [CrossRef]
302. Kabeel, A.E.; Abdelgaied, M. Experimental evaluation of a two-stage indirect solar dryer with reheating coupled with HDH desalination system for remote areas. *Desalination* **2018**, *425*, 22–29. [CrossRef]
303. Abdelaziz, G.B.; El-Said, E.M.S.; Dahab, M.A.; Omara, M.A.; Sharshir, S.W. Hybrid solar desalination systems review. *Energy Sources Part A Recover. Util. Environ. Eff.* **2021**, 1–31. [CrossRef]
304. Moossa, B.; Trivedi, P.; Saleem, H.; Zaidi, S.J. Desalination in the GCC countries—A review. *J. Clean. Prod.* **2022**, *357*, 131717. [CrossRef]
305. Tahri, T.; Abdul-Wahab, S.A.; Bettahar, A.; Douani, M.; Al-Hinai, H.; Al-Mulla, Y. Desalination of seawater using a humidification-dehumidification seawater greenhouse. *Desalin. Water Treat.* **2009**, *12*, 382–388. [CrossRef]
306. Schmack, M.; Ho, G.; Anda, M. The Bubble-Greenhouse: A holistic sustainable approach to small-scale water desalination in remote regions. *Desalination* **2015**, *365*, 250–260. [CrossRef]
307. Kabeel, A.E.; Abdelgaied, M.; Feddaoui, M.B. Hybrid system of an indirect evaporative air cooler and HDH desalination system assisted by solar energy for remote areas. *Desalination* **2018**, *439*, 162–167. [CrossRef]
308. Alkhulaifi, Y.M.; Baata, E.; Al-Sulaiman, F.A.; Ibrahim, N.I.; Ben-Mansour, R. Performance and exergoeconomic assessment of a novel combined ejector cooling with humidification-dehumidification (HDH) desalination system. *Desalination* **2021**, *500*, 114843. [CrossRef]
309. Shalaby, S.M.; Kabeel, A.E.; Moharram, B.M.; Fleafl, A.H. Experimental study of hybrid solar humidification dehumidification system for extremely saline water desalination. *Energy Convers. Manag.* **2021**, *235*, 114021. [CrossRef]
310. Abdelaziz, G.B.; Dahab, M.A.; Omara, M.A.; Sharshir, S.W.; Elsaid, A.M.; El-Said, E.M.S. Humidification dehumidification saline water desalination system utilizing high frequency ultrasonic humidifier and solar heated air stream. *Therm. Sci. Eng. Prog.* **2022**, *27*, 101144. [CrossRef]
311. Gilbert, N. One-third of our greenhouse gas emissions come from agriculture. *Nature* **2012**. [CrossRef]
312. Mahmood, F.; Ghiat, I.; Govindan, R.; Al-Ansari, T. Reduced-order Modelling (ROM) Approach for Optimal Microclimate Control in Agricultural Greenhouses. In Proceedings of the 30 European Symposium on Computer Aided Process Engineering, Milan, Italy, 24–27 May 2020; Pierucci, S., Manenti, F., Bozzano, G.L., Manca, D., Eds.; Elsevier: Amsterdam, The Netherlands, 2020; Volume 48, pp. 1879–1884, ISBN 1570-7946.
313. De Gelder, A.; Dieleman, J.A.; Bot, G.P.A.; Marcelis, L.F.M. An overview of climate and crop yield in closed greenhouses. *J. Hortic. Sci. Biotechnol.* **2012**, *87*, 193–202. [CrossRef]
314. Seven, S.A.; Tastan, Ö.F.; Tas, C.E.; Ünal, H.; Ince, İ.A.; Menceloglu, Y.Z. Insecticide-releasing LLDPE films as greenhouse cover materials. *Mater. Today Commun.* **2019**, *19*, 170–176. [CrossRef]

315. Babaghayou, M.I.; Mourad, A.H.I.; Lorenzo, V.; Chabira, S.F.; Sebaa, M. Anisotropy evolution of low density polyethylene greenhouse covering films during their service life. *Polym. Test.* **2018**, *66*, 146–154. [CrossRef]
316. Sethi, V.P. On the selection of shape and orientation of a greenhouse: Thermal modeling and experimental validation. *Sol. Energy* **2009**, *83*, 21–38. [CrossRef]
317. Campiotti, C.A.; Morosinotto, G.; Puglisi, G.; Schettini, E.; Vox, G. Performance Evaluation of a Solar Cooling Plant Applied for Greenhouse Thermal Control. *Agric. Agric. Sci. Procedia* **2016**, *8*, 664–669. [CrossRef]
318. Singh, M.C.; Sharma, K.K.; Prasad, V. Impact of ventilation rate and its associated characteristics on greenhouse microclimate and energy use. *Arab. J. Geosci.* **2022**, *15*, 288. [CrossRef]
319. Bournet, P.E.; Boulard, T. Effect of ventilator configuration on the distributed climate of greenhouses: A review of experimental and CFD studies. *Comput. Electron. Agric.* **2010**, *74*, 195–217. [CrossRef]
320. Ganguly, A.; Ghosh, S. Model development and experimental validation of a floriculture greenhouse under natural ventilation. *Energy Build.* **2009**, *41*, 521–527. [CrossRef]
321. Su, Y.; Xu, L. Towards discrete time model for greenhouse climate control. *Eng. Agric. Environ. Food* **2017**, *10*, 157–170. [CrossRef]
322. López-Cruz, I.L.; Fitz-Rodríguez, E.; Salazar-Moreno, R.; Rojano-Aguilar, A.; Kacira, M. Development and analysis of dynamical mathematical models of greenhouse climate: A review. *Eur. J. Hortic. Sci.* **2018**, *83*, 269–279. [CrossRef]
323. Cuce, E.; Harjunowibowo, D.; Cuce, P.M. Renewable and sustainable energy saving strategies for greenhouse systems: A comprehensive review. *Renew. Sustain. Energy Rev.* **2016**, *64*, 34–59. [CrossRef]
324. Gasia, J.; Miró, L.; Cabeza, L.F. Review on system and materials requirements for high temperature thermal energy storage. Part 1: General requirements. *Renew. Sustain. Energy Rev.* **2017**, *75*, 1320–1338. [CrossRef]
325. Aljubury, I.M.A.; Ridha, H.D. Enhancement of evaporative cooling system in a greenhouse using geothermal energy. *Renew. Energy* **2017**, *111*, 321–331. [CrossRef]
326. Zhou, N.; Yu, Y.; Yi, J.; Liu, R. A study on thermal calculation method for a plastic greenhouse with solar energy storage and heating. *Sol. Energy* **2017**, *142*, 39–48. [CrossRef]
327. Peters, R.W. Water management, purification, and conservation in arid climates, volume 3: Water conservation, edited by Mattheus, F.A. Goosen and Walid, H. Shayya Technomic Publishing Company Lancaster, PA (2000) 348 pages hardcover ISBN 1-56676-771-7 U.S. list price: $8. *Environ. Prog.* **2001**, *20*, J13.
328. Goosen, M.F.; Al-Hinai, H.; Sablani, S. Capacity-building strategies for desalination: Activities, facilities and educational programs in Oman. *Desalination* **2001**, *141*, 181–189. [CrossRef]
329. Goosen, M.F.A.; Sablani, S.S.; Shayya, W.H.; Paton, C.; Al-Hinai, H. Thermodynamic and economic considerations in solar desalination. *Desalination* **2000**, *129*, 63–89. [CrossRef]
330. Chaibi, M.T. An overview of solar desalination for domestic and agriculture water needs in remote arid areas. *Desalination* **2000**, *127*, 119–133. [CrossRef]
331. Selçuk, M.K.; Tran, V.V. Solar stills for agricultural purposes. *Sol. Energy* **1975**, *17*, 103–109. [CrossRef]
332. Al-Ismaili, A.M.; Suwailam, T.B. Simulation models of the seawater greenhouse. *Int. J. Eng. Technol.* **2018**, *7*, 90–93. [CrossRef]
333. Bailey, B.J. the Environment in Evaporatively Cooled Greenhouses. *Acta Hortic.* **1991**, *287*, 59–66. [CrossRef]
334. Sablani, S.S.; Goosen, M.F.A.; Paton, C.; Shayya, W.H.; Al-Hinai, H. Simulation of fresh water production using a humidification-dehumidification seawater greenhouse. *Desalination* **2003**, *159*, 283–288. [CrossRef]
335. Goosen, M.F.; Sablani, S.; Paton, C.; Perret, J.; Al-Nuaimi, A.; Haffar, I.; Al-Hinai, H.; Shayya, W. Solar energy desalination for arid coastal regions: Development of a humidification–dehumidification seawater greenhouse. *Sol. Energy* **2003**, *75*, 413–419. [CrossRef]
336. Davies, P.A.; Paton, C. The seawater greenhouse in the United Arab Emirates: Thermal modelling and evaluation of design options. *Desalination* **2005**, *173*, 103–111. [CrossRef]
337. Paton, C.; Davies, P. The seawater greenhouse for arid lands. In Proceedings of the Mediterranean Conference on Renewable Energy Sources for Water Production, Santorini, Greece, 10–12 June 1996; pp. 163–166.
338. Davies, P.; Turner, K.; Paton, C. Potential of the Seawater Greenhouse in Middle Eastern Climates. In Proceedings of the International Engineering Conference, Mutah University, Mutah, Jordan, 26–28 April 2004; pp. 523–540.
339. Lovichit, W.; Kubota, C.; Choi, C.Y.; Schoonderbeek, J. Greenhouse water recovery system for crop production in semi-arid climate. In Proceedings of the 2007 ASABE Annual International Meeting, Technical Papers, Minneapolis, MN, US, 17–20 June 2007; American Society of Agricultural and Biological Engineers: St. Joseph, MI, USA, 2007; Volume 8.
340. Chaker, M.; Meher-Homji, C.B. Evaporative Cooling of Gas Turbine Engines: Climatic Analysis and Application in High Humidity Regions. In Proceedings of the ASME Turbo Expo 2007: Power for Land, Sea, and Air, Montreal, QC, Canada, 14–17 May 2007; Volume 3, pp. 761–773.
341. Abdel-Ghany, A.M.; Al-Helal, I.M.; Alzahrani, S.M.; Alsadon, A.A.; Ali, I.M.; Elleithy, R.M. Covering materials incorporating radiation-preventing techniques to meet greenhouse cooling challenges in arid regions: A review. *Sci. World J.* **2012**, *2012*, 906360. [CrossRef]
342. Chaibi, M.T.; Jilar, T. System design, operation and performance of roof-integrated desalination in greenhouses. *Sol. Energy* **2004**, *76*, 545–561. [CrossRef]
343. Torchia-Núñez, J.C.; Porta-Gándara, M.A.; Cervantes-de Gortari, J.G. Exergy analysis of a passive solar still. *Renew. Energy* **2008**, *33*, 608–616. [CrossRef]

344. Ranjan, K.R.; Kaushik, S.C.; Panwar, N.L. Energy and exergy analysis of passive solar distillation systems. *Int. J. Low-Carbon Technol.* **2016**, *11*, 211–221. [CrossRef]
345. Vaithilingam, S.; Esakkimuthu, G.S. Energy and exergy analysis of single slope passive solar still: An experimental investigation. *Desalin. Water Treat.* **2015**, *55*, 1433–1444. [CrossRef]
346. Mamouri, S.J.; Tan, X.; Klausner, J.F.; Yang, R.; Bénard, A. Performance of an integrated greenhouse equipped with Light-Splitting material and an HDH desalination unit. *Energy Convers. Manag. X* **2020**, *7*, 100045. [CrossRef]
347. Rabhy, O.O.; Adam, I.G.; Elsayed Youssef, M.; Rashad, A.B.; Hassan, G.E. Numerical and experimental analyses of a transparent solar distiller for an agricultural greenhouse. *Appl. Energy* **2019**, *253*, 113564. [CrossRef]
348. Mahmood, F.; Al-Ansari, T.A. Design and thermodynamic analysis of a solar powered greenhouse for arid climates. *Desalination* **2021**, *497*, 114769. [CrossRef]
349. Sajid, M.U.; Bicer, Y. Performance Assessment of Spectrum Selective Nanofluid-Based Cooling for a Self-Sustaining Greenhouse. *Energy Technol.* **2021**, *9*, 2000875. [CrossRef]
350. Mahmood, F.; Bicer, Y.; Al-Ansari, T. Design and thermodynamic assessment of a solar powered energy–food–water nexus driven multigeneration system. *Energy Rep.* **2021**, *7*, 3033–3049. [CrossRef]
351. Mangold, D.W.; Bundy, D.S.; Hellickson, M.A. Psychrometrics. In *Ventilation of Agricultural Structures*; Hellickson, M.A., Walker, J.N., Mich, S.J., Eds.; ASAE Monograph: Washington, DC, USA, 1983; pp. 9–22, ISBN 09-161-50569.
352. Zarei, T.; Behyad, R.; Abedini, E. Study on parameters effective on the performance of a humidification-dehumidification seawater greenhouse using support vector regression. *Desalination* **2018**, *435*, 235–245. [CrossRef]
353. Zarei, T.; Behyad, R. Predicting the water production of a solar seawater greenhouse desalination unit using multi-layer perceptron model. *Sol. Energy* **2019**, *177*, 595–603. [CrossRef]
354. Hassanien, R.H.E.; Li, M.; Dong Lin, W. Advanced applications of solar energy in agricultural greenhouses. *Renew. Sustain. Energy Rev.* **2016**, *54*, 989–1001. [CrossRef]
355. La Notte, L.; Giordano, L.; Calabrò, E.; Bedini, R.; Colla, G.; Puglisi, G.; Reale, A. Hybrid and organic photovoltaics for greenhouse applications. *Appl. Energy* **2020**, *278*, 115582. [CrossRef]
356. McCartney, L.; Lefsrud, M.G. Protected agriculture in extreme environments: A review of controlled environment agriculture in Tropical, arid, polar, and urban locations. *Appl. Eng. Agric.* **2018**, *34*, 455–473. [CrossRef]
357. Kumar, M.; Haillot, D.; Gibout, S. Survey and evaluation of solar technologies for agricultural greenhouse application. *Sol. Energy* **2022**, *232*, 18–34. [CrossRef]
358. Panagopoulos, A. A comparative study on minimum and actual energy consumption for the treatment of desalination brine. *Energy* **2020**, *212*, 118733. [CrossRef]
359. Meneses, M.; Pasqualino, J.C.; Céspedes-Sánchez, R.; Castells, F. Alternatives for reducing the environmental impact of the main residue from a desalination plant. *J. Ind. Ecol.* **2010**, *14*, 512–527. [CrossRef]
360. Jones, E.; Qadir, M.; van Vliet, M.T.H.; Smakhtin, V.; Kang, S.-M. The state of desalination and brine production: A global outlook. *Sci. Total Environ.* **2019**, *657*, 1343–1356. [CrossRef]
361. De-la-Ossa-Carretero, J.A.; Del-Pilar-Ruso, Y.; Loya-Fernández, A.; Ferrero-Vicente, L.M.; Marco-Méndez, C.; Martinez-Garcia, E.; Giménez-Casalduero, F.; Sánchez-Lizaso, J.L. Bioindicators as metrics for environmental monitoring of desalination plant discharges. *Mar. Pollut. Bull.* **2016**, *103*, 313–318. [CrossRef]
362. Al-Shammari, S.B.; Lulwa, A. Effect of Brine Disposal on Seawater Quality at Az-Zour Desalination Plant in Kuwait: Physical and Chemical Properties. *J. Environ. Sci. Eng. A* **2018**, *7*, 189–200. [CrossRef]
363. Crisp, G.J. Desalination and water reuse—Sustainably drought proofing Australia. *Desalin. Water Treat.* **2012**, *42*, 323–332. [CrossRef]
364. National Research Council, Division on Earth and Life Studies, Water Science and Technology Board, Committee on Advancing Desalination Technology. *Desalination: A National Perspective*; National Academies Press: Washington, DC, USA, 2008; ISBN 0309119235.
365. Falkenberg, L.J.; Styan, C.A. The use of simulated whole effluents in toxicity assessments: A review of case studies from reverse osmosis desalination plants. *Desalination* **2015**, *368*, 3–9. [CrossRef]
366. Eslamian, S. (Ed.) *Urban Water Reuse Handbook*; CRC Press: Boca Raton, FL, USA, 2016; ISBN 9780429171802.
367. Ziolkowska, J.R. Is Desalination Affordable?—Regional Cost and Price Analysis. *Water Resour. Manag.* **2015**, *29*, 1385–1397. [CrossRef]
368. Panagopoulos, A.; Haralambous, K.J. Environmental impacts of desalination and brine treatment—Challenges and mitigation measures. *Mar. Pollut. Bull.* **2020**, *161*, 111773. [CrossRef]
369. Ziolkowska, J.R.; Reyes, R. Prospects for Desalination in the United States-Experiences From California, Florida, and Texas. In *Competition for Water Resources: Experiences and Management Approaches in the US and Europe*; Ziolkowska, J., Peterson, J., Eds.; Elsevier: Amsterdam, The Netherlands, 2017; pp. 298–316, ISBN 9780128032381.
370. Arafat, H.A. (Ed.) *Desalination Sustainability: A Technical, Socioeconomic, and Environmental Approach*; Elsevier: Amsterdam, The Netherlands, 2017.
371. Alrbai, M.; Enizat, J.; Hayajneh, H.; Qawasmeh, B.; Al-Dahidi, S. Energy and exergy analysis of a novel humidification-dehumidification desalination system with fogging technique. *Desalination* **2022**, *522*, 115421. [CrossRef]

372. El-Said, E.M.S.; Dahab, M.A.; Omara, M.A.; Abdelaziz, G.B. Humidification-dehumidification solar desalination system using porous activated carbon tubes as a humidifier. *Renew. Energy* **2022**, *187*, 657–670. [CrossRef]
373. Tangellapalli, S. Humidification-dehumidification and heat pump integration for water purifier and air conditioning. *Energy Convers. Manag.* **2021**, *244*, 114472. [CrossRef]
374. Rafiei, A.; Loni, R.; Mahadzir, S.B.; Najafi, G.; Pavlovic, S.; Bellos, E. Solar desalination system with a focal point concentrator using different nanofluids. *Appl. Therm. Eng.* **2020**, *174*, 115058. [CrossRef]
375. Kolahi, M.R.; Amidpour, M.; Yari, M. Multi-objective metaheuristic optimization of combined flash-binary geothermal and humidification dehumidification desalination systems. *Desalination* **2020**, *490*, 114456. [CrossRef]
376. Cao, Y.; Dhahad, H.A.; Parikhani, T.; Anqi, A.E.; Mohamed, A.M. Thermo-economic evaluation of a combined Kalina cycle and humidification-dehumidification (HDH) desalination system integrated with thermoelectric generator and solar pond. *Int. J. Heat Mass Transf.* **2021**, *168*, 120844. [CrossRef]
377. Sachdev, T.; Gaba, V.K.; Tiwari, A.K. Performance analysis of desalination system working on humidification-dehumidification coupled with solar assisted air heater and wind tower: Closed and open water cycle. *Sol. Energy* **2020**, *205*, 254–262. [CrossRef]
378. He, W.; Yang, H.; Han, D. Thermodynamic investigation and optimization of a heat pump coupled open-air, open-water humidification dehumidification desalination system with a direct contact dehumidifier. *Desalination* **2019**, *469*, 114101. [CrossRef]
379. Wang, Y.; Qi, Q.; Fan, J.; Wang, W.; Yu, D. Simple and robust MXene/carbon nanotubes/cotton fabrics for textile wastewater purification via solar-driven interfacial water evaporation. *Sep. Purif. Technol.* **2021**, *254*, 117615. [CrossRef]
380. Zhang, Q.; Yang, H.; Xiao, X.; Wang, H.; Yan, L.; Shi, Z.; Chen, Y.; Xu, W.; Wang, X. A new self-desalting solar evaporation system based on a vertically oriented porous polyacrylonitrile foam. *J. Mater. Chem. A* **2019**, *7*, 14620–14628. [CrossRef]
381. Santosh, R.; Kumaresan, G.; Monisha, S.; Kumar, G.K.; Velraj, R. Experimental evaluation of PVA as novel humidifier material for humidification-dehumidification applications. *J. Test. Eval.* **2021**, *49*, 2730–2741. [CrossRef]
382. Santosh, R.; Kumaresan, G.; Paranthaman, V.; Swaminathan, M.R.; Velraj, R. Comparative investigation on heat transfer enhancement of surface-roughened and nano-dispersed phase change material for thermal energy storage. *Int. J. Energy Res.* **2021**, *45*, 15992–16005. [CrossRef]
383. Vijaya Kumar, G.; Cammiade, L.M.F.; Kelm, S.; Arul Prakash, K.; Groß, E.M.; Allelein, H.J.; Kneer, R.; Rohlfs, W. Implementation of a CFD model for wall condensation in the presence of non-condensable gas mixtures. *Appl. Therm. Eng.* **2021**, *187*, 116546. [CrossRef]
384. Ham, M.G.; Jeon, W.J.; Kim, H.J.; Bak, C.-u.; Kim, Y.D. Performance and viability of absorptive dehumidification module using flat-sheet polytetrafluoroethylene/polypropylene composite membranes. *Energy Convers. Manag.* **2020**, *205*, 112393. [CrossRef]
385. Carmona, M.; Palacio Bastos, A.; García, J.D. Experimental evaluation of a hybrid photovoltaic and thermal solar energy collector with integrated phase change material (PVT-PCM) in comparison with a traditional photovoltaic (PV) module. *Renew. Energy* **2021**, *172*, 680–696. [CrossRef]
386. Pramothraj, M.; Santosh, R.; Swaminathan, M.R.; Kumaresan, G. Study of effect of Al and Cu microparticles dispersed in D-Mannitol PCM for effective solar thermal energy storage. *J. Therm. Anal. Calorim.* **2020**, *139*, 895–904. [CrossRef]
387. Zhang, X.; Wang, Y.; Zhao, D.; Guo, J. Improved thermal performance of heat exchanger with TiO_2 nanoparticles coated on the surfaces. *Appl. Therm. Eng.* **2017**, *112*, 1153–1162. [CrossRef]
388. Kurihara, M.; Takeuchi, H. Current Status and Future Trend of Seawater Desalination on Membrane Technology and Biotechnology as Sustainable Green Desalination in the 21st Century. *Gen. Chem.* **2022**, *8*, 210016. [CrossRef]
389. Santosh, R.; Arunkumar, T.; Velraj, R.; Kumaresan, G. Technological advancements in solar energy driven humidification-dehumidification desalination systems—A review. *J. Clean. Prod.* **2019**, *207*, 826–845. [CrossRef]
390. Pavlović, Z.T.; Kostić, L.T. Variation of reflected radiation from all reflectors of a flat plate solar collector during a year. *Energy* **2015**, *80*, 75–84. [CrossRef]
391. Aref, L.; Fallahzadeh, R.; Madadi Avargani, V. An experimental investigation on a portable bubble basin humidification/dehumidification desalination unit utilizing a closed-loop pulsating heat pipe. *Energy Convers. Manag.* **2021**, *228*, 113694. [CrossRef]